Energy, Mines and Resources Canada | Énergie, Mines et Ressources Canada

CANMET

Canada Centre for Mineral and Energy Technology | Centre canadien de la technologie des minéraux et de l'énergie

MECHANICAL PROPERTIES OF ROCK SAMPLES FROM THE LAC DU BONNET BATHOLITH, MANITOBA

A. Annor and R. Jackson
Rock Mechanics Laboratory

December 1985

MICROMEDIA

112 pp

MINERAL AND ENERGY TECHNOLOGY
MINING RESEARCH LABORATORIES
DIVISION REPORT M&ET/MRL 85-41(TR)

This document is an unedited [illegible] report prepared [illegible] for [illegible] and internal [illegible] purposes. It does not [illegible] final [illegible] of the [illegible] for Mineral and Energy Technology (CANMET)

Ce document est un rapport [illegible] rédigé [illegible] pour fin de [illegible] et de documentation [illegible] ne [illegible] l'approbation définitive de l'opinion du Centre canadien de la technologie des minéraux et de l'énergie (CANMET)

MECHANICAL PROPERTIES OF ROCK SAMPLES FROM THE LAC DU BONNET BATHOLITH, MANITOBA

by

A. Annor* and R. Jackson**

ABSTRACT

CANMET and Atomic Energy of Canada Limited (AECL), have undertaken a joint project to investigate the mechanical properties of rock samples from the Lac du Bonnet batholith, near Pinawa, Manitoba. The investigations form a part of research projects within the Canadian Nuclear Fuel Waste Management Program (NFWMP) to find a safe means of disposing of high level nuclear wastes in deep geological structures.

The investigations which comprised uniaxial and triaxial compression measurements, tensile strength tests, and acoustic wave velocity measurements, were undertaken to provide data, and data interpretations for vault design studies, in situ test planning and geosphere modelling activities associated with the NFWMP.

The test results indicated trends of decreasing uniaxial compressive strength, Brazilian tensile strength, Young's modulus and zero pressure compressive wave velocity, and increasing Poisson's ratio with increasing depth. The observed trends conform with the slight compositional variations of the Lac du Bonnet granitic pluton with increasing depth. The altered pink granite samples from the near surface zones of the formation were stronger in compression and deformed much less, than the slightly altered greenish-grey and grey samples from the deeper horizons. Young's modulus for the grey granite samples indicated some stress dependency possibly due to increased crack porosity with stress relaxation.

---

*Physical Scientist, CANMET, Energy, Mines and Resources Canada Ltd.

**Research Engineer, Atomic Energy of Canada Ltd., Seconded to CANMET, Energy, Mines and Resources Canada, Ottawa, Ontario.

Keywords: Compressive strength, Young's modulus, Poisson's ratio, tensile strength, compressive wave velocity.

The test results compare favourably with data in the published literature for granitic rock of similar mineralogical composition as Lac du Bonnet granite. In terms of engineering classification (Deere and Miller, 1966), the formation falls in the range of high strength to very high strength rock with a medium modulus ratio.

PROPRIÉTÉS MÉCANIQUES D'ÉCHANTILLONS DE ROCHES PRÉLEVÉS DANS LE BATHOLITE DU LAC DU BONNET, AU MANITOBA

par

A. Annor* et R. Jackson**

RÉSUMÉ

CANMET et Énergie atomique du Canada Limitée (EACL) se sont associés pour une étude des propriétés mécaniques d'échantillons de roches prélevés dans le batholite du lac du Bonnet, près de Pinawa, au Manitoba. Ces investigations font partie de projets de recherches qui relèvent du Programme canadien de gestion des déchets nucléaires et qui ont pour but de trouver un moyen sûr d'enfouir des déchets nucléaires à forte radioactivité dans des structures géologiques profondes.

Par des mesures de la compression uniaxiale et triaxiale, des essais de résilience et des mesures de la vitesse de propagation des ondes acoustiques, les chercheurs ont obtenu des données qu'ils ont ensuite interprétées en prévision de la conception des voûtes, de la planification des essais sur place et de l'élaboration des modèles de la géosphère dans le cadre du Programme.

Les résultats des essais ont indiqué que la résistance à la compression uniaxiale, la résilience brésilienne, le module de Young et la vitesse des ondes de compression à une pression nulle étaient d'autant plus faibles, et le rapport de Poisson d'autant plus élevé, que la profondeur était grande. Ces tendances sont conformes aux légères variations de la composition du pluton granitique du lac du Bonnet à

---

*Spécialiste des sciences physiques, CANMET, Énergie, Mines et Ressources Canada

**Ingénieur-chercheur, Énergie atomique du Canada Ltée, détaché à CANMET, Énergie, Mines et Ressources Canada, Ottawa, Ontario.

Mots clés : Résistance à la compression, module de Young, rapport de Poisson, résilience, vitesse des ondes de compression.

mesure qu'augmente la profondeur. Les échantillons de granite rose altéré recueillis près de la surface de la formation présentaient une résistance plus élevée en cours de compression et une déformation beaucoup plus faible que les échantillons altérés gris verdâtre et gris provenant des niveaux plus profonds. Le module de Young mesuré sur les échantillons de granite gris a révélé une certaine influence de la contrainte qui peut être attribuable à une augmentation de la porosité des fissures lorsque diminuent les forces exercées sur la roche.

Les résultats des essais se comparent favorablement aux données contenues dans la documentation déjà publiée au sujet des roches granitiques de composition minéralogique semblable à celle du granite du lac du Bonnet. Dans la classification adoptée par les ingénieurs (Deere et Miller, 1966), la formation à l'étude entre dans la catégorie des roches de résistance élevée à très élevée avec un module moyen.

CONTENTS

	Page
ABSTRACT	i
RÉSUMÉ	iii
INTRODUCTION	1
GEOLOGICAL DESCRIPTION OF CORE SAMPLES	2
DESCRIPTION OF MEASUREMENTS	3
Sampl Preparation	4
Compressive wave velocity measurements	4
Data treatment	5
Uniaxial compressive strength measurements	6
URL-1 standard samples	6
The effect of moisture content on the mechanical properties of laboratory samples	7
Uniaxial compression data treatment	7
Brazilian tensile strength measurement	7
Data treatment	7
Triaxial compression measurements	8
Data reduction	8
DATA ANALYSIS AND RESULTS	9
Data Summary	9
DISCUSSIONS	10
Engineering design considerations	10
Classification in terms of rock sample colouration	10
Generalized observations	11
Examination of stress relaxation effects on the measured properties	11
Effects of stress relaxation on Young's modulus of rock	11
Anisotropic characteristics	12
Triaxial compression test results	13
Strength properties of intact rock samples	14
Strength properties of jointed rock samples	17
SCALE EFFECTS	19
CONCLUSIONS	20
ACKNOWLEDGEMENTS	21
REFERENCES	22

TABLES

No.		Page
1.	Summary of uniaxial mechanical properties and compressive wave velocity data for borehole URL-1 samples	27
2.	Summary of uniaxial mechanical properties and compressive wave velocity data for borehole URL-2 samples	30
3.	Summary of uniaxial mechanical properties and compressive wave velocity data for borehole URL-5 samples	31
4.	Summary of uniaxial mechanical properties and compressive wave velocity data for boreholes URL-2, URL-5 and URL-6 "Deep" samples	33
5.	Summary of test data on the effects of specimen conditioning on uniaxial compression test results	35
5a.	Summary of uniaxial mechanical properties of surface air dried and oven dried URL specimens	35
5b.	Summary of uniaxial mechanical properties of surface air dried WN-1 specimens	36
5c.	Summary of uniaxial mechanical properties of oven dried WN-1 specimens	37
5d.	Summary of uniaxial mechanical properties of water saturated WN-1 specimens	38
5e.	Statistical distributions of uniaxial mechanical properties for conditioned WN-1 specimens	39
6.	Summary of Brazilian tensile strength test data for borehole URL-2 "deep" samples	40
7.	Statistical summary of mechanical properties data for Lac du Bonnet granitic samples on the basis of engineering sub-divisions (URL-sites)	43
8.	Statistical summary of mechanical properties data for Lac du Bonnet granitic samples (WNRE-site)	44
9.	Statistical summary of uniaxial strength deformation and acoustive wave velocity data for Lac du Bonnet granitic samples (combined URL and WNRE-sites)	45
10.	Summary of literature-referenced uniaxial mechanical properties data for granitic rocks	46

TABLES (Cont'd)

No.		Page
11.	Summary of triaxial compression test data for Lac du Bonnet granitic samples (URL-site)	47
12.	Summary of triaxial compression test data for Lac du Bonnet granitic samples (WNRE-site)	50
13.	Summary of triaxial compression test data for Atikokan granitic samples	50
14.	Analysis of rock fracture data (based on Hoek and Brown, 1980)	51
15.	Summary of rock joint characterization data for Lac du Bonnet drill core samples	53

FIGURES

1. Standard sample 54
2. Generalized lithology, occurrence of natural fractures, fracture fillings, alteration zones and zones of discontinuous hairline fractures in borehole URL-1 55
3. Generalized lithology, occurrence of natural fracture infillings, alteration zones, and zones of discontinuous hairline fractures in borehole URL-2 56
4. Generalized lithology, occurrence of natural fractures, fracture infillings, alteration zones and zones of discontinuous hairline fractures in borehole URL-5 57
5. Generalized lithology, occurrence of natural fractures in fillings, alteration zones, and zones of discontinuous hairline fractures in borehole URL-6 58
6. Generalized lithology, occurrence of natural fractures in fillings, alteration zones, and zones of discontinuous hairline fractures in borehole URL-7 59
7. Depth profiles of uniaxial compressive strength and Poisson's ratio (URL and WNRE-sites combined) 60
8. Depth profiles of tangent modulus of elasticity and zero pressure dilatational wave velocity for Lac du Bonnet granitic samples (URL and WNRE-sites combined) 61

FIGURES (Cont'd)

No.		Page
9.	Engineering classification of intact rock for Lac du Bonnet granitic samples (boreholes URL-1, URL-2, URL-5, URL-6, URL-7 and WN-2, and WN-4)	62
10.	Histogram of bulk density for upper zone (0-50 m vertical depth) Lac du Bonnet granitic samples (URL-site)	63
11.	Histogram of uniaxial compressive strength for upper zone (0-50 m vertical depth) Lac du Bonnet granitic samples (URL-site)	64
12.	Histogram of tangent modulus of elasticity for upper zone (0-50 m vertical depth) Lac du Bonnet granitic samples (URL-site)	65
13.	Histogram of Poisson's ratio, for upper zone (0-50 m vertical depth) Lac du Bonnet granitic samples (URL-site)	66
14.	Histogram of zero pressure compressive wave velocity for upper zone (0-50 m vertical depth) Lac du Bonnet granitic samples (URL-site)	66
15.	Histogram of bulk density for intermediate zone (51-260 m) Lac du Bonnet granitic samples (URL-site)	67
16.	Histogram of uniaxial compressive strength for intermediate zone (51-260 m vertical depth) Lac du Bonnet granitic samples (URL-site)	68
17.	Histogram of Brazilian tensile strength for intermediate zone (51-260 m vertical depth) Lac du Bonnet granitic samples (URL-site)	69
18.	Histogram of tangent modulus for intermediate zone (51-260 m vertical depth), Lac du Bonnet granitic samples (URL-site)	70
19.	Histogram of Poisson's ratio for intermediate zone (51-260 m vertical depth) Lac du Bonnet granitic samples (URL-site)	71
20.	Histogram of zero pressure compressive wave velocity for intermediate zone (51-260 m vertical depth) Lac du Bonnet granitic samples (URL-site)	72
21.	Histogram of bulk density for lower zone (below 260 m vertical depth) Lac du Bonnet granitic samples (URL-site)	73
22.	Histogram of uniaxial compressive strength for lower zone (below 260 m vertical depth) Lac du Bonnet granitic samples (URL-site)	74

FIGURES (Cont'd)

No.		Page
23.	Histogram of Brazilian tensile strength for lower zone (below 260 m vertical depth) Lac du Bonnet granitic samples (URL-site)	75
24.	Histogram of tangent modulus of elasticity for lower zone (below 260 vertical depth) Lac du Bonnet granitic samples (URL-site)	76
25.	Histogram of Poisson's ratio for lower zone (below 260 m vertical depth) Lac du Bonnet granitic samples (URL-site)	77
26.	Histogram of zero pressure compressive wave velocity for lower zone (below 260 m vertical depth) Lac du Bonnet granitic samples (URL-site)	78
27.	Histogram of uniaxial compressive strength for Lac du Bonnet granitic samples (URL and WNRE combined data)	79
28.	Histogram of tangent modulus for Lac du Bonnet granitic samples (URL and WNRE combined data)	80
29.	Histogram of Poisson's ratio for Lac du Bonnet granitic samples (URL and WNRE combined data)	81
30.	Histogram of Brazilian tensile strength for Lac du Bonnet granitic samples (URL and WNRE combined data)	82
31.	Histogram of zero pressure compressive wave velocity for Lac du Bonnet granite samples (URL and WNRE combined data)	83
32.	Variation of tangent modulus of elasticity versus confining pressure for URL upper zone samples	84
33.	Variation of tangent modulus of elasticity versus confining pressure for boreholes URL-2, 5, and 6 deep samples	85
34.	Normalized strength envelope for Lac du Bonnet granitic samples from the URL-site	86
35.	Mohr's circle and strength envelope for Lac du Bonnet granitic samples at 21°C	87
36.	Mohr's circle and strength envelope for Lac du Bonnet granitic samples at 100°C	88
37.	Mohr's circle and strength envelope for Lac du Bonnet granitic samples at 200°C	89
38.	Relationship between principal stresses at failure for Lac du Bonnet granitic samples at 21°C	90

FIGURES (Cont'd)

No.		Page
39.	Relationship between principal stessses at failure for Lac du Bonnet pink granite samples at 21°C	91
40.	Relationship between principal stresses at failure for Lac du Bonnet grey granite samples at 21°C	92
41.	Relationship between principal stresses at failure for Atikokan granite samples at 21°C	93
42.	Relationship between principal stresses at failure for Atikokan and Lac du Bonnet granite samples at 21°C	94
43.	Relationship between principal stresses at failure for Lac du Bonnet granitic samples at 100°C	95
44.	Relationship between principal stresses at failure for Atikokan granitic samples at 100°C	96
45.	Relationship between principal stresses at failure for Atikokan and Lac du Bonnet granitic samples at 100°C	97
46.	Relationship between principal stresses at failure for Lac du Bonnet granitic samples at 200°C	98
47.	Relationship between principal stresses at failure for Atikokan granitic samples at 200°C	99
48.	Relationship between principal stresses at failure for Atikokan and Lac du Bonnet granitic samples at 200°C	100
49.	Frictional strength of saw-cuts in Lac du Bonnet granitic samples as a function of temperature	101

INTRODUCTION

CANMET and other branches of Energy, Mines and Resources Canada are involved in geomechanics research towards the safe disposal of nuclear fuel wastes in deep geological formations. The investigations form part of comprehensive research studies by Atomic Energy of Canada Limited, to assess the concept of disposing of nuclear waste in plutonic rock.

Four plutonic rock bodies designated as research areas have been studied to date. Three of the research areas are located in the Chalk River, Atikokan, and East Bull Lake regions of Ontario. A fourth area is situated on the Lac du Bonnet batholith, near Pinawa, Manitoba. At this location, an underground research laboratory (URL) is currently under construction by Atomic Energy of Canada Limited as part of the above mentioned research activity.

A comprehensive mechanical and thermomechanical rock properties study program has been followed over the past few years on rock samples from the URL site. The objectives of the investigations have been to provide data, and data interpretations for vault design studies, as well as, to fulfill URL and geosphere modelling requirements. A two stage on-going laboratory study program was initiated in 1982 for this purpose (Baumgartner, 1983). The first stage of the study involved uniaxial strength and deformational properties (Young's modulus and Poisson's ratio), and acoustic wave velocity measurements on URL area core samples at ambient room temperature. Initial results of this study was reported by Annor and Jackson (1982). Additional measurements have since been carried out. These measurements have also included tests to identify factors such as, the effects of moisture, and stress relaxation on the mechanical property data (Jackson 1983; Jackson and Boudreau, 1985, Jackson and Paquette, 1984, Jackson and Annor, 1985a).

The second phase of the study involved thermal expansion measurements under variable constraint, and elevated temperature triaxial compression measurements. The test results are reported elsewhere, [Jackson 1984), Annor and Jackson (1982) and Jackson and Annor, (1985b)].

The objectives of this report are:

1. To summarize the mechanical rock properties data for the Lac du Bonnet formation at the URL site which has been collected to date under the EMR's rock property task.
2. To fulfill geosphere modelling task requirements by accounting for, in some detail, how the test data were obtained.

GEOLOGICAL DESCRIPTION OF CORE SAMPLES

The test samples originated from twelve surface drilled shallow and deep boreholes in the Lac du Bonnet batholith in the URL lease area. The samples were mainly of granitic composition, and medium to coarse grained. Mineralogical compositions were approximately: 30% K-feldspar, 30% plageoclase, 30% or slightly less quartz, and 10% or slightly more, mafic minerals (mainly biotite), (Wong, 1984).

The samples were either pink, greenish-grey, or grey coloured. The pink colouration has been associated with rock alteration. On the other hand, grey colour has been identified with very little or no alteration (Kamineni et al., 1984). The pink granitic samples originated from relatively shallow zones of the formation between surface of bedrock and about 260 m depth. In contrast, the grey coloured samples were taken from the deep zones of the formation. The greenish-grey samples originated between the pink and grey granite.

In terms of the Energy, Mines and Resources' rock properties activity designations (Larocque and Annor, 1984), three types of samples were used for the measurements. These were respectively:

(i) standard engineering,
(ii) extended engineering, and
(iii) special engineering samples.

The standard engineering samples were generally representative of a lithology. These samples were selected and distributed according to a set of criteria based on borehole lithological, geologic and geophysical information, (Larocque, 1978), (Figure 1).

The extended engineering samples were selected from zones of specific interest, such as the two originally proposed operating levels of the

underground research laboratory (URL). In terms of borehole length, the specific zones of interest were as follows:

URL-1	URL-5	URL-6
175-200 m	122-138 m	224-260 m
282-295 m	272-284 m	

The special engineering samples were usually selected for specific purposes. These samples originated from the shallow BH-group of boreholes, as well as the lower reaches of the deepest boreholes in the URL-lease area. The special engineering samples were used to investigate the effects of moisture content on the uniaxial strength and deformation characteristics of the URL rock samples. The effects of stress relief on the core samples were also investigated using the special engineering samples. The boreholes and the corresponding zones of interest were:

URL-1	URL-2	URL-5
664.85-666.34 m	1080.14-1082-63 m	441.56-443.07 m

URL-6	URL-7
373.68-375.68 m	61.36-198.00 m
391.17-392.43 m	

Additionally, some special engineering samples were selected from shallow boreholes BH-01, BH-09, BH-10 and BH-11.

The generalized lithological variation of the URL formation in boreholes URL-1, URL-2, URL-5, URL-6 and URL-7 are provided in Fig. 2, 3, 4, 5 and 6, respectively.

DESCRIPTION OF MEASUREMENTS

Sample preparation and testing were carried out to conform as closely as possible with the American Society for Testing and Materials (ASTM) standards (ASTM 1971a, 1971b), and CANMET's Pit Slope Manual Specifications (Gyenge and Herget, 1977). Sample preparation, equipment, and testing

procedures are also described in the following reports: Annor, (1984); Annor and Wong, (1984), Annor and Jackson, (1984).

SAMPLE PREPARATION

Cylindrical test specimens with an average length to diameter (L/D) ratio of about 2.2, were used for the uniaxial compression and dilatational wave velocity measurements described in this report. With regard to the Brazilian tensile strength tests, discs with thickness to diameter ratios of about 0.5 were used. In the case of the triaxial compression measurements, the length to diameter ratio of the test samples was about 2.8.

The test samples were cut slightly larger than their final dimensions, using a water cooled diamond-saw. Sample ends were then ground parallel to each other to within 0.03 mm and at right angles to the longitudinal axis. Hardened steel jigs and a lapping wheel were used for this purpose. Sample dimensions and weight were measured, and recorded for future computations. The samples were generally tested in a dry state after surface air drying in the laboratory, except where indicated.

To carry out uniaxial elastic deformation measurements strain gauges, oriented to measure axial and circumferential strains, were located equidistant from the two ends of the specimen. Gauges of similar orientations were located on the opposite sides of the sample. The axial and circumferential gauges were connected in series, to form single active gauges.

The gauges were used in a half bridge configuration for strain measurements. BLH Electronics Co. SR-4, FAE Series, and Micro-Measurements Division EA-500 BH Series gauges were used.

Compressive Wave Velocity Measurements

The testing equipment consisted of transmitting and receiving specimen platens containing piezoelectric transducers, a high voltage pulse generator, a signal amplifier, a Tektronix Type 555 dual beam oscilloscope with a delay sweep and a time base resolution to 0.1 micro seconds per centimeter, and a Hoek triaxial cell. For one set of measurements, the velocity equipment was used with a hydraulic press (Tinius Olsen Universal Testing Machine) to measure specimen compressive wave transit time, as a function of applied axial load. For a second set of test samples, the velocity equipment was used in conjunction with a manually operated hydraulic

pump, and a loading frame to measure specimen compressive wave transit time as a function of applied hydrostatic pressure.

In the case of axial compressive wave velocity measurements, the test sample and transducer assembly, was placed between the platens of the hydraulic press and was axially stressed in increments of about 2.7 MPa to a maximum stress level. Due to the structural limitations of the transducer platens, the maximum applied stress used was about 43 MPa. At each incremental stress level, the transmitter's piezoelectric transducer excited by a pulse generator, was used to send stress waves into the specimen which were detected by the receiver's piezoelectric platen.

The compressive wave velocity measurements as a function of variable hydrostatic pressure, were almost similar to the axial compressive wave velocity tests described above. There were, however, slight differences in the procedure used. Initially, the lapped test specimens were encased in a rubber membrane and then placed into a Hoek cell. Phenyl salicyclate was used to attach the pulsing heads to the test samples. A hydraulic loading frame was used to apply a small axial load through the pulsing heads to a predetermined stress value. Confining pressure was then applied until equilibrium was reached. The travel time of the compression wave was determined with the Tektronix osciloscope. Measurements were carried out over the confining pressure range of 0.1 to 70 MPa. Delayed arrival time readings were taken at various pre-determined stress levels. The measured delayed arrival time of the seismic disturbance, the specimen length, and the measured zero delay of the sonic system were used to determine specimen dilatational velocity. Prior to individual specimen time delay measurements, the transmitting and receiving platens were placed together and the zero delay time of the sonic system determined. Delay time was measured to 0.1 micro-second, (Annor et al. 1979; Gyenge and Herget, 1977).

Data Treatment

Dilatational velocity, (V_p), of a specimen was determined from the relationship:

$$Vp = \frac{L}{(tp - to)} \qquad \text{Eq 1}$$

where: L = specimen length (m)
tp = time of transit (s)
to = zero delay time of the sonic system(s).

Uniaxial Compressive Strength Measurements

Equipment used to measure axial and circumferential specimen deformation under applied axial load consisted of two Bruel and Kjaer Type 1526 strain indicators, and a Hewlett Packard 7046 B X-7 recorder. The bridges were used in a half-bridge configuration. Axial and circumferential strain gauges were used to provide voltage analog outputs of the axial and circumferential strains produced in the sample by axial loading. These analogs were then used to drive the two Y-axis plotters of the Hewlett Packard recorder independently. Axial and circumferential stress-strain curves were obtained in this manner for each of the specimens tested. The curves were used to determine Young's modulus and Poisson's ratio. The axial load was increased until failure occurred and the failure load noted. Recorder outputs of the axial stress versus strain curves are provided by Jackson, (1982); Jackson and Boudreau, (1983); Jackson and Paquette, (1984); and Jackson and Annor, (1985a).

URL-1 Standard Samples

A method similar to that described above was used for carrying out the uniaxial compression measurements of the URL-1 Standard samples. Each specimen, however, was subjected to three loading and unloading cycles to compensate for the effects of stress relaxation due to drilling. Reported Young's modulus and Poisson's ratio, were determined from the average value of the final two loading and unloading cycles. Recorder output of the stress versus strain curves are reported by McKay (1982).

In addition to the standard uniaxial compression measurements, two studies were undertaken to investigate (1) the effects of moisture content on the mechanical properties of laboratory core samples; and (2) the effects of stress relaxation on the observed mechanical properties data.

The Effects of Moisture Content on the Mechanical Properties of Laboratory Samples

The methods of testing were identical to those already described under acoustic wave velocity and uniaxial compression measurements. The test samples were, however, conditioned differently prior to testing.

One set of test specimens was heated slowly (0.35°C/min) to about 63°C and cooled down to room temperature before testing. A second set of specimens was surface air dried in the laboratory before testing. A third set of specimens was immersed in water for at least seven days prior to testing. The calculated uniaxial compressive strengths, Poisson's ratios and Young's moduli of the three sample populations were then compared. A detailed description of the test procedure is given in the following reports: Jackson, (1983); and Jackson and Annor (1985).

Uniaxial Compression Data Treatment

Young's modulus was calculated for each sample by determining the value of the tangent to the axial strain curve at 50% of failure load. The ratio of the tangent to the axial strain curve to the tangent to the transverse strain curve at 50% failure load, was used to determine the sample's Poisson's ratio. The ultimate compressive strength of each sample was calculated by dividing the sample failure load by sample cross sectional area.

Brazilian Tensile Strength Measurement

Specimens were tested according to ASTM specification C496-71. The test specimens were loaded diametrically between two hardened steel platens in a hydraulic press. Load was applied until the specimen failed.

In the case of tests to determine the strength anisotropy of the Lac du Bonnet granitic samples, adjacent, paired core samples were selected. One of the two samples was loaded along the core reference line while the other was loaded perpendicular to the line.

Data Treatment

The tensile strength of a specimen was determined from the relationship:

$$\sigma_t = \frac{2P}{\pi Dt} \qquad \text{Eq 2}$$

where: σ_t = specimen tensile strength (MPa)
P = failure load (MN)
D = diameter of disc (m)
t = thickness of disc (m)

Triaxial Compression Measurements

The equipment and the procedure used to carry out triaxial compression measurements at ambient room temperature are described by Jackson and Boudreau (1984), and Annor et al. (1981). However, a brief description of the methods is provided below. Initially, the lapped samples were encased in an annealed copper sleeve with dimensions close to that of the test samples. Tne jacketed sample assembly was then sealed at both ends with hardened steel rings forced over tapered end platens. Two pairs of foil resistance strain gauges, oriented to measure axial deformation, were connected in two nalf bridge configurations so that, two independent axial deformation measurements could be obtained. The readings were simultaneously recorded on an HP 7046 B-X-Y recorder, and by a Fluke Data Logger. A recording interval of 10 seconds was used in the case of the Fluke Data Logging.

Prior to actual measurements, a series of calibration tests were conducted using a hardened steel dummy sample. The objective of the calibration tests was to evaluate the performance of the strain gauges under constraint. The effect of confining pressure on gauge performance was found to be insignificant at the stress levels used in the investigations.

Data Reduction

The data was reduced by plotting the recorded strain readings as a function of stress. A third degree equation of the form shown in Eq 4 was fitted to the stress versus strain points:

$$\sigma = A_1\varepsilon + a_2\varepsilon^2 + a_3\varepsilon^3 \qquad \text{Eq 4}$$

where: σ = stress

ε = strain

and a_1, a_2, and a_3 are coefficients.

The derivative of the equation was used to estimate the tangent Young's modulus of each test sample at the 50% the failure strength. This procedure compares well with the conventional graphical approach for estimating the Young's modulus of a rock specimen (Jackson, 1984).

DATA ANALYSIS AND RESULTS

DATA SUMMARY

Uniaxial strength, deformation, and acoustic wave velocity test results for individual boreholes, are summarized in Tables 1 to 6. A statistical summary of the estimated parameters for the URL site test samples is provided in Table 7. The results have been summarized in terms of depth intervals relevant to engineering studies.

A statistical summary of the uniaxial mechanical properties data for Lac du Bonnet granitic samples from borehole WN1, 2 and 4 from the WNRE* site (Annor, 1984) is also provided in Table 8. A summary of the combined rock properties data from URL and WNRE sites is given in Table 9.

Depth profiles of uniaxial compressive strength, Poisson's ratio, tangent modulus of elasticity and zero pressure compressive wave velocity for the combined URL and WNRE sites test samples are provided in Fig. 7 and 8.

The results of applying the Deere and Miller (1966) classification for intact rock based on Young's modulus, and the uniaxial compressive strength of the Lac du Bonnet rock samples are shown in Fig. 9. The modulus ratio for this classification is defined as follows:

$$\text{Modulus ratio} = \frac{\text{tangential Young's modulus at 50\% ultimate strength}}{\text{uniaxial compressive strength}},$$

and is interpreted as follows:

high modulus ratio	>500
medium modulus ratio	200 < modulus <500
low modulus ratio	<200

*Whiteshell Nuclear Research Establishment.

Statistical distributions of the calculated properties, in terms of sample population for the Lac du Bonnet formation, are provided in Fig. 10-31 in the form of histograms.

A summary of the triaxial compression data for ambient room temperature tests are given in Tables 11, 12 and 13 for Lac du Bonnet (URL site, WNRE site) and Atikokan granitic samples. The Atikokan samples have been included for the purpose of data comparison.

DISCUSSIONS

Engineering Design Considerations

The test results have been summarized statistically in terms of depth intervals required for the purposes of engineering design. The rock mass was grouped into three zones for this purpose (Baumgartner, 1983).

The first zone is from rock surface, to a vertical depth of about 50 m. This interval is assumed to represent the maximum penetration depth for surfacial effects such as fracturing and weathering. The second zone lies between the vertical depths of about 50 to 250 m. Initially, this represented the zone of maximum interest in terms of geotechnical experimentation. As originally proposed, the two operating levels of the underground research facility, were to be located in this zone. The third zone pertains to vertical depths greater than 260 m. The test samples from this zone were used for the following purposes:

a) to identify the generalized strength and deformational behaviour of the Lac du Bonnet granitic formation at depth; and
b) to evaluate the effects of stress relaxation on the mechanical properties of the Lac du Bonnet rock samples.

Classification in Terms of Rock Sample Colouration

A sub-classification has also been made in terms of specimen colouration. According to this sub-division, the rock mass falls into pink, greenish grey, and grey zones. The pink rock zone extends from surface bedrock to a vertical depth of about 290 m, the transitional zone consisting of greyish pink to greenish grey rock from about 290 m to 635 m, and the grey rock zone below 635 m.

Generalized Observations

In terms of generalized behaviour, the strength and deformation properties of the Lac du Bonnet formation can be classified into three principal zones. These are: upper, transitional and lower zones. These sub-divisions also correspond approximately to the three principal zones of rock alteration found in the Lac du Bonnet batholith (Kamineni et al., 1984).

The test results indicated trends of decreasing uniaxial compression strength, zero pressure compressive wave velocity and Young's modulus and increasing Poisson's ratio values with increasing depth (Fig. 7 and 8). While the observed trends can be explained in terms of the slight compositional differences between the test samples from the three principal zones, they also suggest some effects of stress relaxation after drilling (Annor and Jackson, 1982). The stress relaxation effect seems to apply primarily to samples originating from the deeper horizons of the formation.

Examination of Stress Relaxation Effects on the Measured Properties

To examine the effects of stress relaxation on the elastic deformation and acoustic wave velocity test data, rock core samples were selected from the lower reaches of the deepest boreholes at the URL site for various mechanical properties tests (Jackson and Boudreau, 1983). Specifically, the following tests were carried out; uniaxial compression, triaxial compression, compressive wave velocity and Brazilian tensile strength measurements. The triaxial compression tests and the compressive wave velocity measurements were carried out at confining pressures ranging between 5 and 70 MPa. These values corresponded to the estimated principal stresses prevailing at the sample depths of interest, at the URL lease area (Herget, 1980). The core samples used for the investigations originated from boreholes URL-2, URL-5 and URL-6.

Effects of Stress Relaxation on Young's Modulus of Rock

Generally, the variation of Young's modulus with confining pressure, provides some indication of the degree of micro-cracking to which a test sample has been subjected. In the case of hard crystalline, or homogeneous rock with low porosities, the elastic modulus is generally not affected by confining pressure (Fig. 32). On the the other hand, porous rocks usually exhibits a large stress dependency on Young's modulus (Lama and Vutukuri,

1978). The variation of elastic modulus with confining pressure for the Lac du Bonnet grey granitic samples (Fig. 33), indicates considerable stress dependency at low confining pressure levels. The extent of the stress dependency is more apparent when compared with the changes from similar tests for the predominantly Lac du Bonnet pink granitic samples from shallower depths (Fig. 32).

Significant differences are noticed between the elastic behaviour of the rock core samples taken from the lower reaches of the URL area boreholes, and those taken from other zones of this formation. Young's modulus values, which were determined on the basis of uniaxial compression measurements, differed from those estimated on the basis of triaxial compression tests. This was particularly true when values determined at relatively high confining pressures were compared to values determined at low confining pressures. However, these differences for URL-2 core samples seem to be eliminated when confining pressure above 20 MPa are applied (Jackson and Boudreau, 1983). It is interesting to note that this confining pressure value corresponds to the overburden stress to which the samples subjected when located at a depth of 1025 m.

The observations therefore suggest that for the grey granitic samples from the deeper levels of boreholes in the Lac du Bonnet batholith, there is a significant stress relaxation effect on mechanical properties. The increase in sample porosity due to the stress relaxation, was responsible for the observed low modulus values.

In terms of possible in-situ rockmass behaviour, stress relaxation could result in the slabbing of walls in underground excavations located at depth in this formation.

Anisotropic Characteristics

The stress distribution in a rock mass surrounding an underground excavation, can be influenced significantly by the directional variation in the strength and deformation properties of the rock. The estimation of such directional variation in the deformational characteristics of a rock mass is generally of importance, with regards to mechanical property determinations involving layered rock formations. In the case of igneous rocks such as granite, for the sake of simplicity, a rock mass is generally assumed to be elastic, homogeneous and isotropic for most engineering applications.

However, strength and deformational anisotropy can also occur in these types of formations. As a result, the strength and deformational anisotropic characteristics of crystalline igneous rocks are also required for detailed geotechnical investigations. Often, core samples taken from three orthogonal directions of the rock mass are used for this purpose.

With regard to mechanical property determinations on Lac du Bonnet formation, small sample size and random drill core orientation have prevented the determination of the directional variation of the strength and deformation properties of the URL rockmass. Strength anisotropy has, however, been estimated from Brazilian tensile strength data for the URL site rock.

The test procedure used to determine Brazilian tensile strength was described in the section treating test procedures. In the case of measurements carried out to investigate directional variation in rock strength, the following modification to the described test procedure was made. Two disc specimens were cut adjacent to each other from the same core sample. After initial sample preparation, one specimen was loaded diametrically parallel to the plane formed by the axis of the core and the drill core reference line. The other specimen was loaded diametrically on a line perpendicular to this plane.

For the test samples which originated from the deeper levels of URL area boreholes, the tensile strength values of the samples tested in an orientation perpendicular to the drill core reference line plane, were about 10% lower than those tested parallel to this plane. Although this directional variation in tensile strength values suggests some degree of strength anisotropy in the test samples, transferring of the core sample orientations to the co-ordinates of the in situ rock mass was not possible, because of the random orientation of the core samples.

Triaxial Compression Test Results

Underground excavations in rock can produce compressive stresses which result in shear failure of the boundary rock mass. Laboratory mechanical rock property investigations are generally undertaken to provide comprehensive engineering design data for safe underground construction. These investigations are often undertaken at variable stresses to duplicate the in situ stress conditions existing in the rock mass. The test data are

then used to develop a relationship between the in situ compressive and shear stress, that could exist under failure conditions (Hoek and Brown, 1980).

Two strength envelopes are generally required for this purpose, depending on the condition of the rock mass, and also on the purpose of the excavation. These are the (peak) shear strength envelope of the relatively intact rock material; and the residual strength envelope of the jointed rock mass.

Strength Properties of Intact Rock Samples

The strength properties of the intact rock material, can be expressed in terms of established empirical criteria. Two commonly employed criteria, are the Mohr-Coulomb failure criterion (Jaeger and Cook, 1976) and the Hoek and Brown (1980) failure criterion for rocks.

The Mohr-Coulomb criterion, can be expressed in terms of the principal stresses at peak load conditions as follows:

$$\sigma_1 = \sigma_c + \sigma_3 \tan^2 (45° + \phi/2) \qquad \text{Eq 6}$$

where: σ_1 = principal stress at failure (MPa)
σ_c = uniaxial compressive strength (MPa)
σ_3 = confining pressure (MPa)
ϕ = angle of internal friction (deg)

This expression yields a curved failure envelope. However, the envelope can also be approximated by a straight line for practical purposes as has been done for Lac du Bonnet samples in Fig. 34.

With regards to the Hoek and Brown (1980) failure criterion for rocks, the relationship expresses the principal stresses associated with the failure of the rock as follows:

$$\sigma_1 = \sigma_3 + \sqrt{m\sigma_c \cdot \sigma_3 + s(\sigma_c)^2} \qquad \text{Eq 8}$$

where: σ_1 = the major principal stress at failure

σ_3 = the minor principal stress applied to the specimen

σ_c = the uniaxial compressive strength of the intact rock material in the specimen

m and s = constants which depend on the properties of the rock and its structure

For this analysis, the uniaxial compressive strength of an intact rock specimen (σ_{cs}) is calculated from the relationship:

$$\sigma_{cs} = \sqrt{s\ \sigma_c^2} \qquad \text{Eq 8}$$

This relationship is obtained by substituting $\sigma_3 = 0$ in Eq 7. For the intact rock, $\sigma_{cs} = \sigma_c$ and s is taken to be 1. On the other hand, for previously broken rock, s is taken to be less than 1, and the unconfined strength (σ_c) of the rock is given by Eq 8. Also, the uniaxial tensile strength (σ_t) of a rock specimen can be estimated from the following relationship (Hoek and Brown (1980):

$$\sigma_t = 1/2\ \sigma_c\ (m - \sqrt{m^2 + 4s}) \qquad \text{Eq 9}$$

The Hoek and Brown (1980) criterion has been used to develop strength envelopes for the Lac du Bonnet and Atikokan area rock specimens. The results of the analyses are summarized in Table 14, and in Fig. 28 through 38. The results have been compiled in terms of rock colouration, as well as, test temperature.

The accuracy of the Hoek and Brown (1980) analysis depends on the availability of both uniaxial tensile and compressive strength data, as well as triaxial compressive strength data. Data from all the three strength tests were only available for tests carried out at ambient room temperature. In cases where data were available from the three strength tests, agreement between the calculated material constant "m" values, and those reported in the publisned literature was very good. This was particularly true for

those measurements carried out at ambient room temperature, involving Lac du Bonnet granitic samples.

With regards to the elevated temperature test results, no comparisons could be made between the estimated material constants "m" values, and values from reference sources. This was due to the fact that, no values are reported in the published literature, for granitic rock samples at elevated temperatures. It is felt, however, that the calculated material constants values for the Lac du Bonnet and Atikokan granitic samples at elevated temperatures (Table 14) are slightly higher than anticipated. The high values can be attributed to the lack of uniaxial tensile and compressive strength data at elevated temperatures for these rock types.

The bulk of the Lac du Bonnet granitic test samples used to develop strength analysis data originated between the 50 and 260 m vertical depths at the URL lease area. The operating levels of URL were originally planned to be located in this zone. In addition, WN-1 core test data were included for the analysis. It has been established in previous investigations that the strength and deformation properties of the Lac du Bonnet formation at the URL and WNRE sites are very similar (Annor and Jackson, 1982). Therefore, combining the test data from the two sites for the purpose of this analysis is considered justified.

Graphical representations of a linearized approximation of the Mohr strength envelope, as well as the Hoek and Brown (1980) analysis for Lac du Bonnet granitic samples, are provided in Fig. 34. The test data have been normalized to the mean uniaxial compressive strength of the Lac du Bonnet granitic samples.

In terms of Mohr circle analysis, the angle of internal friction for the Lac du Bonnet granitic samples was found to vary between 45° and 64°, depending on confining pressure, (Annor et al, 1981; Jackson, 1984) Figs 35 to 37.

For Hoek and Brown (1980) analysis, test data were divided into two principal groups on the basis of sample colouration, pink and grey. Other colour sub-groups of test samples were also considered. The "m" values for these subdivisions are also presented in Table 14, and graphically in Fig. 38 to 48.

The m-values reported in the published literature for granitic rocks, range between 20.8 and 32.8 (Hoek and Brown, 1980). The average "m" value

established for these rocks was 29.2. These reported values can be compared with those presented in Table 14 for the Lac du Bonnet and the Eye Dashwa Lakes (Atikokan) granitic samples. The Eye Dashwa Lakes data have been presented here for the purpose of data comparison. On the basis of a sample population of 250, the mean "m" value for the aggregate unheated Lac du Bonnet granitic samples, was found to be 29.9. The mean values for the unheated pink and grey Lac du Bonnet granitic samples were 31.17 and 30.54, respectively. There is a very good agreement between the "m" values for the Lac du Bonnet granitic samples, and those reported in the literature by Hoek and Brown (1980).

The material constant "m" values for the heated Lac du Bonnet granitic samples are also summarized in Table 14. The elevated temperature testing was carried out at two temperature levels: 100°C and 200°C. The "m" values for the two temperature levels were 33.66, and 32.79, respectively. By inspection, these values are similar to those determined for unheated samples. It can be concluded, on the basis of the analysis that, temperature levels of up to 200°C does not significantly influence the strength properties of the Lac du Bonnet granitic samples. It should be noted, however, that the estimated uniaxial compressive strength of the Lac du Bonnet granitic samples decreased slightly with increasing temperature between ambient room temperature and 200°C. There was about a 7% decrease in the estimated uniaxial compressive strength between ambient room temperature and 100°C. This decrease should be compared with a 14% total reduction in strength between 21° and 200°C.

Strength Properties of Jointed Rock Samples

The values presented in Table 14, represent basically intact rock material properties. Test data on fractured rock material, are also essential for the prediction of in situ rock mass behaviour. The strength envelope of the fractured rock material, can be determined from stiff tests conducted on failed rock specimens. An essential parameter of the strength envelope of the fractured rock material is the basic friction angle (ϕ_b).

With regards to the Lac du Bonnet granitic samples, the basic friction angle had previously been determined on saw-cut specimens, (Fig. 49) (Annor et al, 1981), and on core samples containing predominantly clean joints (Jackson et al, 1985). The basic friction angle of the Lac du Bonnet granitic

samples was estimated to be about 30° by Annor et al. (1981), and 31°, by Jackson et al. (1985). These values agree very well with basic friction angle values published in the literature (Barton and Choubey, 1978). It was also found that, for the Lac du Bonnet granitic samples, the basic friction angle value, was not affected significantly by temperature, over the range of 21° and 200°C (Annor et al, 1981).

The failure envelope of the joint systems in the rock, can also be described in terms of the Barton-Bandis rock joint characterization model (Barton and Bakhtar, 1983). This model is expressed as follows:

$$\tau = \sigma_n \tan (JRC \log_{10} \frac{JCS}{\sigma_n} + \phi_r) \qquad \text{Eq 9}$$

where: τ = shear strength of the joint (MPa)

σ_n = normal force acting across the joint surface (MPa)

JRC = joint roughness coefficient

JCS = joint wall compressive strength (MPa)

ϕ_r = residual friction angle

A major advantage of the above model is that values of ϕ_r, JCS, and JRC can be determined easily, using simple index tests. For example, a Schmidt rebound hammer is utilized to obtain an estimate of the weathered joint wall compressive strength (JCS), and the host rock's unweathered intact strength. Similarly, the basic friction angle (ϕ_b), can be determined for most rocks, by performing tilt tests on flat unweathered rock surfaces (generally two intact core surfaces). Having determined (ϕ_b), and the related rebound values for the fractures under consideration, the residual friction angle, (ϕ_r), can be estimated using the relationship:

$$\phi_r = (\phi_b - 20) + \frac{r}{R} \times 20 \qquad \text{Eq 10}$$

where: r = Schmidt rebound value on weathered joint surface

R = Schmidt rebound value on unweathered surface.

The value of JRC is calculated by performing self-weight shear tests in the form of tilt tests on the fracture surfaces (Jackson et al, 1985). A

statistical summary of estimated rock fracture parameters for Lac du Bonnet drill core samples is provided in Table 15.

SCALE EFFECTS

Laboratory determined mechanical rock property data can provide useful information for stability analysis, as well as, for estimating a rock mass response to mechanical and thermal loads. Sometimes, however, agreement between the actual rock mass response and predictions based on laboratory test data can be poor. As a matter of sound engineering practice, large scale in situ tests are often carried out to obtain necessary design data. This is done prior to undertaking any large scale geotechnical projects. In the absence of such tests, appropriate scale reduction factors are often applied to laboratory small scale test data, to provide an estimate of in-situ values.

Some empirical relationships have been developed by various investigators (Hoek and Brown, 1980; Hauze, 1980), for relating laboratory rock strength and deformation property values to in situ conditions. Hoek and Brown (1980), have suggested the following approximate empirical relationship for relating laboratory determined small size sample strength, to in-situ rock mass unconfined strength (Qu):

$$Q_u = Qu_{50} \left(\frac{50}{d}\right)^{0.18} \qquad \text{Eq 11}$$

where: $Q_{u_{50}}$ = the uniaxial compressive strength of a specimen of 50 mm diameter

and d = diameter of the laboratory specimen in (mm).

This relationship is applicable to unjointed intact rock specimen diameters between 10 and 200 mm. In the case of a jointed rock mass, Hoek and Brown (1980) suggest that strength variation be linked to discontinuity spacing.

In terms of in situ rock mass deformation, Hauze (1980) has proposed the following generalized relationship between field and laboratory determined Young's modulus values:

$$0.20 < E_f/E_1 < 0.60$$

where E_f and E_l refer to Young's modulus determined in the field, and laboratory, respectively. This empirical relationship was determined from a literature review of large geotechnical projects. On the basis of the above relationsnip, the estimated rock mass modulus for the Lac du Bonnet formation ranges between 12 GPa and 60 GPa, and is expected to increase with increasing depth due to confinement.

CONCLUSIONS

A summary of mechanical rock property data for Lac du Bonnet granitic samples and testing procedures have been provided to assist vault design studies, in situ test planning and geosphere modelling activities, within the Canadian Nuclear Fuel Waste Management Program.

The following generalized observations have also been made on the mechanical behaviour of Lac du Bonnet granite based on the data contained in this report.

1. The formation is characterized by trends of decreasing uniaxial compressive strength, Young's modulus and zero pressure compressive wave velocity and increasing Poisson's ratio with increasing sample depth. The trends seem to be more pronounced for the grey granitic samples from the lower reaches of the boreholes at the URL site. The behaviour suggests that significant stress relaxation can occur at depth in the grey granite zone when excavated.
2. With reference to in situ conditions, stress relaxation could result in slabbing along the walls of an excavation founded at depth in the grey granitic rock.
3. For purposes of geomechanical rock properties classification, the URL formation may be subdivided into upper, transitional and lower zones. These subdivisions seem to correspond approximately to the three principal rock alteration zones found at the URL site.
4. Tne strength, deformation and acoustic wave velocity values of the Lac du Bonnet granitic samples, compare favourably with published data on granitic rock with similar mineralogical

compositions. The acoustic wave velocity values were found to be affected by the moisture content of the rock.

5. The Lac du Bonnet granitic formation can be classified for engineering applications as a high strength to very high strength rock with a medium modulus ratio. This classification is with reference to the engineering classification for intact rock by Deere and Miller (1966).
6. It can be concluded on the basis of the Hoek and Brown (1980) analysis involving principal stresses at failure for rocks that, for purposes of design, "m" value of 29.9 can be considered to be representative of the unfractured Lac du Bonnet granitic formation at 21°C. This value may not be affected significantly by temperatures up to 200°C. There is a very good agreement between the calculated "m" values for the unheated Lac du Bonnet granite samples and "m" values reported in the published literature for granitic rocks of similar mineralogical composition.
7. The basic friction angle (ϕ_b) for Lac du Bonnet granitic samples was estimated to be about 30°. This value was unaffected significantly by temperature level of up to 200°C.
8. The angle of internal friction (ϕ) for the intact Lac du Bonnet granitic samples varied between 45° and 64° for tests carried out at ambient room temperature depending on confining pressure. These values did not change significantly with increasing temperature between 21° and 200°C.

ACKNOWLEDGEMENTS

The authors wish to thank the following people for their contributions to this report: F. Kapeller for equipment and methodology development, J. Folta and D. Dugmore for preparing the drawings, A.S. Wong for his assistance with the geological description, and D. Paquette for assisting with the data analysis.

REFERENCES

1. Annor, A., Larocque, G.E. and Chernis, P.; Uniaxial compression tests, Brazilian tensile strength and dilatational velocity measurements on rock specimens from Pinawa and Chalk River; CANMET, Mining Research Laboratories; Report MRP/MRL 79-60(TR), Energy, Mines and Resources Canada, Ottawa; 1979.

2. Annor, A., Miles, P., Kapeller, F. and Larocque, G.; High temperature and pressure triaxial compression tests on rock samples from Pinawa and Creighton Mine; Atomic energy of Canada Ltd., Techn Record TR-158, WNRE, Pinawa, Manitoba; 1981.

3. Annor, A. and Jackson, R.; Summary of uniaxial elastic properties and thermal expansion data for Pinawa granite samples (URL-1, 2, 5 and WN-1, 2 and 4); CANMET, Mining Research Laboratories; Report MRP/MRL 82-82(OP); Energy, Mines and Resources Canada, Ottawa; 1982.

4. Annor, A.; Mechanical properties of rock samples from Pinawa, Manitoba; CANMET, Division Report ERP/MRL 84-48(TR); Energy, Mines and Resources Canada, Ottawa; 1984.

5. Annor, A. and Wong, A.S.; Mechanical properties of rock samples from Chalk River, Ontario; CANMET, Mining Research Laboratories; Report ERP/MRL 84-33(TR); Energy, Mines and Resources Canada, Ottawa; 1984.

6. Annor, A. and Jackson, R.; Mechanical properties of rock samples from Atikokan, Ontario; CANMET, Mining Research Laboratories; Report ERP/MRL 84-63(TR); Energy, Mines and Resources Canada, Ottawa; 1984.

7. ASTM. 1971a; Standard test for unconfined compressive strength of intact rock specimens; ASTM test D2937-71A.

8. ASTM, 1971b; Standard test for splitting tensile strength of cylindrical concrete specimens; ASTM test C496-71.

9. Barton, N. and Bakhtar, K.; Rock joint description and modelling for the hydrothermomechanical design of nuclear waste repositories; Tera Tek Engineering; Report TRE-83-10; University Research Park, Salt Lake City, Utah; 1983.

10. Barton, N. and Choubey, V.; The shear strength of rock joints in theory and practice; Norweigian Geotechnical Institute Publication No. 119; Oslo, Norway; 1978.

11. Baumgartner, P.; Summary of rock properties testing (Phase II) and data base generation; ACEL Whiteshell Nuclear Research Establishment Memorandum No. AGHB 83-120; 1983.

12. Coates, P.J. and Parsons, R.C.; Experimental criteria for classification of rock substances; Int. J. Rock. Mech. Min. Sci. Vol 3; pp. 181-189; 1966.

13. Deere, J.J. and Miller, R.P.; Engineering classification and index properties for intact rock; Air Force Weapons Laboratory, Technical Report No. AFWL-TR-65-116; 1966.

14. Dugal, J.J.; Unpublished notes on Sperry-Sun directional survey reports for drillholes URL-1, URL-2, URL-5, URL-6 and URL-7; Terrain Sciences Division, Geological Surveys of Canada, Ottawa; 1984.

15. Gyenge, M. and Herget, G; Pit slope manual supplement 3-2, laboratory tests for design parameters; CANMET Report 77-26, Energy, Mines and Resources Canada, Ottawa; p. 74; 1977.

16. Hauze, F.E.; Scale effects in the determination of rock mass strength and deformability; Rock Mech. 12; p. 167-192; 1980.

17. Hawkes, I., Mellor, M. and Gariepy, S.; Deformation of rocks under uniaxial tension; Int. J. Rock. Mech. Min. Sci. and Geomech. Abstr.; Vol 10; pp. 493-507; 1973.

18. Herget, G.; Regional stresses in the Canadian shield; CANMET, Mining Research Laboratories; Report MRP/MRL 80-8(OP), Energy, Mines and Resources Canada, Ottawa; 1980.

19. Huang, C. and Hunter, J.S.; The 1978 progress report on the Seismic and Downhole surveys at the Chalk River and Whiteshell Research Areas; Atomic Energy of Canada Limited Report TR-31; Pinawa, Manitoba, 1980.

20. Hoek, E. and Brown, E.T.; Underground excavation in rock; The Institution of Mining and Metallurgy, London; pp. 131-159; 1980.

21. Jackson, R.; The effect of oven drying specimens on uniaxial elastic properties; CANMET, Division Report ERP/MRL 83-16(TR); Energy, Mines and Resources Canada, Ottawa; 1983.

22. Jackson, R. and Boudreau, C.; Special ambient temperature mechanical properties studies to determine the effects of stress release on URL core samples; CANMET, Division Report ERP/MRL 84-17(TR); Energy, Mines and Resources Canada, Ottawa; 1983.

23. Jackson, R. and Paquette, D.; A summary of mechanical property test data on samples from borehole URL-7, URL-B9-1, 2, and 3, URL-B10-1, and URL-B26-1 at Lac du Bonnet, Manitoba; CANMET, Division Report ERP/MRL 84-31(INT); Energy, Mines and Resources Canada, Ottawa; 1984.

24. Jackson, R.; High temperature and pressure triaxial compression tests on samples from borehole URL-6; CANMET, Division Report ERP/MRL 84-22(TR); Energy, Mines and Resources Canada, Ottawa; 1984.

25. Jackson, R. and Annor, A.; The effects of water content on the uniaxial mechanical properties of WN1 core samples; CANMET, Division Report ERP/MRL 85-118(TR); Energy, Mines and Resources Canada, Ottawa; 1985a.

26. Jackson, R. and Annor, A.; Thermomechanical properties of rock samples from the Lac du Bonnet and the Eye Dashwa Lakes plutons; CANMET, Division Report ERP/MRL 85-42(TR); Energy, Mines and Resources Canada, Ottawa; 1985b.

27. Jackson, R., Annor, A., Wong, A.S. and Bétournay, M.; Preliminary results of rock joint testing on URL core; CANMET, Division Report ERP/MRL 85-14(TR), Energy, Mines and Resources Canada, Ottawa; 1985.

28. Jaeger, J.C. and Cook, N.G.W.; Fundamentals of rock mechanics; Chapman and Hall, London; pp. 585; 1976.

29. Kamineni, D.C., Dugal, J.J.B. and Ejeckam, R.B.; Geochemical investigation of granitic core samples from boreholes at the Underground Research Laboratory site, near Lac du Bonnet, Manitoba; Atomic Energy of Canada Limited; Whiteshell Nuclear Research Establishment, Pinawa, Manitoba; Report No. (TR-221); May 1984.

30. Larocque, G.E.; Memorandum on standard sample selection; Rock Mechanics Laboratory; CANMET, Energy, Mines and Resources Canada, Ottawa; 1978.

31. Larocque, G.E. and Annor, A.; Overview: rock mechanics/rock properties; CANMET, Mining Research Laboratories, Report ERP/MRL 84-10(OP,J); Energy, Mines and Resources Canada, Ottawa; 1984.

32. Lama, R.D. and Vutukuri, V.S.; Handbook on mechanical properties of rock; Trans. Tech. Publications; Vol. II; Appendix II; pp. 315-465; 1978.

33. McKay, D.A.; AECL core testing program, URL-1 series cores; Ontario Hydro Research; Division Report 82-431-K; 1982.

34. Michalopoulos, A.P. and Triandafilidis, G.E.; Influence of water on hardness, strength and compressibility of rock; Bull. Association of Eng. Geol.; Vol. XIII, No. 1; pp. 1-22; 1976.

35. Miller, R.P.; Engineering classification and index properties for intact rock; PhD. Thesis, Univ. Ill, Urbana, Ill.; 1965.

36. Obert, L., Windes, S.L. and Duval, W.I.; Standardized test for determining the physical properties of mine rock; US Bureau of Mines Report of Investigation 3891; 1946.

37. Price, N.J.; The compressive strength of coal measured rocks; Coll. Engineering; Vol. 37, pp. 283-292; 1960.

38. Wild, V.S. and McKittrick, D.P.; Northfield Mountain Underground Power Station Symposium Underground Rock Chambers, Arizona, Amer. Soc. Civil Engineers; pp. 287-331; 1971.

39. Wong, A.S.; Modal analyses of URL-01, URL-02, URL-05 and URL-06 extended engineering core samples from the underground research laboratory site near Lac du Bonnet, Manitoba; CANMET, Division Report ERP/MEL 84-27(TR), Energy, Mines and Resources Canada, Ottawa; 1984.

40. Wylie, M.R.J., Gregory, A.R. and Gardner, G.H.F.; An experimental investigation of factors affecting elastic wave velocities in porous media; Geophysics vol. 23, pp. 459-493; 1958.

Table 1 - Summary of uniaxial mechanical properties and compressive wave velocity data for borehole URL-1 samples

Specimen identification	Borehole characteristics: Vertical depth (m)	Borehole characteristics: Elevation (m)	Specimen characteristics: Length (mm)	Specimen characteristics: Diameter (mm)	Specimen characteristics: Bulk density (Mg/m^3)	Compressive strength (MPa)	Elastic modulus (GPa)	Poisson's ratio	Compressive wave velocity: Vo (at 0.1 MPa) (km/s)	Compressive wave velocity: Velocity at overburden pressure: σ_v (MPa)	Compressive wave velocity: Velocity at overburden pressure: V_p (km/s)	Rock type: Name	Rock type: Special features
URL-1- 46.40	45.84	246.5			2.65	229	77.1	0.24	5.67	1.19	5.65	Granite	light olive green coloration medium to slightly coarsed grained massive,
URL-1- 68.50	66.36	226.0			2.65	186	82.2	0.25	6.06	1.73	6.07		
URL-1-100.60	97.10	195.3			2.69	248	86.0	0.29	5.68	2.56	5.62	Granite	medium to slightly coarse grained light olive green coloration
URL-1--177.10	170.37	122.0			2.61	200	83.4	0.27	5.18	4.36	5.31	Granite	massive equigranular medium to coarse grained
URL-1-177.40	170.67	121.7	97.0	44.3	2.63	184	69.7	0.25	4.90	4.40	5.06	Mafic Tonalite	weakly-foliated medium to coarse grained
URL-1-184.68+	177.95	114.4	95.9	44.8	2.62	192	70.9	0.27	5.06	4.57	5.14	Pink granite	massive and porphyritic

Table 1 - (Cont'd)

Specimen identification	Borehole characteristics		Specimen characteristics						Compressive wave velocity			Rock type	
	Vertical depth (m)	Elevation (m)	Length (mm)	Diameter (mm)	Bulk density (Mg/m^3)	Compressive strength (MPa)	Elastic modulus (GPa)	Poisson's ratio	Vo (at 0.1 MPa) (km/s)	Velocity at overburden pressure σ_v (MPa)	Velocity at overburden pressure V_p (km/s)	Name	Special features
URL-1-191.38+	184.65	107.7	96.7	44.8	2.62	176	71.4	0.25	5.17	4.75	5.28	Pink granite	massive medium to coarse grained, porphyritic
URL-1-230.50	221.12	71.3			2.61	189	84.9	0.23	5.26	5.66	5.35	Pink granite	massive slightly porphyritic
URL-1-254.30	244.92	47.5			2.62	197	75.0	0.26	4.51	6.29	4.71	Grey granite	massive inequigranular medium grained
URL-1-282.68++	272.35	20.0	94.4	44.8	2.63	203	70.9	0.19	4.57	7.03	4.73	Grey granite	massive light olive green coloration
URL-1-292.90++	280.53	11.9	92.8	44.6	2.65	160	65.8	0.22	4.85	7.29	5.01	Pink granite	massive and porphyritic
URL-1-299.90++	287.53	4.9	96.7	44.9	2.62	177	65.8	0.24	4.51	7.39	4.63	Pink granite	massive medium to coarse grained, porpyrite
URL-1-302.40++	290.03	2.4	96.7	44.9	2.63	208	74.5	0.25	4.74	7.48	5.08	Pink granite Grey granite	massive slightly porphyritic massive inequigranular medium grained

Table 1 - (Cont'd)

Specimen identification	Borehole characteristics		Specimen characteristics			Compressive strength (MPa)	Elastic modulus (GPa)	Poisson's ratio	Compressive wave velocity			Rock type	
	Vertical depth (m)	Elevation (m)	Length (mm)	Diameter (mm)	Bulk density (Mg/m^3)				Vo (at 0.1 MPa) (km/s)	Velocity at overburden pressure			
										σ_v (MPa)	V_p (km/s)	Name	Special features
URL-1-397.80++	397.80	-87.4			2.66	155	61.4	0.26	4.32	10.38	4.78	Grey granite	massive light olive green coloration
URL-1-443.20	422.68	-130.3			2.61	146	68.6	0.30	2.87	10.82	4.19		
URL-1-496.70	472.14	-179.8			2.64	154	64.61	0.31	3.47	12.23	4.34		
URL-1-527.40	501.14	-208.8			2.64	180	66.4	0.32	3.57	12.98	4.47		
URL-1-592.60	561.46	-269.1			2.64	167	64.4	0.30	3.38	15.54	4.70		
URL-1-615.90	582.69	-290.3			2.65	181	62.4	0.32	3.75	15.15	4.66		
URL-1-662.40	635.67				2.66	166	63.6	0.36	3.61	16.59	4.90		

+Compiled from basic test data provided by Ontario Hydro (McKay, 1982).

++Data were compiled from URL-extended engineering studies (Jackson, 1982, 1983).

*Elevations are with reference to mean sea level.

Table 2 - Summary of uniaxial mechanical properties and compressive wave velocity data for borehole URL-2 samples

Specimen identification	Borehole characteristics		Specimen characteristics			Compressive strength (MPa)	Elastic modulus (GPa)	Poisson's ratio	Compressive wave velocity			Rock type
	Vertical depth (m)	Elevation* (m)	Length (mm)	Diameter (mm)	Bulk density (Mg/m^3)				Vo (at 0.1 MPa) (km/s)	Velocity at overburden pressure σ_v (MPa)	Velocity at overburden pressure V_p (km/s)	Special features
URL-2-256.0	247.06	33.9	97.5	45.0	2.63	203	64.9	0.25	3.84	6.37	4.21	
URL-2-448.1	430.32	-149.4	96.7	44.9	2.64	179	53.5	0.22	3.70	11.14	4.34	
URL-2-586.0	559.82	-278.9	97.3	44.9	2.62	181	53.6	0.26	3.16	14.39	4.40	
URL-2-705.70	668.89	-388.0	94.2	44.9	2.63	152	56.2	0.23	3.49	17.26	4.69	
URL-2-798.6	752.73	-471.8	97.3	45.1	2.64	158	58.5	0.13	3.66	19.49	4.95	
URL-2-871.5	815.63	-534.7	97.3	44.9	2.63	163	53.8	0.29	3.45	21.04	4.55	medium to coarse grained inequigranular
URL-2-1001.2	929.83	-648.9	97.0	45.0	2.63	156	51.0	0.25	2.82	23.99	4.37	
URL-2-1094.8	1000.26	-719.3	98.2	45.0	2.63	172	55.9	0.30	1.91	25.81	4.58	

*Elevations are with reference to mean sea level.

Table 3 - Summary of uniaxial mechanical properties and compressive wave velocity data for URL-5 samples

Specimen identification	Borehole characteristics		Specimen characteristics			Compressive strength (MPa)	Elastic modulus (GPa)	Poisson's ratio	Compressive wave velocity			Rock type	
	Vertical depth (m)	Elevation* (m)	Length (mm)	Diameter (mm)	Bulk density (Mg/m^3)				Vo (at 0.1 MPa) (km/s)	Velocity at overburden pressure σ_v (MPa)	Velocity at overburden pressure V_p (km/s)	Name	Special features
URL-5- 16.40	16.17	27.16	98.6	44.9	2.62	219	73.0	0.27	5.07	0.42	5.10	Pink granite	
URL-5- 76.90	74.69	213.0	97.1	45.0	2.65	230	71.9	0.22	5.67	1.94	5.68	Pink granite	
URL-5-108.30	104.60	183.1	96.8	44.9	2.59	199	72.5	0.38	5.14	2.66	5.30	Pink granite	
URL-5-126.60	122.66	165.1	95.6	45.0	2.64	175	70.4	0.18	5.05	3.18	5.15	Pink granite	
URL-5-127.99	124.05	163.7	97.3	45.0	2.63	196	71.4	0.29	4.87			Pink granite	
URL-5-133.00	128.81	158.9	96.8	45.0	2.64	221	80.0	0.30	5.00			Pink granite	
URL-5-138.63	134.44	153.33	97.0	44.8	2.62	189	69.9	0.32	4.79			Pink granite	
URL-5-157.20	152.76	135.0	96.2	44.8	2.59	180	71.4	0.26	4.97	3.88	5.12	Pink granite	
URL-5-199.10	192.87	94.9	98.1	44.8	2.63	191	73.5	0.31	5.09	4.98	5.25	Pink granite	
URL-5-246.50	238.45	49.3	97.6	44.9	2.63	226	69.0	0.25	5.45	6.15	5.50	Pink granodiorite	
URL-5-274.51	265.89	21.8	95.6	45.1	2.64	180	53.1	0.22	4.03			Grey granodiorite	
URL-5-277.57	268.95	18.8	96.9	45.0	2.62	193	64.9	0.26	3.95			Grey granodiorite	
URL-5-281.63	271.71	16.0	96.1	45.0	2.62	191	61.4	0.24	4.08			Grey granodiorite	

Table 3 - (Cont'd)

Specimen identification	Borehole characteristics		Specimen characteristics			Compressive strength (MPa)	Elastic modulus (GPa)	Poisson's ratio	Compressive wave velocity			Rock type	
	Vertical depth (m)	Elevation[a] (m)	Length (mm)	Diameter (mm)	Bulk density (Mg/m^3)				Vo (at 0.1 MPa) (km/s)	Velocity at overburden pressure σ_v (MPa)	Velocity at overburden pressure V_p (km/s)	Name	Special features
URL-5-289.70	279.78	8.0	94.9	45.0	2.63	197	66.2	0.25	4.07	7.22	4.51	Grey granodiorite	
URL-5-334.00	323.12	-35.4	96.9	44.6	2.68	130	58.8	0.25	4.40	8.50	4.68	Grey granodiorite	
URL-5-370.00	357.45	-69.7	97.4	45.1	2.63	176	56.2	0.25	3.77	9.22	4.32	Grey granite	
URL-5-450.90	434.86	-147.1	97.0	45.2	2.65	163	54.1	0.37	3.48	11.30	4.07	Grey granite	
URL-5-496.80	478.95	-191.2	97.1	44.7	2.65	186	53.1	0.27	3.52	12.45	4.16	Grey granite	

[a]Elevations are with reference to mean sea level.

Table 4 - Summary of uniaxial mechanical properties and compressive wave velocity data for boreholes URL-2, URL-5 and URL-6 "deep" samples

Specimen identification	Borehole characteristics		Specimen characteristics			Compressive strength	Elastic modulus	Poisson's ratio	Compressive wave velocity			Rock type	
									Vo	Velocity at overburden pressure			
	Vertical depth (m)	Elevation* (m)	Length (mm)	Diameter (mm)	Bulk density (Mg/m^3)	(MPa)	(GPa)		(at 0.1 MPa) (km/s)	σ_v (MPa)	V_p (km/s)	Name	Special features
URL-2-1080.32	991.0	-710.0	96.44	45.08	2.618	198.42	51.58	0.30	2.53	25.0	5.24	Granite grey	
URL-2-1080.55	991.2	-710.3	96.02	45.03	2.627	189.04	51.82	0.22	2.45	-	-	Granite grey	
URL-2-1080.83	991.5	-710.6	94.90	45.03	2.629	163.26	51.90	0.40	2.52	25.0	4.99	Granite grey	
URL-2-1081.06	991.7	-710.8	95.92	45.03	2.625	166.40	52.54	0.30	2.48	-	-	Granite grey	
URL-2-1081.67	992.2	-711.3	95.80	45.03	2.632	178.33	54.26	0.34	2.62	-	-	Granite grey	
URL-2-1081.90	992.4	-711.5	97.30	45.06	2.628	162.41	51.78	0.36	2.86	25.0	5.80	Granite grey	
URL-2-1082.21	992.7	-711.8	96.30	45.03	2.632	160.12	51.99	0.43	2.88	-	-	Granite grey	
URL-2-1082.44	992.9	-712.0	96.52	45.04	2.623	180.13	46.62	0.35	2.71	25.0	4.76	Granite grey	
URL-5-441.75	426.0	-138.3	94.46	45.15	2.655	226.73	56.06	0.31	3.70	15.0	5.01	Granite grey	
URL-5-441.98	426.3	-138.6	95.44	45.13	2.659	186.29	52.90	0.30	3.57	-	-	Granite grey	
URL-5-442.26	426.5	-138.8	96.20	45.15	2.651	223.60	56.69	0.27	3.64	-	-	Granite grey	
URL-5-442.54	426.8	-139.1	95.11	45.15	2.652	199.87	56.63	0.29	3.83	15.0	4.09	Granite grey	
URL-6-373.80	373.8	-83.7	97.63	45.03	2.634	180.84	59.20	0.39	3.73	10.0	4.80	Granite grey	
URL-6-374.70	374.7	-84.6	97.57	45.05	2.631	170.02	61.73	0.31	3.84	10.0	4.65	Granite grey	

Table 4 (Cont'd)

Specimen identification	Borehole characteristics: Vertical depth (m)	Borehole characteristics: Elevation* (m)	Specimen characteristics: Length (mm)	Specimen characteristics: Diameter (mm)	Specimen characteristics: Bulk density (Mg/m^3)	Compressive strength (MPa)	Elastic modulus (GPa)	Poisson's ratio	Compressive wave velocity: Vo (at 0.1 MPa) (km/s)	Compressive wave velocity: Velocity at overburden pressure: σ_v (MPa)	Compressive wave velocity: Velocity at overburden pressure: V_p (km/s)	Rock type: Name	Rock type: Special features
URL-6-374.98	375.0	-84.9	96.12	45.04	2.633	203.98	58.54	0.33	3.76	-	-	Granite grey	
URL-6-391.38	391.4	-101.3	95.30	45.02	2.625	196.63	55.52	0.32	3.71	10.0	4.67	Granite grey	
URL-6-391.61	391.6	-101.5	95.29	45.01	2.648	170.32	56.58	0.29	3.55	-	-	Granite grey	
URL-6-391.89	391.9	-101.8	97.65	44.98	2.630	183.13	56.44	0.31	3.73	10.0	4.48	Granite grey	
URL-6-392.17	392.2	-102.1	96.14	45.00	2.598	147.76	58.23	0.30	3.47	-	-	Granite grey	

*Elevations are with reference to mean sea level.

Table 5 - Summary of test data on the effects of specimen conditioning on uniaxial compression test results

Table 5(a) - Summary of uniaxial mechanical properties of surface air dried and oven dried URL-specimens

Specimen identification	Borehole characteristics: Vertical depth (m)	Borehole characteristics: Elevation* (m)	Specimen characteristics: Length (mm)	Specimen characteristics: Diameter (mm)	Specimen characteristics: Bulk density (Mg/m^3)	Compressive strength (MPa)	Elastic modulus (GPa)	Poisson's ratio	Rock type: Color	Rock type: Name	Rock type: Special features
URL-1-283.80	273.36	19.02	97.6	44.8	2.63	192	60.2	0.19	Grey	Granite	surface air dried prior to testing
URL-1-283.90	273.46	18.92	94.9	44.9	2.63	187	60.2	0.23	Grey	Granite	oven dried to 80°C prior to testing
URL-5-129.30	125.30	162.43	97.1	45.0	2.63	200	66.2	0.30	Pink	Granite	surface air dried prior to testing
URL-5-129.40	125.40	162.33	97.7	45.0	2.63	198	66.7	0.24	Pink	Granite	oven dried to 80°C prior to testing
URL-5-134.80	131.03	156.70	95.0	45.0	2.63	190	67.1	0.23	Pink	Granite	air dried prior to testing
URL-5-134.90	131.13	156.60	96.2	45.0	2.63	203	63.7	0.25	Pink	Granite	oven dried to 80°C prior to testing

*Elevations are with reference to sea level.

Table 5(b) - Summary of uniaxial mechanical properties of surface air dried WN-1 specimens

Specimen identification	Length (mm)	Diameter (mm)	Bulk Density (Mg/m^3)	Uniaxial compressive strength (MPa)	Tangent modulus (GPa)	Poissons's ratio	Zero pressure wave velocity (km/s) B.C.	Zero pressure wave velocity (km/s) A.C.	dynamic modulus A.C.
WW1-74.03	107.67	44.72	2.63	209	67.54	0.28	4.77	4.77	61.27
WW1-74.25	108.76	44.74	2.54	180	62.70	0.30	4.60	4.60	53.94
WW1-74.76	107.53	44.76	2.63	176	62.64	0.44	4.70	4.70	50.96
WW1-75.05	105.01	44.76	2.76	199	64.67	0.20	4.71	4.71	61.78
WW1-75.27	108.39	44.76	2.63	190	68.58	0.25	4.95	4.95	68.64
WW1-76.03	108.66	44.76	2.63	197	70.37	0.24	4.74	4.74	60.37
WW1-76.25	103.33	44.78	2.62	208	68.28	0.24	4.63	4.63	60.54
WW1-76.63	108.60	44.78	2.62	218	71.02	0.26	4.91	4.91	66.72
WW1-76.74	104.13	44.78	2.62	208	81.16	0.37	4.90	4.90	65.58
WW1-78.00	108.89	44.78	2.63	05	71.39	0.23	4.90	4.81	65.96
WW1-78.11	103.21	44.78	2.64	206	71.39	0.23	4.81	4.81	65.96
WW1-79.41	103.21	44.78	2.62	199	71.80	0.30	4.60	4.60	58.86

Table 5(c) - Summary of uniaxial mechanical properties of oven dried WN-1 specimens

Specimen identification	Length (mm)	Diameter (mm)	Bulk Density (Mg/m^3)	Uniaxial compressive strength (MPa)	Tangent modulus (GPa)	Poissons's ratio	Zero pressure wave velocity (km/s) B.C.	Zero pressure wave velocity (km/s) A.C.	dynamic modulus A.C.
WW1-74.36	108.11	44.77	2.61	175	67.21	0.28	4.70	4.47	50.03
WW1-76.36	107.97	44.81	2.61	216	67.71	0.18	5.00	4.89	67.39
WW1-77.30	107.05	44.78	2.63	201	75.63	0.28	5.34	4.97	67.29
WW1-78.69	108.49	44.79	2.62	190	68.22	0.28	4.91	4.75	59.91
WW1-335.54	108.29	45.02	2.62	212	62.79	0.29	4.63	4.60	53.66
WW1-335.76	107.99	45.02	2.62	201	66.79	0.28	4.73	4.66	57.12
WW1-335.76	107.98	45.02	2.62	211	65.60	0.24	4.73	4.59	54.26
WW1-335.98	108.56	45.02	2.62	181	63.00	0.18	4.68	4.65	57.58
WW1-336.09	108.51	45.01	2.62	199	64.32	0.24	4.66	4.62	55.33

Table 5(d) - Summary of uniaxial mechanical properties of water saturated WN-1 specimens

Specimen identification	Length (mm)	Diameter (mm)	Bulk Density (Mg/m^3)	Uniaxial compressive strength (MPa)	Tangent modulus (GPa)	Poissons's ratio	Zero pressure wave velocity (km/s) B.C.	Zero pressure wave velocity (km/s) A.C.	dynamic modulus A.C.
WW1-74.14	105.40	44.74	2.62	188	61.99	0.26	N/A	5.91	119.84
WW1-74.54	107.64	44.74	2.63	190	74.50	0.27	N/A	6.06	125.99
WW1-74.65	104.23	44.72	2.63	178	73.37	0.36	N/A	6.16	131.93
WW1-75.16	104.40	44.76	2.63	172	71.95	0.27	N/A	5.86	117.28
WW1-76.85	105.48	44.79	2.62	218	72.66	0.29	N/A	5.92	118.57
WW1-78.22	109.01	44.77	2.63	213	75.26	0.28	N/A	6.11	126.55
WW1-78.36	105.34	44.79	2.62	216	67.37	0.25	N/A	5.93	121.35
WW1-78.47	105.27	44.79	2.62	210	71.26	0.28	4.70	5.97	121.72
WW1-79.30	103.23	44.74	2.62	184	73.68	0.28	N/A	5.79	114.18
WW1-79.52	103.21	44.68	2.62	215	70.40	0.26	N/A	5.88	120.49

Table 5(e) - Statistical distribution of uniaxial mechanical properties for conditioned WN-1 specimens

Mechanical properties		Initial conditioning: Oven dried	Surface air dried	Saturated
Compressive Wave Velocity (km/sec)	Mean	4.69	4.79	5.96
	Std dev	0.16	0.17	0.12
Dynamic Modulus (GPa)	Mean	58.06	61.89	121.79
	Std dev	5.93	5.38	5.14
Poisson's ratio	Mean	0.25	0.28	0.28
	Std dev	0.04	0.07	0.03
Uniaxial Compressive strength (MPa)	Mean	198	200	198
	Std dev	14	12	18
Tangent Young's Modulus (GPa)	Mean	66.81	69.29	71.24
	Std dev	3.59	5.00	3.96

Table 6 - Summary of Brazilian tensile strength test data for borehole URL-2 "deep" samples

	Borehole characteristics		Specimen characteristics				
Specimen identification	Vertical depth (m)	*Elevation (m)	Length (mm)	Diameter (mm)	Bulk density (Mg/m^3)	Tensile strength (MPa)	Test Orientation
URL-2-1080.29	991.0		23.56	45.06	2.62	6.79	⊕
URL-2-1080.29			20.92	45.04	2.61	6.94	⊖
URL-2-1080.78			23.28	45.03	2.62	7.12	⊕
URL-2-1080.80	991.4		23.22	45.03	2.63	6.63	⊖
URL-2-1081.64			22.97	45.03	2.62	7.46	⊕
URL-2-1082.17			21.87	45.02	2.62	7.69	⊕
URL-2-1082.19	992.7		22.84	45.03	2.63	6.22	⊖

*Elevation measurements are with reference to mean sea level.

Table - 6 (Cont'd)

Specimen identification	Borehole characteristics: Vertical depth (m)	Borehole characteristics: *Elevation (m)	Specimen characteristics: Length (mm)	Specimen characteristics: Diameter (mm)	Specimen characteristics: Bulk density (Mg/m^3)	Specimen characteristics: Tensile strength (MPa)	Specimen characteristics: Test Orientation
URL-5-441.70	426.0		23.02	45.17	2.65	9.31	⦶
URL-5-441.73			22.91	45.17	2.65	9.87	⊖
URL-5-442.08			24.16	45.16	2.65	9.97	⦶
URL-5-442.10	426.4		20.92	45.16	2.64	8.75	⊖
URL-5-442.49			22.98	45.15	2.64	10.51	⦶
URL-5-445.51			22.90	45.15	2.65	9.95	⊖
URL-5-442.77			22.42	45.17	2.65	10.10	⊖
URL-5-442.80	427.1		24.08	46.16	2.66	9.46	⦶

*Elevation measurements are with reference to mean sea level.

Table - 6 (Cont'd)

Specimen identification	Borehole characteristics: Vertical depth (m)	Borehole characteristics: *Elevation (m)	Specimen characteristics: Length (mm)	Specimen characteristics: Diameter (mm)	Specimen characteristics: Bulk density (Mg/m^3)	Specimen characteristics: Tensile strength (MPa)	Test Orientation
URL-6-374.46	374.46		22.92	45.07	2.63	8.71	⊖
URL-6-374.48			22.63	45.06	2.63	8.66	⊕
URL-6-374.80			21.27	45.07	2.62	8.46	⊕
URL-6-374.82			21.99	45.07	2.62	8.39	⊖
URL-6-391.60			22.96	45.04	2.63	5.96	⊕
URL-6-391.84			22.07	45.00	2.63	7.82	⊕
URL-6-391.87	391.9		22.19	44.98	2.63	7.80	⊖

*Elevation measurements are with reference to mean sea level.

Table 7 - Statistical summary of mechanical properties data for Lac du Bonnet granitic samples on the basis of engineering sub-divisions (URL lease area)

Borehole identification	Zone (m)	Principal rock type(s)	Ave. length (mm)	Ave. diameter (mm)	Ave. density (Mg/m^3)		Compressive strength (MPa)	Tangent modulus (E) (GPa)	Poisson's ratio	P-wave velocity at 0.1 MPa km/sec	Brazilian tensile strength (MPa)
						No. of values	6	6	6	6	
			(N=5)	(N=5)	(N=6)	Range	134 to 229	53.6 to 77.1	0.24 to 0.29	4.34 to 5.67	
URL-1, 5 B9,	0-50		98.6	46.8	2.63	Mean	189	66.4	0.27	5.05	
						Standard Deviation	34	8.1	0.02	0.56	
						No. of values	27	27	27	27	24
			(N=22)	(N=46)	(N=51)	Range	175 to 248	64.7 to 86.0	0.18 to 0.38	3.84 to 6.06	7.41 to 12.07
URL-1, 2, 5 7	51-260		98.2	44.8	2.63	Mean	201	72.2	0.26	5.14	9.86
						Standard Deviation	20	6.0	0.04	0.45	1.08
						No of values	44	44	44	44	30
			(N=38)	(N=68)	(N=79)	Range	130 to 227	46.6 to 74.5	0.13 to 0.43	1.91 to 4.85	5.96 to 10.51
URL-1, 2, 5 6	below 260		93.9	45.0	2.63	Mean	177	57.0	0.29	3.53	8.23
						Standard Deviation	20	10.4	0.06	0.66	1.25

Table 8 - Statistical summary of mechanical properties data for Lac du Bonnet granitic samples (WNRE-site)

Borehole identification	Zone vertical depth (m)	Principal rock type(s)	No. of specimens tested	Ave. length (mm)	Ave. diameter (mm)	Ave. density (Mg/m^3)		Compressive strength (MPa)	Tangent modulus (E) (GPa)	Poisson's ratio	P-wave velocity at 0.1 MPa km/sec	Brazilian tensile strength (MPa)
							No. of values	18	18	18	18	17
WN-4	389.8-830.1	Grey granite	18				Range	95 to 211	27.4 to 79.0	0.20 to 0.39	2.5 to 4.4	8.6 to 13.0
							Mean	173	66.7	0.275	3.5	11.1
							Standard Deviation	19	5.9	0.05	0.6	1.1
							No. of values	14	14	14	14	14
WN-1,2	23.9-438.2	Pink granite	14	97.8	44.7	2.67	Range	191 to 235	64.0 to 74.0	0.20 to 0.29	4.34 to 5.0	7.5 to 10.0
							Mean	220	69.0	0.24	4.89	8.9
							Standard Deviation	12	2.4	0.03	0.2	0.9
							No. of values	2	2	2		-
WN-2	53.5- 82.2	Tonalite	2	99.3	44.7	2.74	Range	159 to 173	73 to 74	0.21 to 0.23	5.1 to 5.4	-
							Mean	166	74.0	0.22	5.2	-
							Standard Deviation	10	7.1	0.01	0.2	

*Not applicable to Brazilian tensile strength specimens (after Annor, 1984).

Table 9 - Statistical Summary of uniaxial strength deformation and acoustic wave velocity data for Lac du Bonnet granitic samples (combined URL and WNRE sites)

Borehole identification	Principal rock type		Density (Mg/m^3)	Uniaxial compressive strength (MPa)	Tangent Young's modulus (GPa)	Poisson's ratio	P-wave velocity at 0.1 (MPa) (km/s)	Brazilian tensile strength (MPa)
Pinawa WN-1, 2, & 4 + URL-1, 2, 5&6 (combined) Boreholes	granite	No. of values	156	156	156	156	146	79
		Range	2.54 to 2.75	130 to 248	46.6 to 86.0	0.13 to 0.44	2.45 to 6.06	5.96 to 12.99
WN-1,2 & 4 URL-1,2,5 6,7 & BH-07		Mean	2.63	192	66.0	0.27	4.32	9.45
		St. Dev.	0.02	23	7.5	0.05	0.86	1.59
(WN-1,2, & 4) URL-1,2,5,6 & 7 URL-1,2,5 BH-09 Boreholes	Pink granite	No. of values	101	101	101	101	91	39
		Range	2.54 to 2.75	159 to 248	58.1 to 86.0	0.18 to 0.44	3.84 to 6.06	6.17 to 12.99
		Mean	2.63	200	69.2	0.26	4.87	9.32
		St. Dev.	0.02	19	5.4	0.04	0.41	1.26
WN-1,2, & 4 & 7 URL-1,2,5 6 & 7	Grey granite	No. of values	55	55	55	55	55	40
		Range	2.60 to 2.66	130 to 231	46.6 to 78.7	0.13 to 0.43	2.45 to 4.80	5.96 to 12.99
		Mean	2.64	176	60.1	0.29	3.41	9.58
		St. Dev.	0.01	21	7.2	0.06	0.57	1.87

Table 10 - Summary of literature-referenced uniaxial mechanical properties data for granitic rocks

	Location and granitic rock description	Density (Mg/m^3)	Uniaxial compressive strength Qu (MPa)	Modulus of elasticity E (GPa)	Poisson's ratio ν	Tensile strength σt (MPa)	Reference
1	U.S.A. Md., contains quartz and syenite	2.65	250.97	52.54	-	20.68 (R)	Wuerker, 1956
2	U.S.A. Pikes Peak, dense, mg	2.64	226.0	70.6	0.18	11.9	Miller, 1965
3	U.S.A. Barre, Vt, and syenite	2.64	194.4	61.4	0.39	10.7	Miller, 1965
4	U.S.A. Rose Granite Pedernal Hills, N.M.	2.64	308.0	69.64	0.28	-	Michalopoulos and Triandafilidis, 1976
5	U.aS.A. Raymond, Calf. Raymond granite	2.64	178.0	58.6	0.26	-	Michalopoulos & Triandafilidis, 1976
6	Canada, Grenville Que, Cg, 80% orthoclase	2.61	172.0	65.8	-	-	Coates & Parsons, 1966
7	U.S.A., Barre, Vt. Perpendicular to bedding	2.64	200.0	58.6	-	13.5	Hawkes et al. 1973
8	U.S.A., Mg-Cg (a)	2.66	228.91	30.4*	0.04*	19.99	Obert et al. 1946
	(b)	2.66	225.15	27.4*	0.10	25.37 (R)	
	(c)	2.66	244.07	44.2*	0.31*	18.41 (R)	
9	Atikokan granite Mean	2.65	212	73.9	0.26	-	Annor and Jackson, 1982
	(N=50 samples) Std. Dev.	0.02	26	15.2	0.05		

Numbers 1-8 were compiled and condensed from : Lama and Vutukuri (1978).

* Dynamic test values.

R - refers to test in bending.

Table 11 - Summary of triaxial compression test data for Lac du Bonnet Granitic Samples (URL-site)

Specimen identification	Length (mm)	Diameter (mm)	Density (Mg/m^3)	Confining pressure (MPa)	Temperature (°C)	Triaxial strength (MPa)	Young's modulus (GPa)
URL 1 179.82	121.18	44.72	2.64	3.5	21	272	65.79
URL 1 189.62	122.66	44.86	2.64	3.5	21	276	70.00
URL 5 127.62	121.84	44.45	2.64	3.5	21	285	67.94
URL 5 136.90	121.39	44.68	N/A	3.5	21	299	71.30
URL 6 224.50	117.65	44.50	2.65	3.5	21	280	68.87
URL 6 256.67	116.05	44.79	2.62	3.5	21	302	68.08
URL 7 132.00	118.07	44.51	2.68	3.5	21	315	70.66
URL 7 188.20	119.82	44.84	2.65	3.5	21	264	68.33
URL 6 374.22	125.50	44.28	2.63	5.0	21	303	56.59
URL 6 392.04	126.50	44.51	2.63	5.0	21	288	63.28
URL 1 179.70	114.74	44.76	2.64	10.0	21	344	67.03
URL 1 189.23	115.23	44.50	2.64	10.0	21	363	67.61
URL 2 1080.14	125.49	44.79	2.63	10.0	21	345	60.16
URL 2 1081.77	125.55	44.66	2.63	10.0	21	356	60.55
URL 5 128.46	115.00	44.30	2.65	10.0	21	371	70.99
URL 5 137.15	121.52	44.68	2.63	10.0	21	365	67.06
URL 6 224.62	115.10	44.80	2.65	10.0	21	384	68.26
URL 6 257.60	117.28	44.55	2.62	10.0	21	364	70.86
URL 6 373.69	118.03	44.55	2.63	10.0	21	344	66.32
URL 6 391.25	124.16	44.62	2.63	10.0	21	361	65.42
URL 7 144.00	118.02	44.41	2.63	10.0	21	383	69.75
URL 7 174.42	115.95	44.47	2.63	10.0	21	376	68.33
URL 5 442.13	126.59	44.64	2.66	15.0	21	419	58.67
URL 5 442.94	118.31	44.42	2.66	15.0	21	367	59.34
URL 1 179.45	119.80	44.76	2.64	17.0	21	429	69.42
URL 1 189.49	121.84	44.68	2.64	17.0	21	405	64.93
URL 5 127.74	122.54	44.68	2.62	17.0	21	436	71.11
URL 5 136.69	122.94	44.65	2.64	17.0	21	435	72.00
URL 6 224.74	114.72	44.80	2.65	17.0	21	435	66.63
URL 6 257.72	115.42	44.52	2.63	17.0	21	434	68.69

Table 11 - (Cont'd)

Specimen identification	Length (mm)	Diameter (mm)	Density (Mg/m^3)	Confining pressure (MPa)	Temperature (°C)	Triaxial strength (MPa)	Elastic modulus (GPa)
URL 6 391.48	124.38	44.58	2.63	25.0	21	488	68.87
URL 6 391.71	122.61	44.49	2.63	25.0	21	488	63.36
URL 1 179.58	121.86	44.88	2.672	26.0	21	516	67.33
URL 1 179.95	121.18	44.78	2.64	26.0	21	479	69.33
URL 5 128.33	115.24	44.53	2.65	26.0	21	506	66.41
URL 5 137.28	122.96	44.68	2.63	26.0	21	505	64.88
URL 6 225.50	118.05	44.77	2.64	26.0	21	507	64.86
URL 6 257.84	113.07	44.51	2.64	26.0	21	513	66.21
URL 7 150.26	119.34	44.45	2.59	26.0	21	506	66.31
URL 7 166.55	119.75	44.55	2.63	26.0	21	543	69.16
URL 5 441.85	125.59	44.53	2.66	30.0	21	534	60.99
URL 5 442.64	125.63	44.64	2.66	30.0	21	539	61.25
URL 1 180.20	123.14	44.74	2.63	35.0	21	534	71.03
URL 1 189.20	120.12	44.72	2.63	35.0	21	563	69.26
URL 2 1080.41	12[illegible]	44.61	2.63	35.0	21	601	65.44
URL 2 1081.49	1[illegible]	44.67	2.63	35.0	21	532	67.04
URL 5 128.20	11	44.45	2.63	35.0	21	562	69.41
URL 5 137.02	121.72	44.68	2.64	35.0	21	534	65.54
URL 6 224.90	118.21	44.81	2.65	35.0	21	552	69.46
URL 6 258.08	118.63	44.52	2.63	35.0	21	551	70.10
URL 7 134.16	117.94	44.94	2.63	35.0	21	611	69.02
URL 7 181.00	119.20	44.46	2.64	35.0	21	558	69.18
URL B4 9.75	117.95	44.08	2.64	35.0	21	606	70.01
URL B26 5.00	115.87	44.68	2.63	35.0	21	576	76.20
URL 2 1080.93	126.64	44.49	2.62	50	21	674	67.46
URL 2 1082.31	125.60	44.63	2.64	50	21	636	64.57
URl 2 1080.63*	120.75	44.52	2.63	50	21	651	66.74
URL 2 1082.03*	124.60	44.69	2.63	50	21	638	64.11
URL 6 374.85	124.76	44.47	2.65	50	21	597	69.21
URL 6 392.27	125.79	44.73	2.63	50	21	629	68.52

Table 11 - (Cont'd)

Specimen identification	Length (mm)	Diameter (mm)	Density (Mg/m^3)	Confining pressure (MPa)	Temperature (°C)	Triaxial strength (MPa)	Elastic modulus (GPa)
URL 5 441.57	122.05	44.63	2.66	55	21	317**	62.94
URL 5 442.36	125.61	44.64	2.66	55	21	708	63.80
URL 2 1080.63	120.75	44.52	2.63	70	21	727†	66.71
URL 2 1082.03	124.60	44.69	2.63	70	21	713†	66.27

*Samples were previously cycled at σ_3 = 70.0 MPa.

**Failure occurred along a pre-existing fracture plane.

†Triaxial strengths were estimated using failure strength determined at σ_3 = 50 MPa.

Table 12 - Summary of triaxial compression test data for Lac du Bonnet granitic samples (WNRE-site)*

Specimen identification	Length (mm)	Diameter (mm)	Density (Mg/m^3)	Confining pressure (MPa)	Temperature (°C)	Triaxial strength (MPa)	Elastic modulus (GPa)
WN 1 323.93	N/A	44.93	N/A	3.5	21	283	71.02
WN 1 324.75	N/A	44.69	N/A	3.5	21	241	68.33
WN 1 169.70	111.29	44.56	2.65	3.5	21	273	53.10
WN 1 323.82	N/A	44.91	N/A	17.0	21	459	74.88
WN 1 324.16	N/A	44.93	N/A	17.0	21	445	66.40
WN 1 169.24	111.29	44.56	2.65	17.0	21	492	56.89
WN 1 323.70	N/A	44.93	N/A	35.0	21	552	68.74
WN 1 324.06	N/A	44.96	N/A	35.0	21	558	64.26
WN 1 169.8	111.30	44.45	N/A	35.0	21	609	60.55
WN 1 169.48	111.11	44.45	N/A	35.0	21	545	60.28

*Compiles from Annor et al. (1981)

Table 13 - *Summary of triaxial compression test data for Atikokan granitic samples

Specimen identification	Length (mm)	Diameter (mm)	Density (Mg/m^3)	Confining pressure (MPa)	Temperature (°C)	Triaxial strength (MPa)	Elastic modulus (GPa)
ATK 1 660.54	125.78	44.37	2.68	3.5	21	262	53.19
ATK 1 660.80	128.80	44.40	2.65	3.5	21	266	44.90
ATK 1 660.93	129.10	44.54	2.65	17.0	21	422	64.74
ATK 1 661.06	128.32	44.37	2.65	17.0	21	427	60.00
ATK 1 661.19	129.24	44.63	2.64	35.0	21	541	65.48
ATK 1 661.45	129.08	44.53	2.65	35.0	21	538	62.13

*Compiled from Jackson (1984).

Table 14 - Analysis of rock fracture data (based on Hoek and Brown, 1980)

Rock type	Number of samples N	Mean uniaxial compressive strength (σ_c) MPa	m	s	r	Comments
Lac du Bonnet granite (combined URL and WNRE samples)	250	232	29.85	1.00	0.933	Includes pink and grey samples (unheated)
Lac du Bonnet granite (combined URL and WNRE Pink coloured samples)	91	241	31.17	1.00	0.965	Pink samples (unheated)
Lac du Bonnet granite (combined URL and WNRE grey coloured samples	174	222	30.54	1.00	0.924	Grey samples (unheated)
Eye Dashwa Lakes -Atikokan granite (All samples)	56	214	33.55	1.00	0.958	Includes both grey and pink (unheated samples)
Eye Dashwa Lakes -Atikokan granite grey samples	35	212	34.08	1.00	0.973	Grey-unheated samples
Lac du Bonnet and Eye Dashwa Lakes Atikokan samples combined	306	226	30.4	1.00	0.932	All data combined (unheated samples)
Lac du Bonnet and Eye Dashwa Lakes Atikokan pink granite samples	112	236	31.91	1.00	0.962	Unheated samples
Lac du Bonnet and Eye Dashwa Lakes Atikokan grey granitic samples	209	220	30.83	1.00	0.926	Unheated samples
Lac du Bonnet and Eye Dashwa Lakes -Atikokan granitic samples	27	211	33.66	1.00	0.964	Combined pink and grey coloured samples Test temperature = 100°C

Table 14 - (Cont'd)

Rock type	Number of samples N	Mean uniaxial compressive strength (σ_c) MPa	m	s	r	Comments
Lac du Bonnet and Eye Dashwa Lakes -Atikokan granitic samples	31	195	32.79	1.00	0.969	Combined pink and grey coloured samples Test temperature = 200°C

Table 15 - Summary of rock joint characterization data for Lac du Bonnet drill core samples (After Jackson et al., 1985)

	Unconfined* compressive strength intact rock material (σ_c) (MPa)	Joint wall* compressive strength (JCS) (MPa)	Joint roughness coefficient JRC		
			Calculated	Visually estimated	Combined
No. of samples	139	139	62	77	139
Range	82-241	45-196	2.99-8.86	3.50-13.00	2.99-13.00
Mean	179.8	114.3	6.45	6.00	6.28
Std Dev	34.99	33.3	1.40	1.90	1.55

*Based on Schmidt hammer (Model-L) results.

ROCK PROPERTY ACTIVITY; STANDARD SAMPLE DISTRIBUTION SCHEME (1979/80)

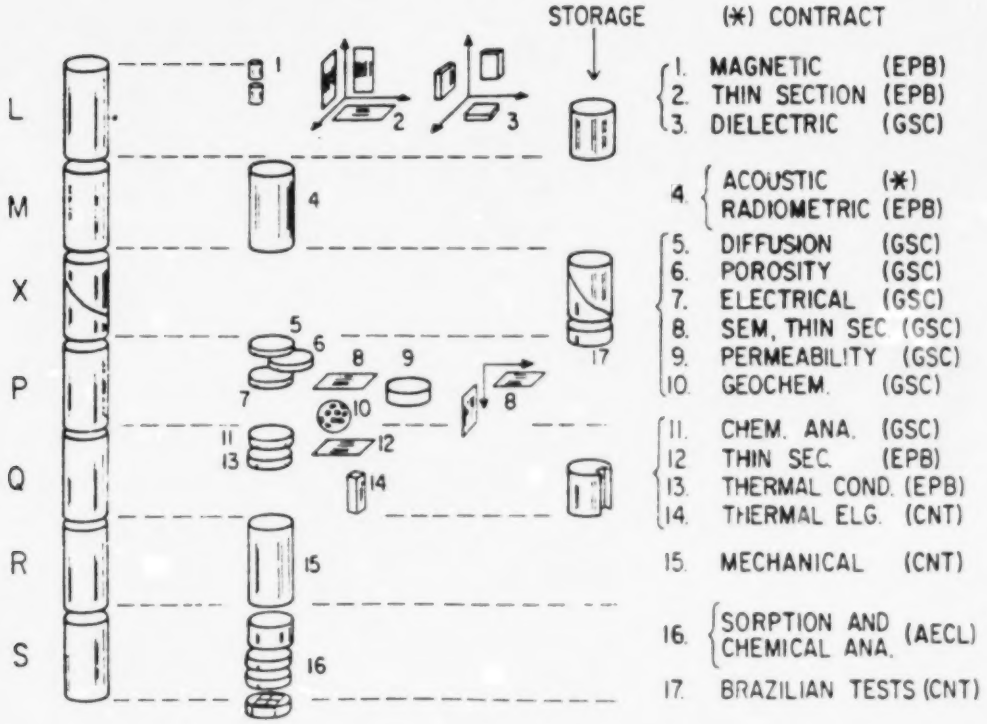

Fig. 1 - Standard sample

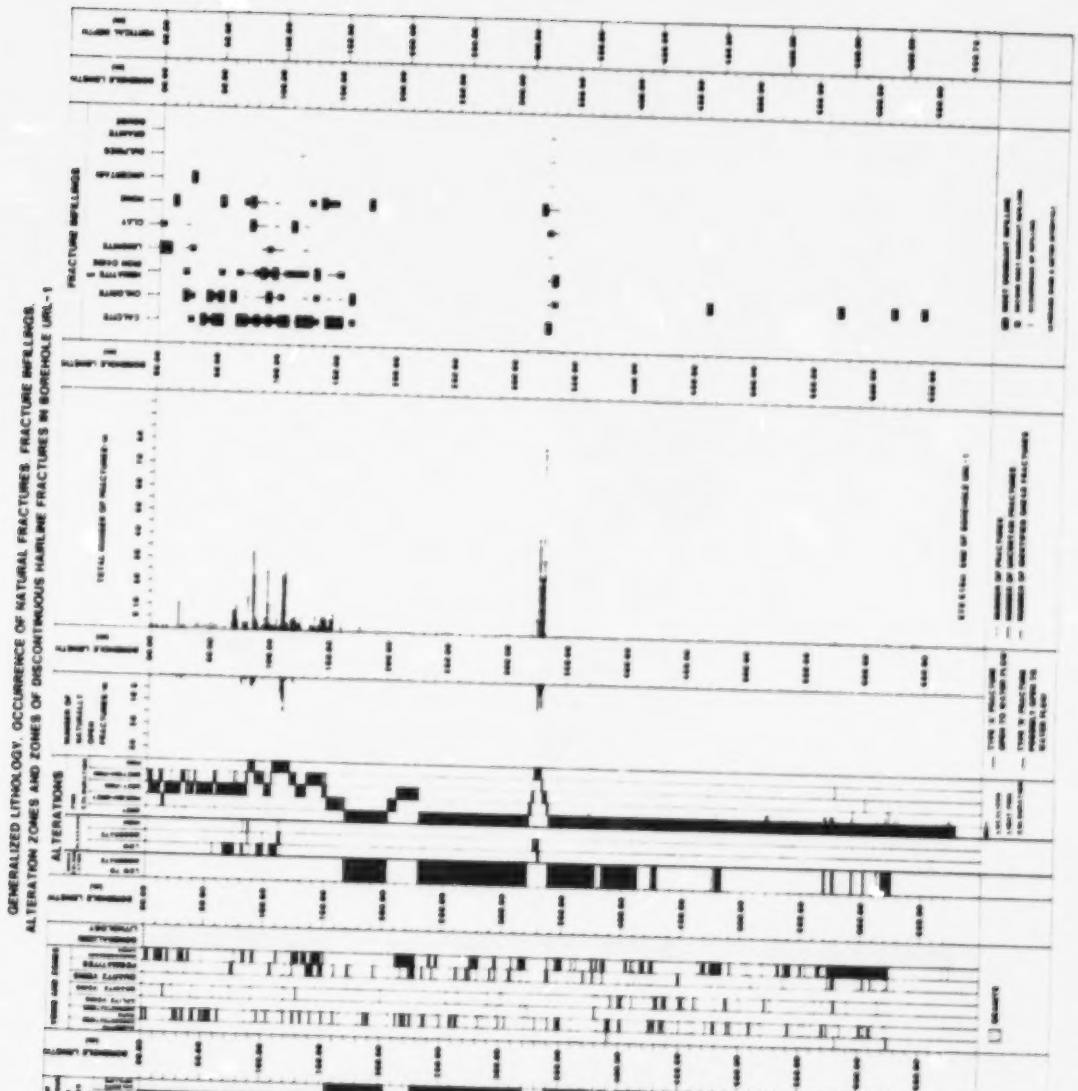
GENERALIZED LITHOLOGY, OCCURRENCE OF NATURAL FRACTURES, FRACTURE INFILLINGS,
ALTERATION ZONES AND ZONES OF DISCONTINUOUS HAIRLINE FRACTURES IN BOREHOLE URL-1
FRACTURE INFILLINGS
ALTERATIONS

Fig. 2 - Generalized lithology, occurrence of natural fractures, fracture fillings, alteration zones and zones of discontinuous hairline fractures in borehole URL-1

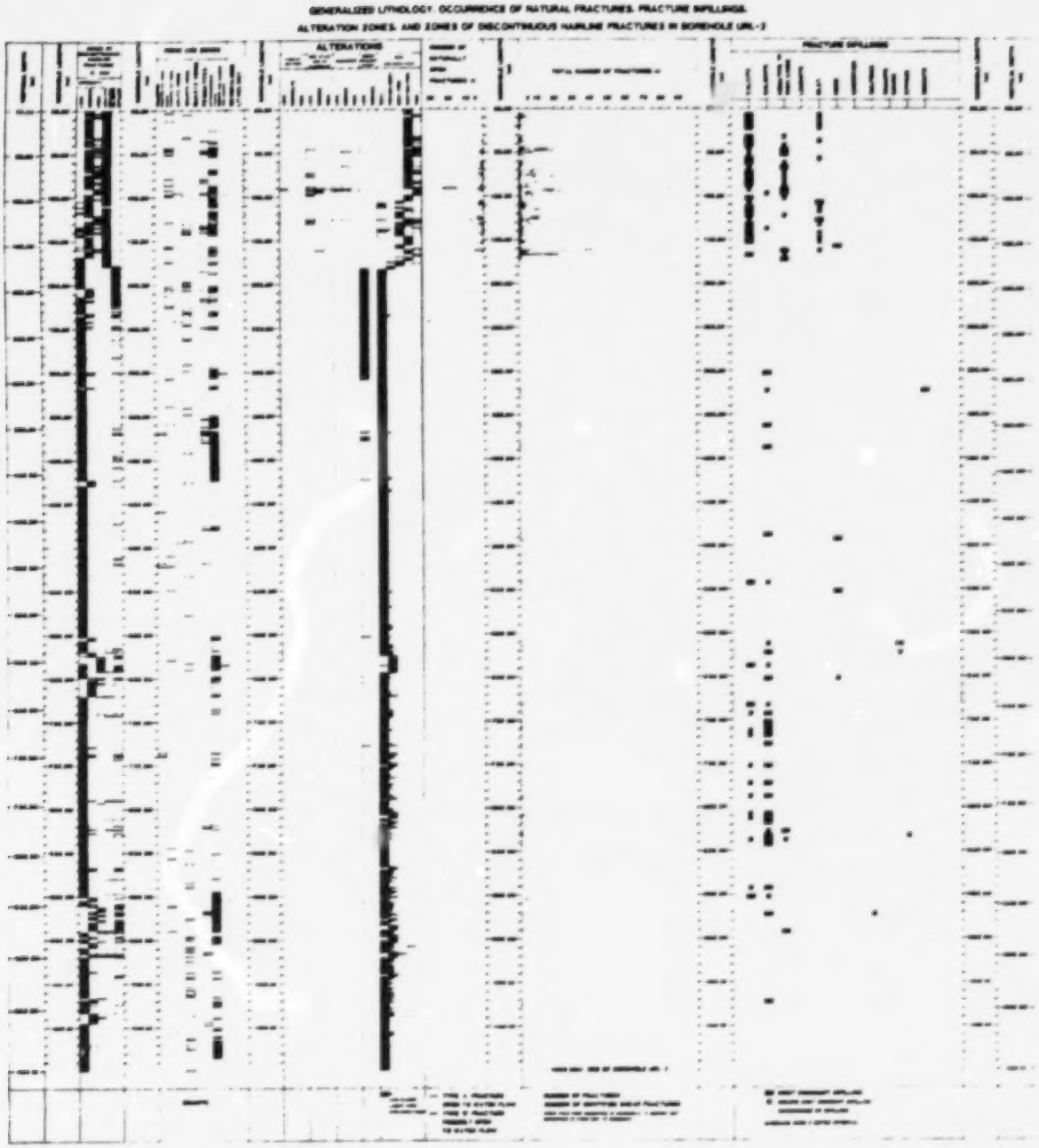

Fig. 3 - Generalized lithology, occurrence of natural fracture infillings, alteration zones, and zones of discontinuous hairline fractures in borehole URL-2

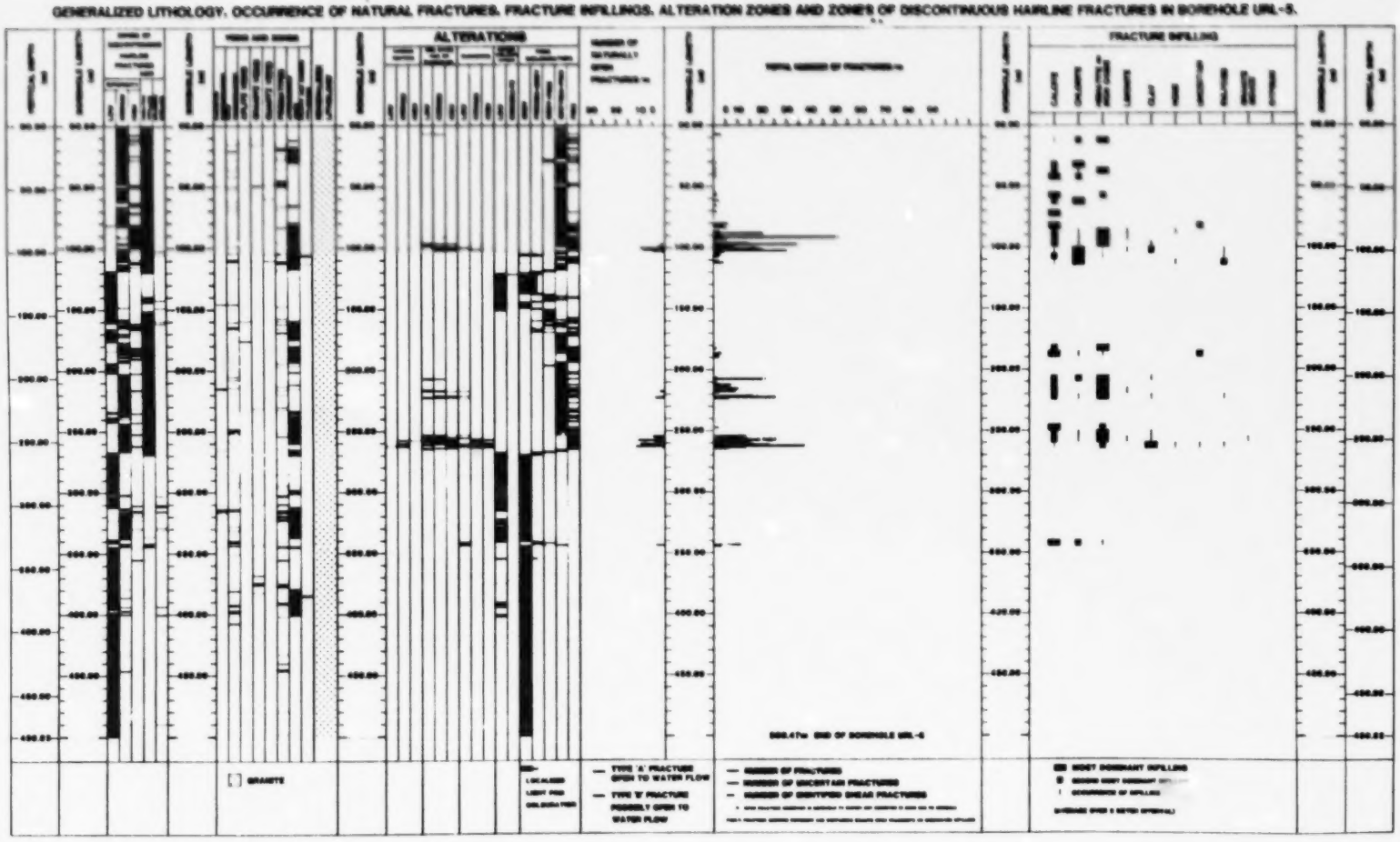
GENERALIZED LITHOLOGY, OCCURRENCE OF NATURAL FRACTURES, FRACTURE INFILLINGS, ALTERATION ZONES AND ZONES OF DISCONTINUOUS HAIRLINE FRACTURES IN BOREHOLE URL-5.
ALTERATIONS
FRACTURE INFILLING
GRANITE

Fig. 4 - Generalized lithology, occurrence of natural fractures, fracture infillings, alteration zones and zones of discontinuous hairline fractures in borehole URL-5

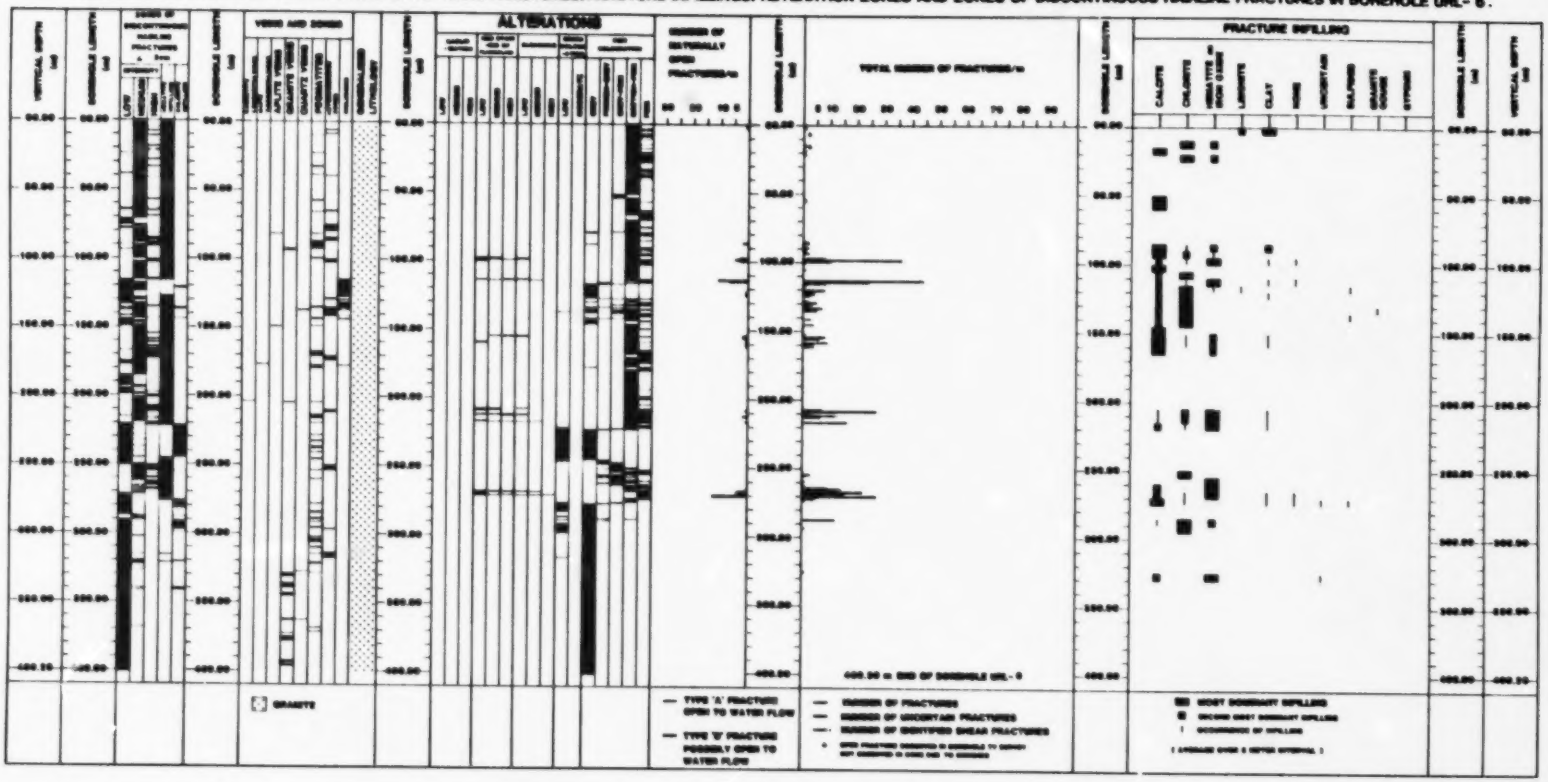

Fig. 5 - Generalized lithology, occurrence of natural fractures in fillings, alteration zones, and zones of discontinuous hairline fractures in borehole URL-6

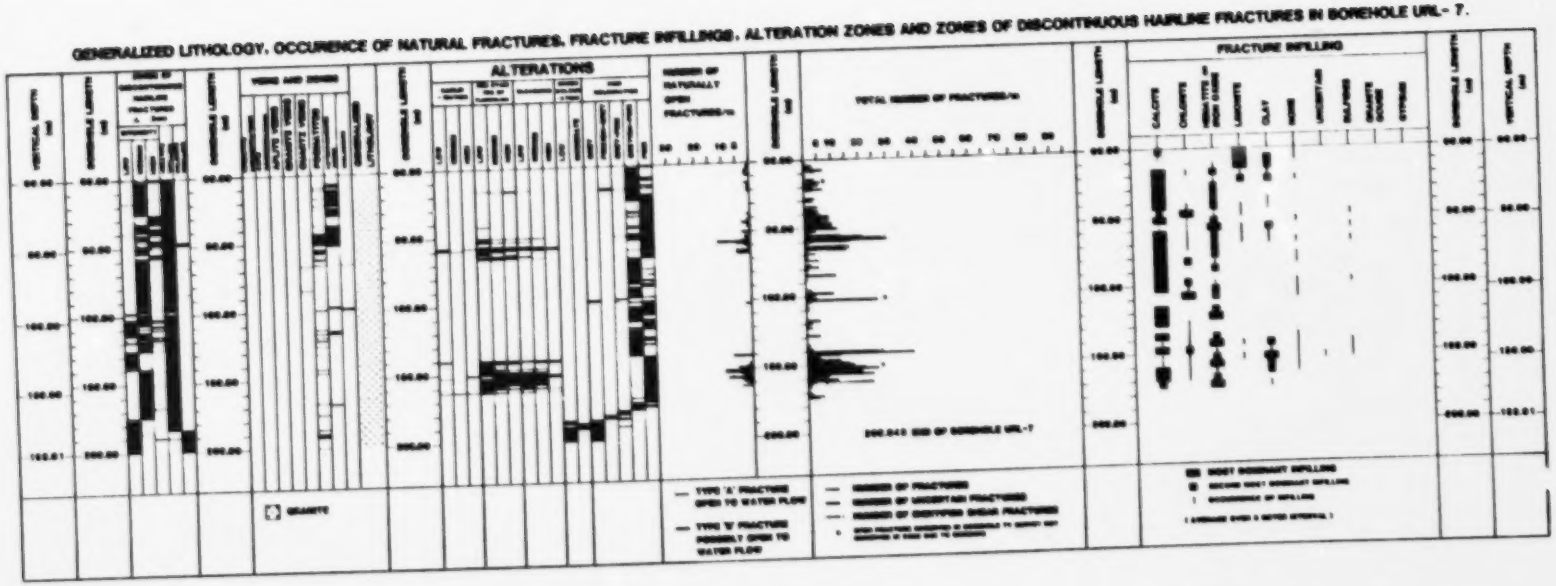
GENERALIZED LITHOLOGY, OCCURENCE OF NATURAL FRACTURES, FRACTURE INFILLINGS, ALTERATION ZONES AND ZONES OF DISCONTINUOUS HAIRLINE FRACTURES IN BOREHOLE URL- 7.
ALTERATIONS
FRACTURE INFILLING

Fig 6 - Generalized lithology, occurrence of natural fractures in fillings, alteration zones, and zones of discontinuous hairline fractures in borehole URL-7

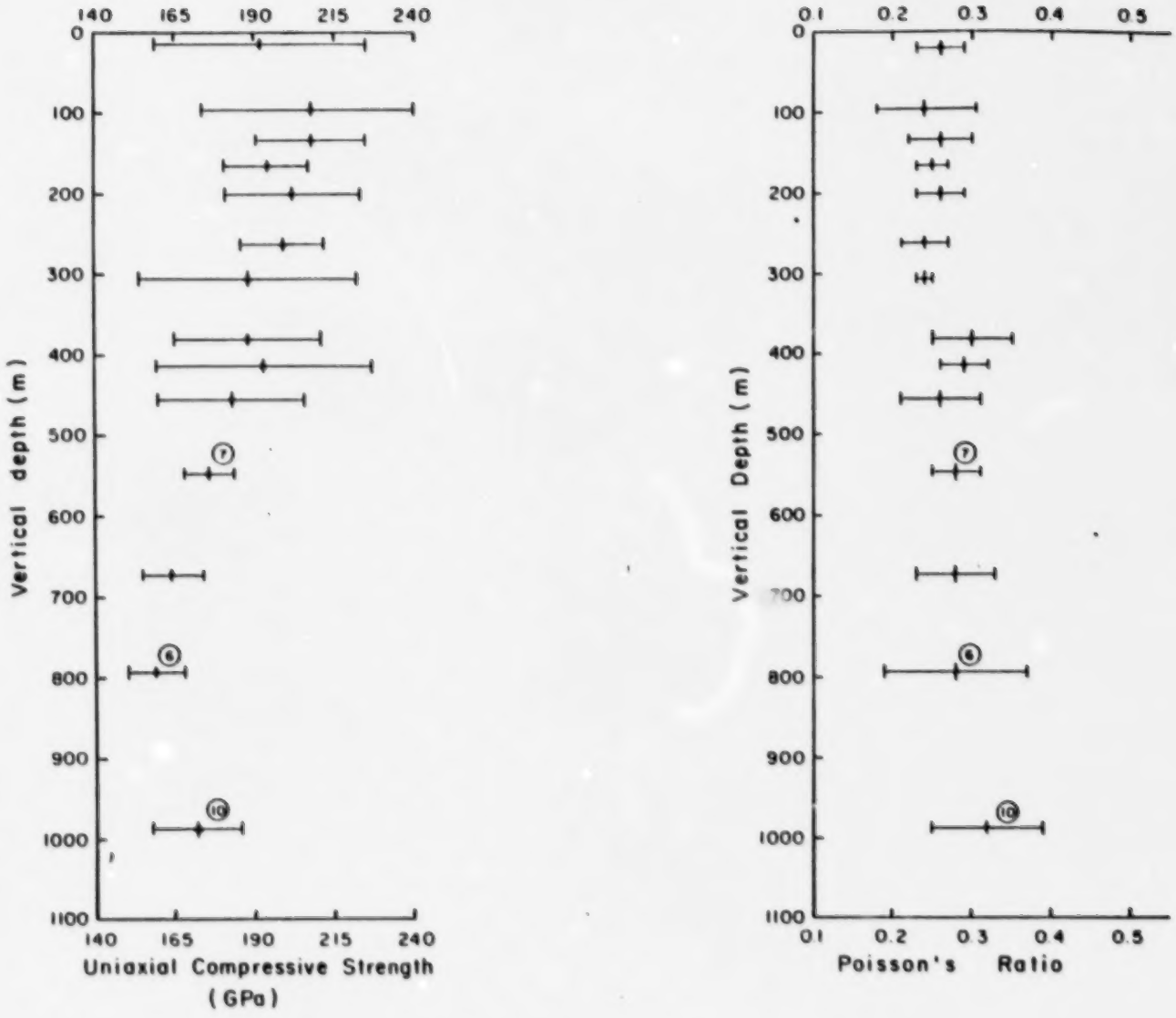

Fig. 7 - Depth profiles of uniaxial compressive strength and Poisson's ratio (URL and WNRE-sites combined)

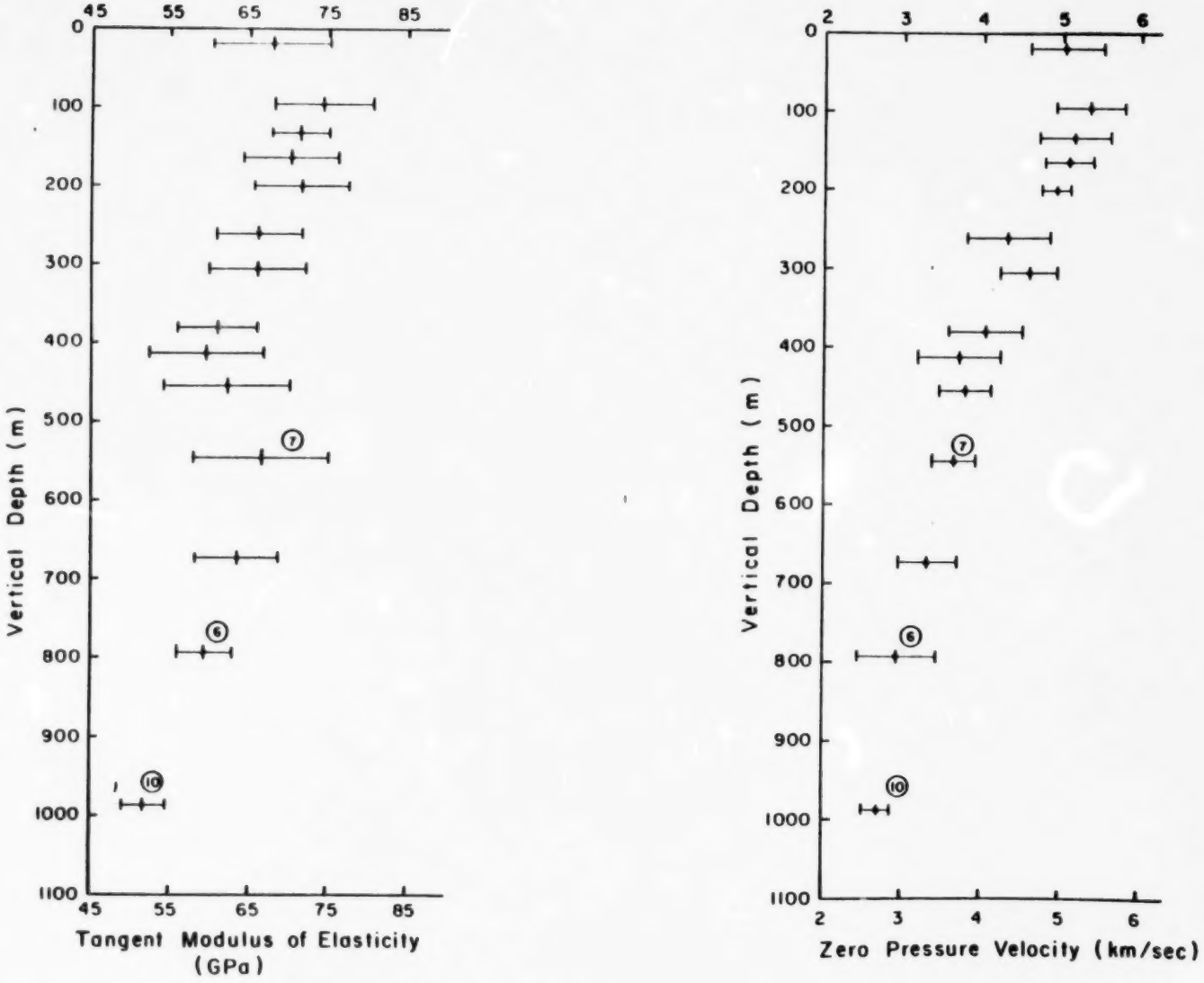

Fig. 8 - Depth profiles of tangent modulus of elasticity and zero pressure dilatational wave velocity for Lac du Bonnet granitic samples (URL and WNRE-sites combined)

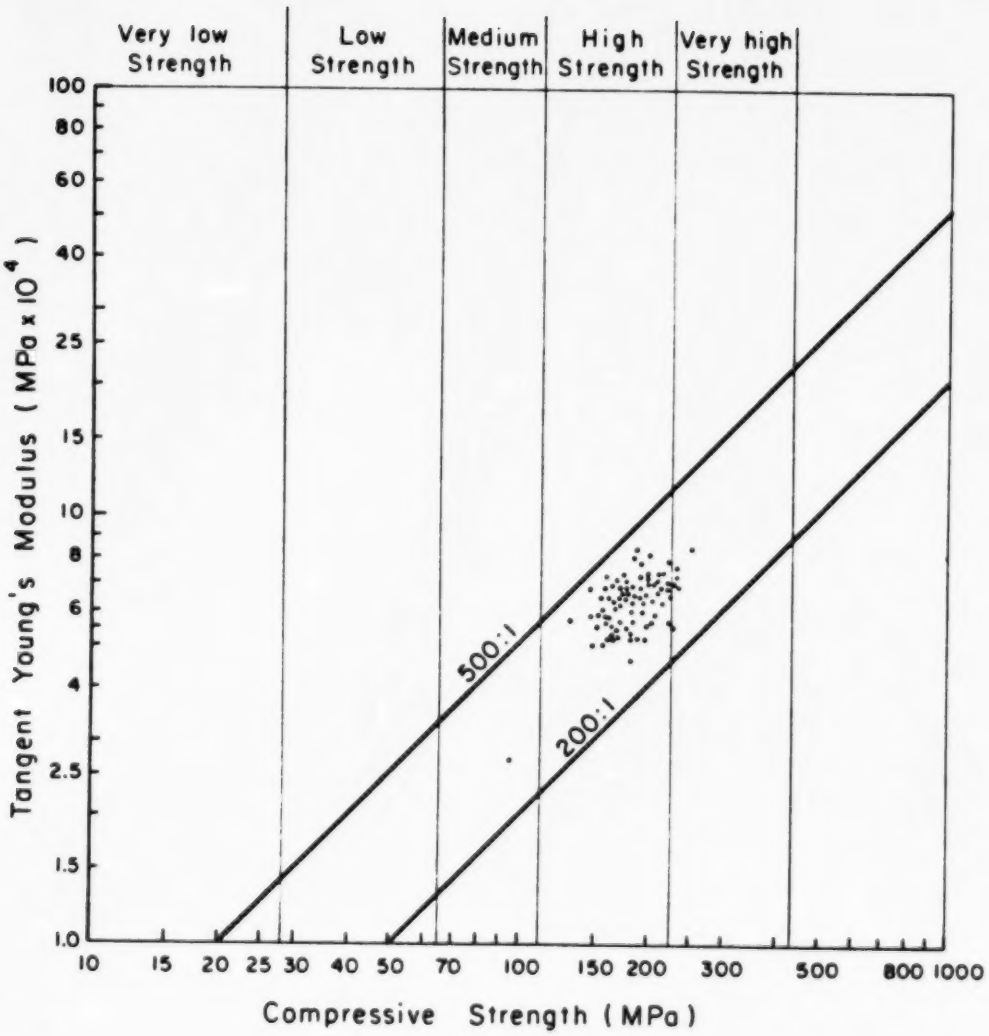

Fig. 9 - Engineering classification of intact rock for Lac du Bonnet granitic samples (boreholes URL-1, URL-2, URL-5, URL-6, URL-7 and WN-2, and WN-4)

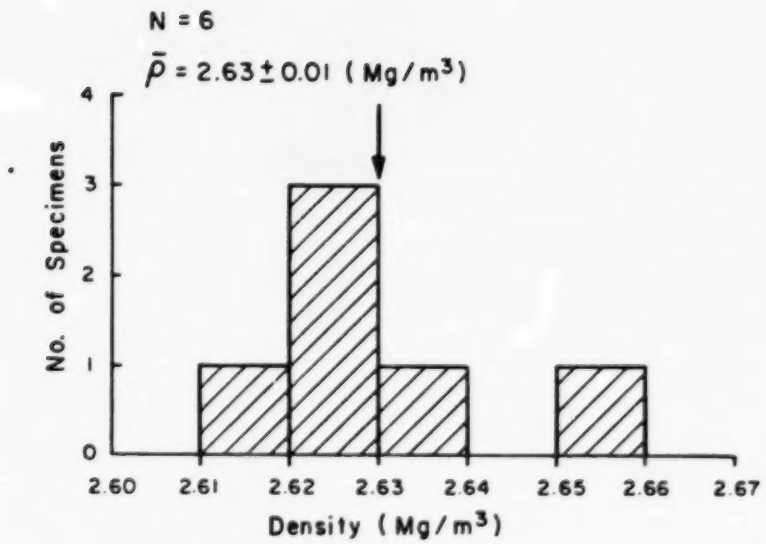

Fig. 10 - Histogram of bulk density for upper zone (0-50 m vertical depth) Lac du Bonnet granitic samples (URL-site) *

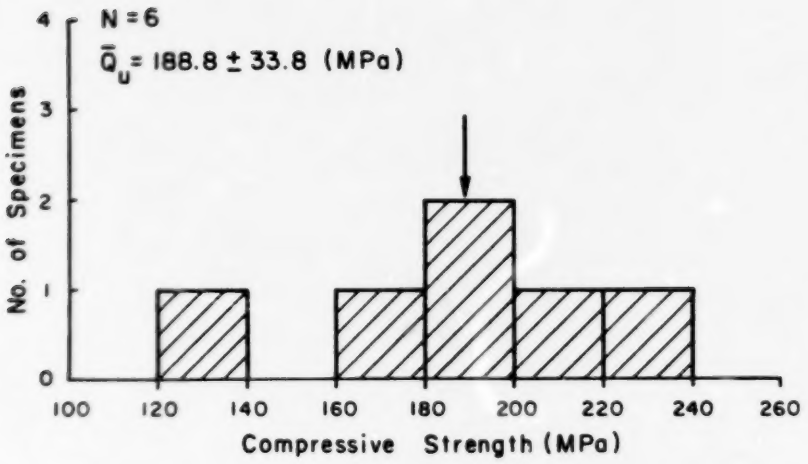

Fig. 11 - Histogram of uniaxial compressive strength for upper zone (0-50 m vertical depth) Lac du Bonnet granitic samples (URL-site)

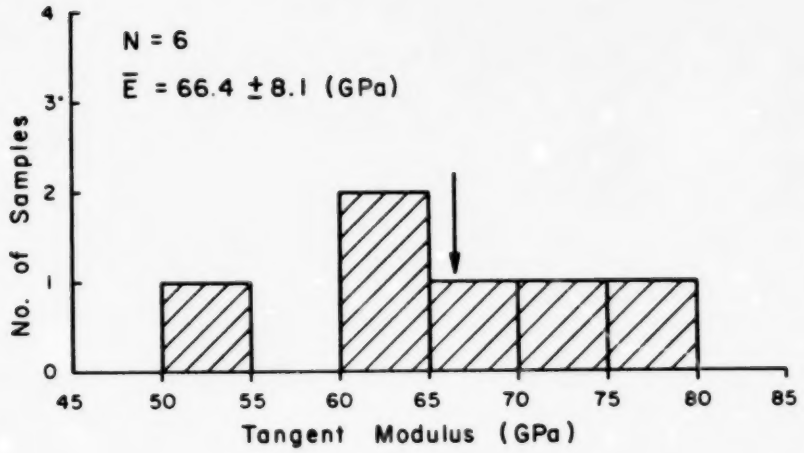

Fig. 12 - Histogram of tangent modulus of elasticity for upper zone (0-50 m vertical depth) Lac du Bonnet granitic samples (URL-site)

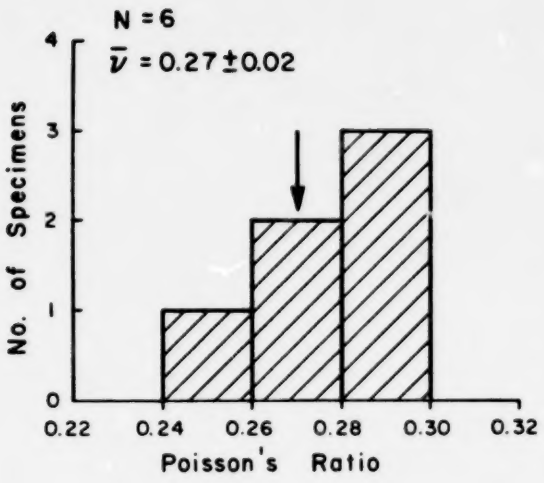

Fig. 13 - Histogram of Poisson's ratio, for upper zone (0-50 m vertical depth) Lac du Bonnet granitic samples (URL-site)

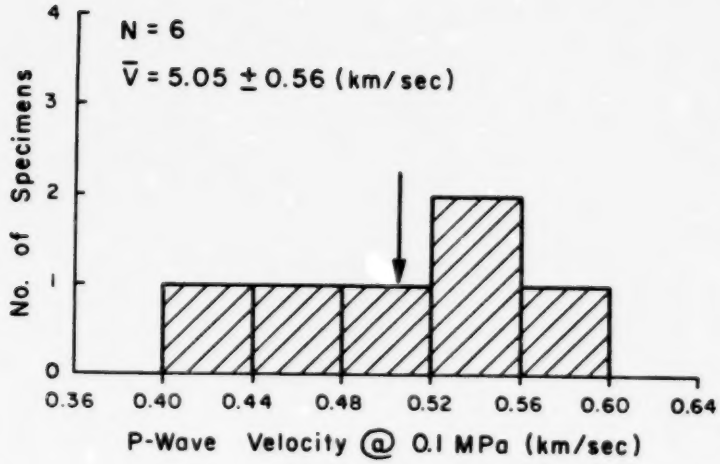

Fig. 14 - Histogram of zero pressure compressive wave velocity for upper zone (0-50 m vertical depth) Lac du Bonnet granitic samples (URL-site)

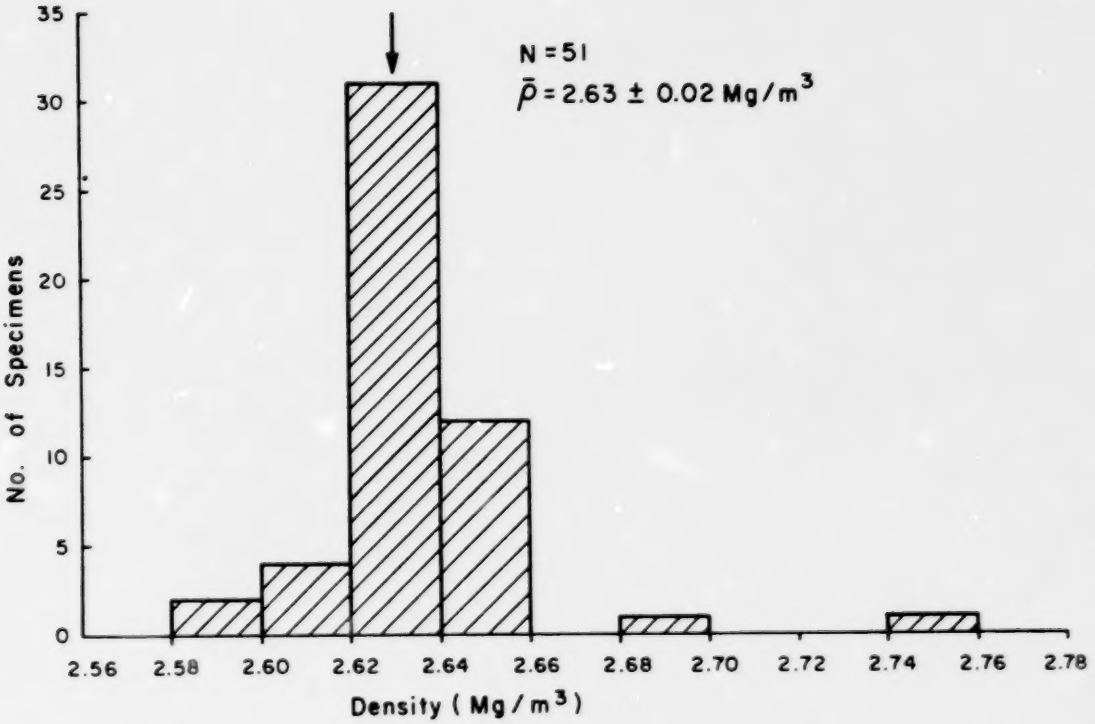

Fig. 15 - Histogram of bulk density for intermediate zone (51-260 m) Lac du Bonnet granitic samples (URL-site)

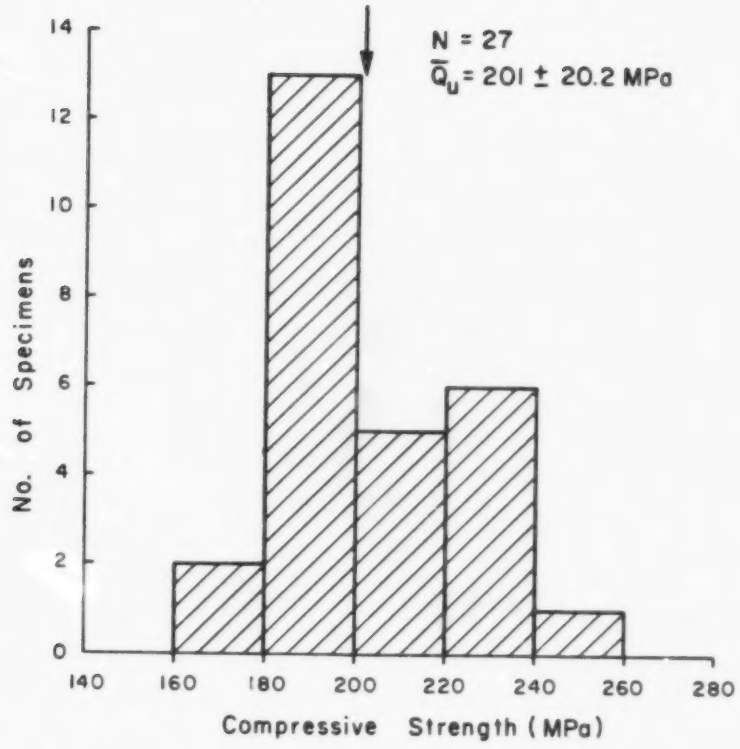

Fig. 16 - Histogram of uniaxial compressive strength for intermediate zone (51-260 m vertical depth) Lac du Bonnet granitic samples (URL-site)

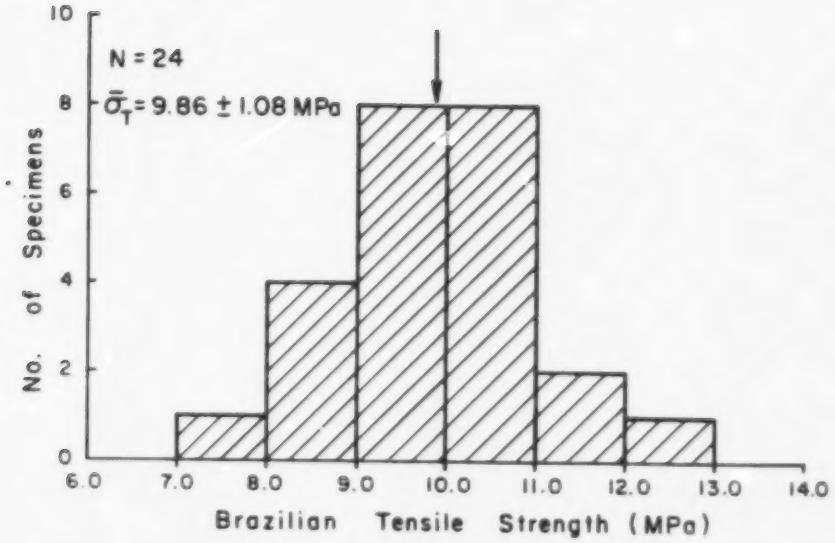

Fig. 17 - Histogram of Brazilian tensile strength for intermediate zone (51-260 m vertical depth) Lac du Bonnet granitic samples (URL-site)

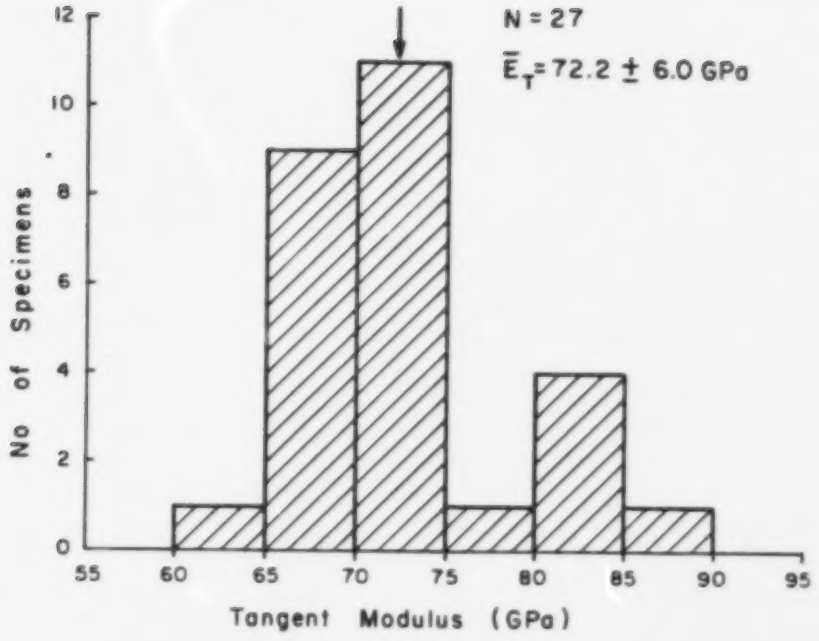

Fig. 18 - Histogram of tangent modulus for intermediate zone (51-260 m vertical depth), Lac du Bonnet granitic samples (URL-site)

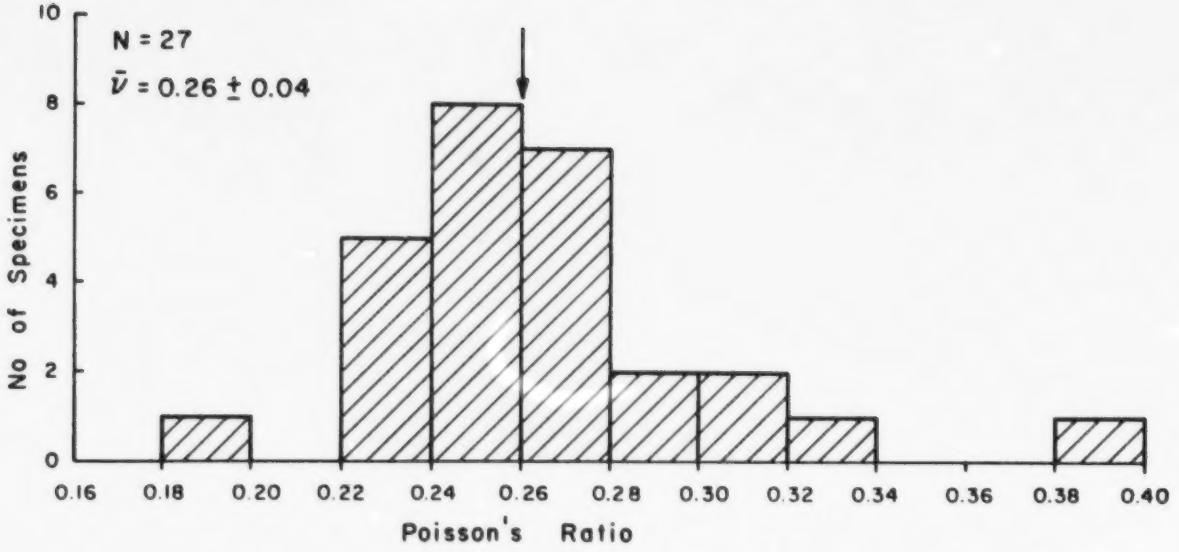

Fig. 19 - Histogram of Poisson's ratio for intermediate zone (51-260 m vertical depth) Lac du Bonnet granitic samples (URL-site)

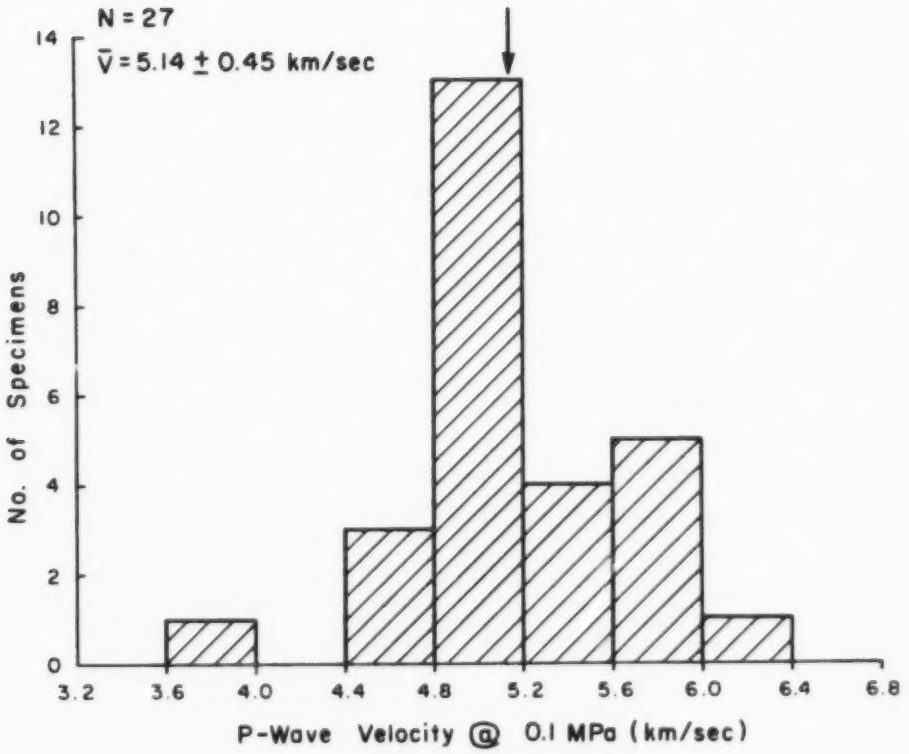

Fig. 20 - Histogram of zero pressure compressive wave velocity for intermediate zone (51-260 m vertical depth) Lac du Bonnet granitic samples (URL-site)

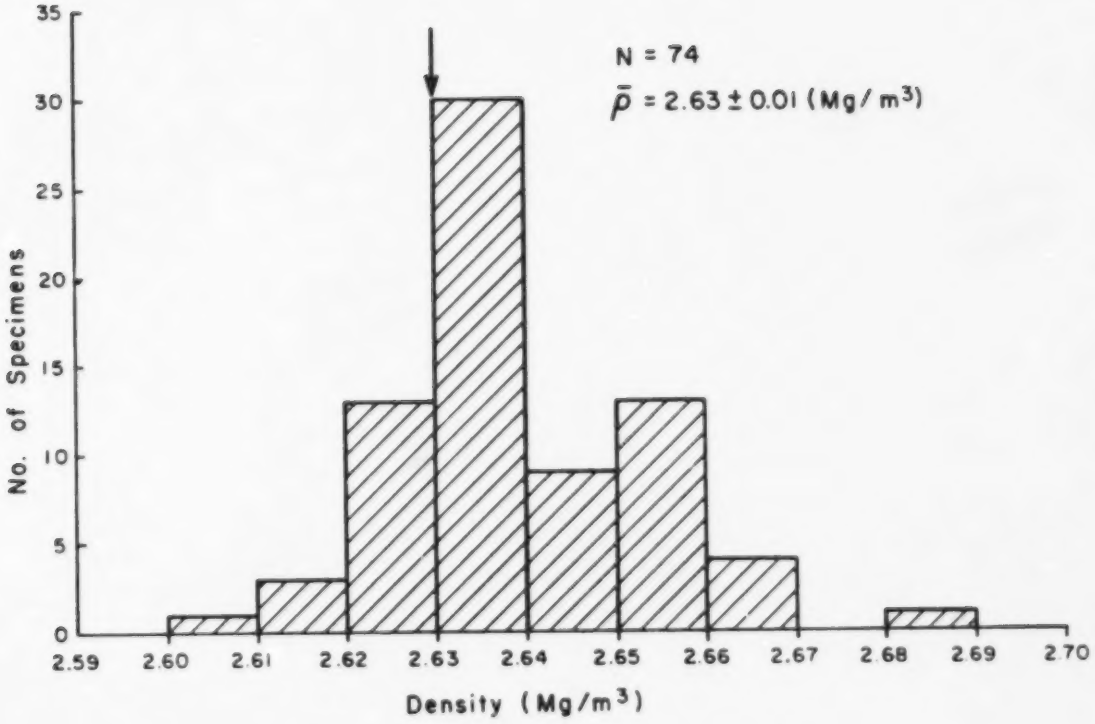

Fig. 21 - Histogram of bulk density for lower zone (below 260 m vertical depth) Lac du Bonnet granitic samples (URL-site)

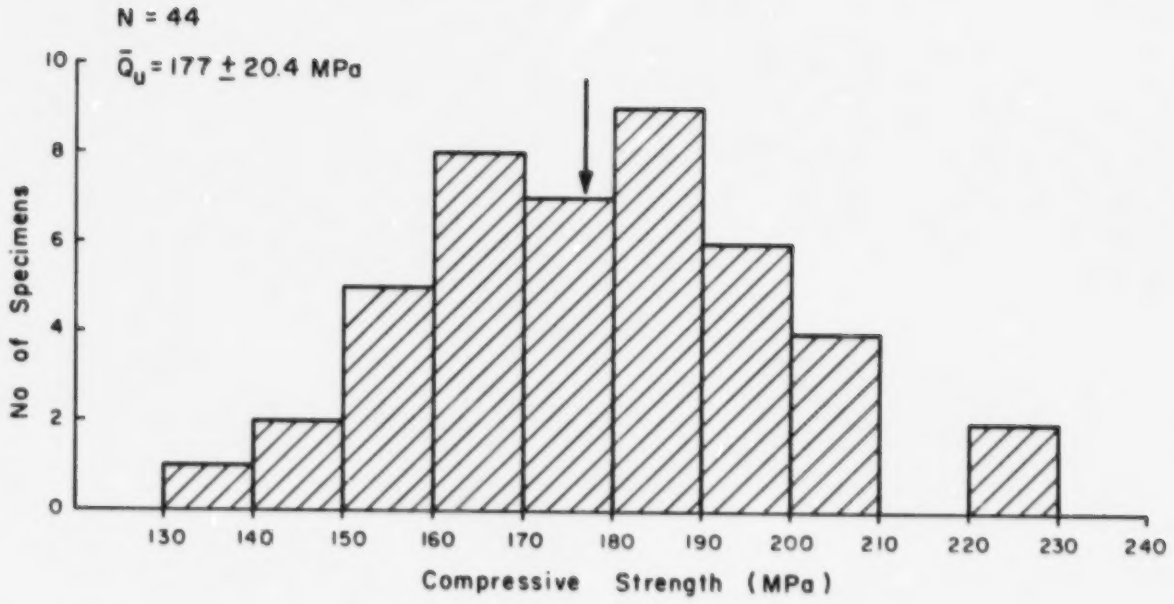

Fig. 22 - Histogram of uniaxial compressive strength for lower zone (below 260 m vertical depth) Lac du Bonnet granitic samples (URL-site)

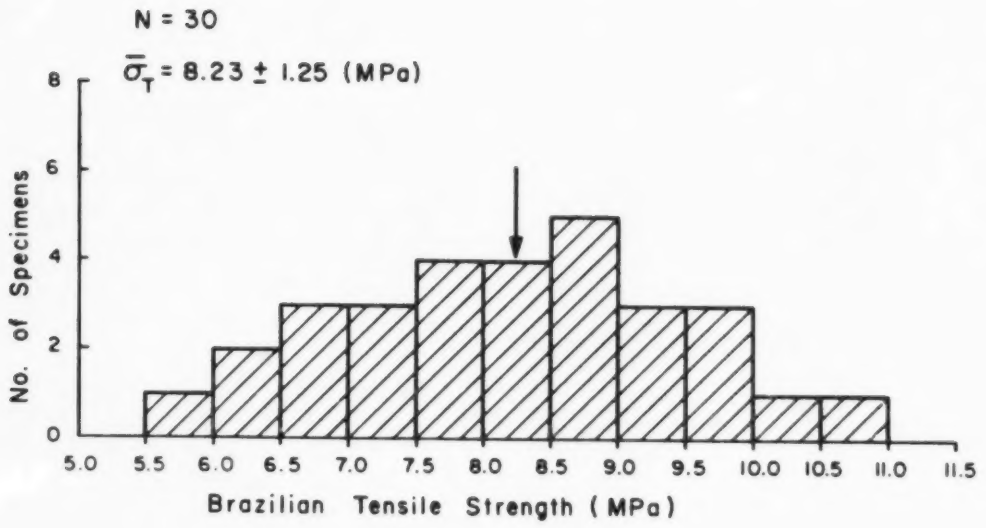

Fig. 23 - Histogram of Brazilian tensile strength for lower zone (below 260 m vertical depth) Lac du Bonnet granitic samples (URL-site)

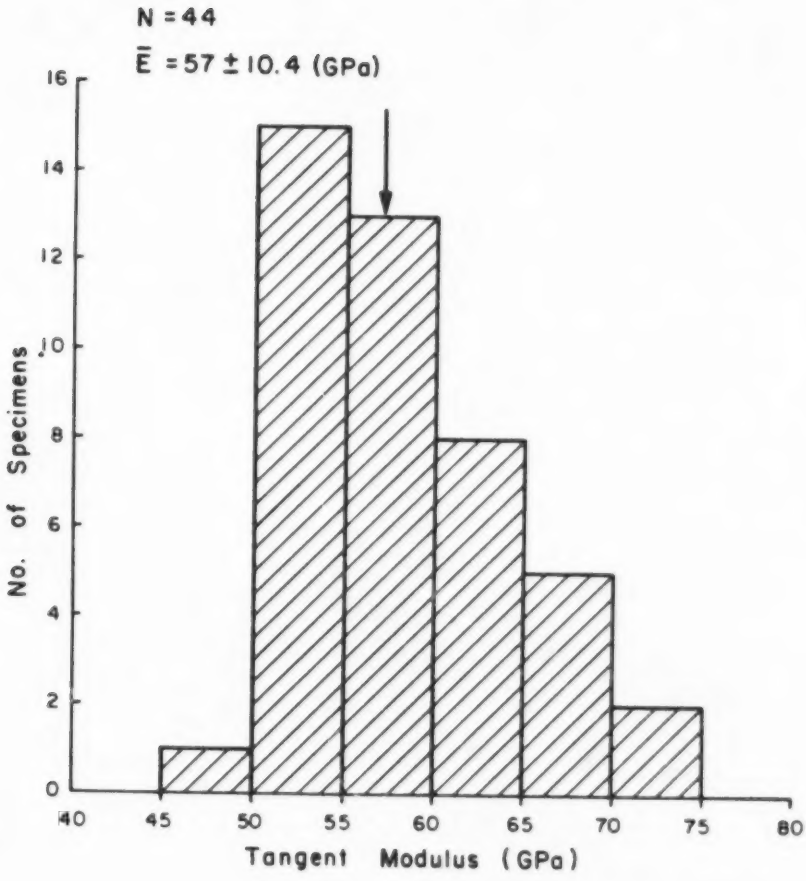

Fig. 24 - Histogram of tangent modulus of elasticity for lower zone (below 260 vertical depth) Lac du Bonnet granitic samples (URL-site)

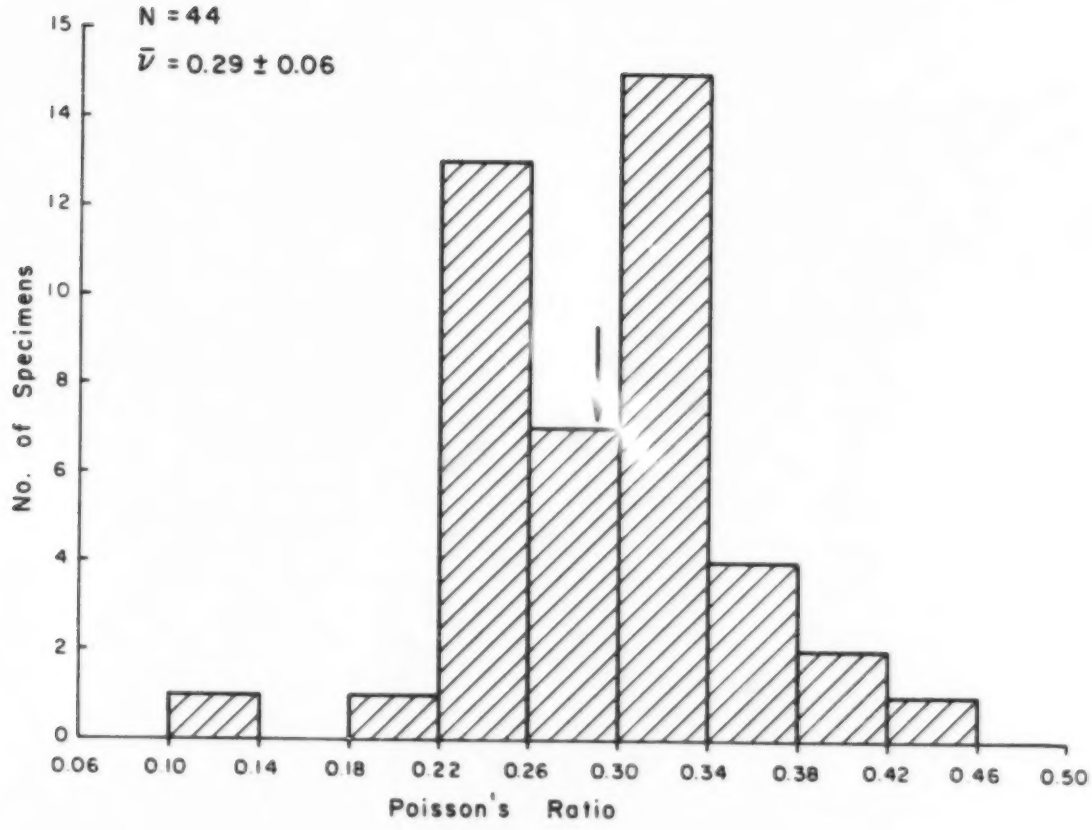

Fig. 25 - Histogram of Poisson's ratio for lower zone (below 260 m vertical depth) Lac du Bonnet granitic samples (URL-site)

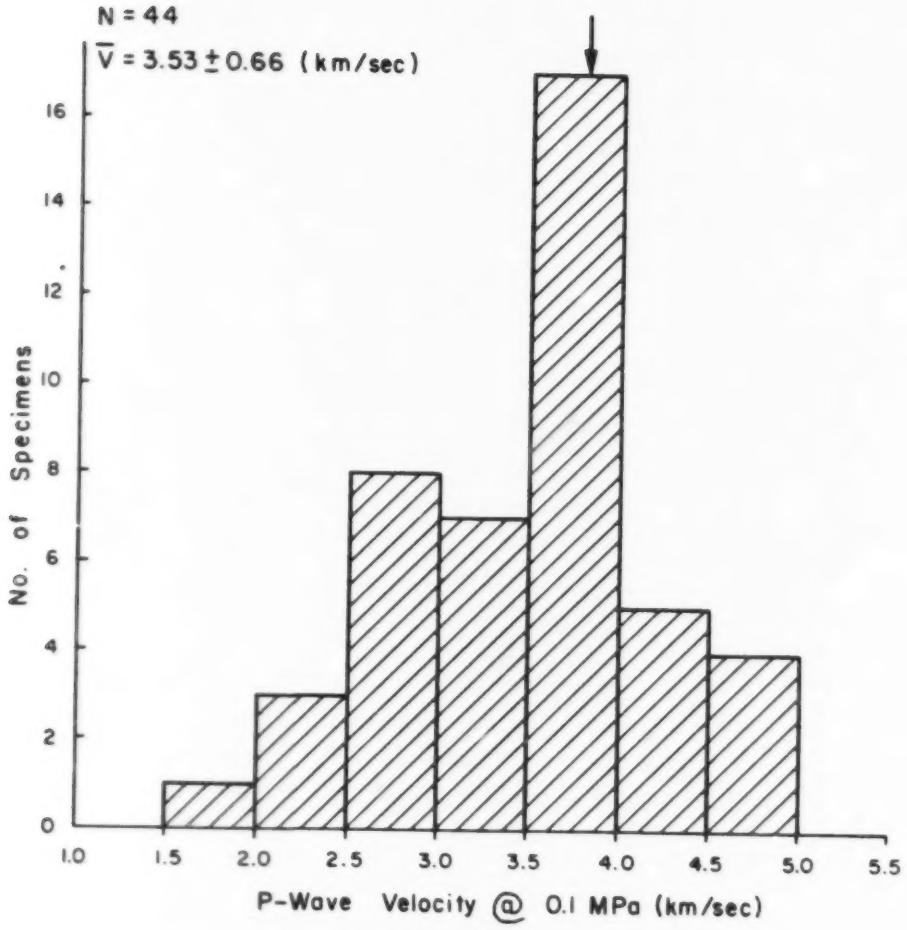

Fig. 26 - Histogram of zero pressure compressive wave velocity for lower zone (below 260 m vertical depth) Lac du Bonnet granitic samples (URL-site)

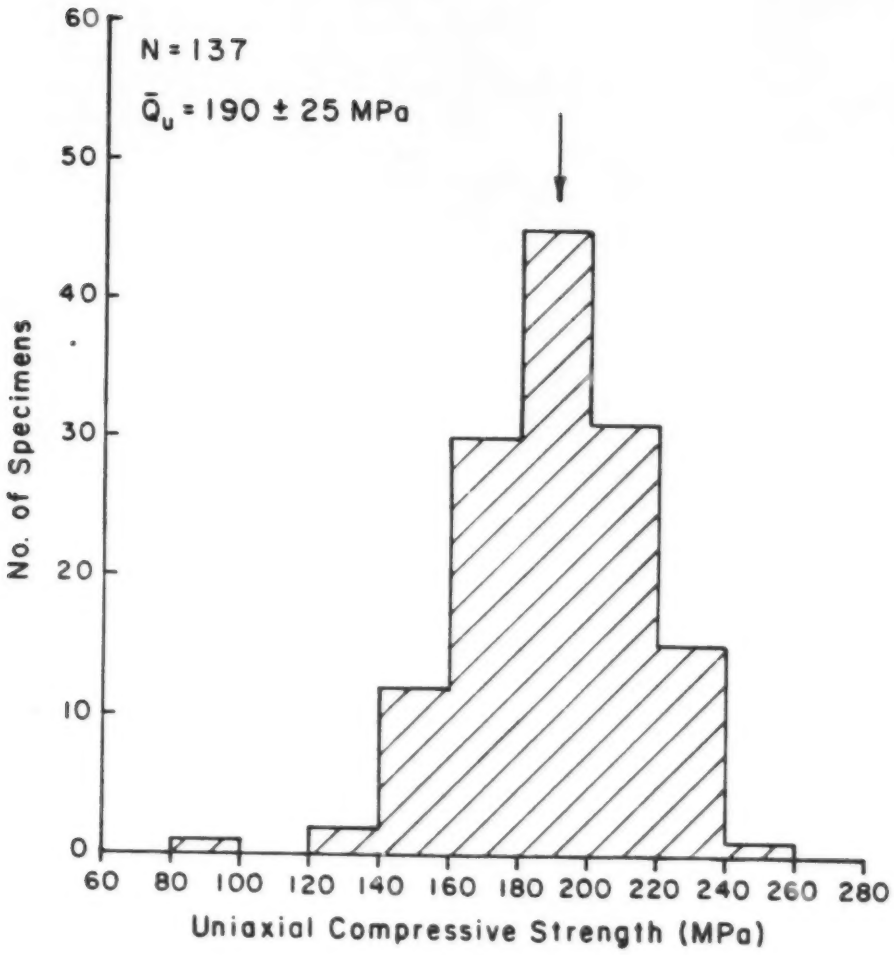

Fig. 27 - Histogram of uniaxial compressive strength for Lac du Bonnet granitic samples (URL and WNRE combined data)

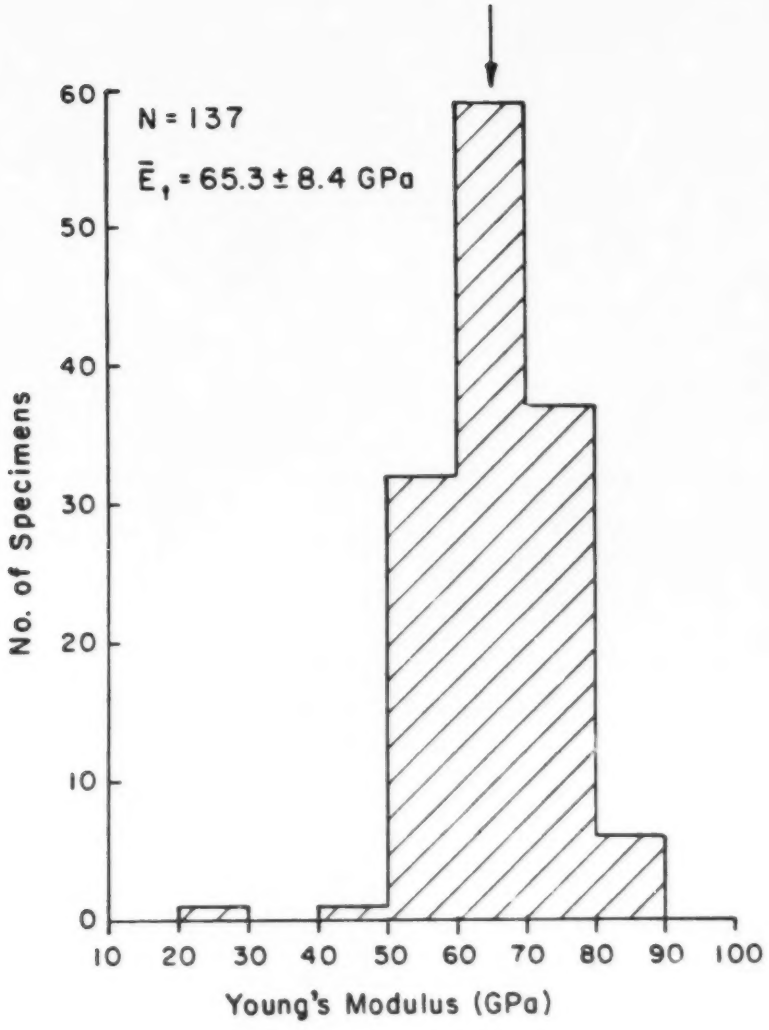

Fig. 28 - Histogram of tangent modulus for Lac du Bonnet granitic samples (URL and WNRE combined data)

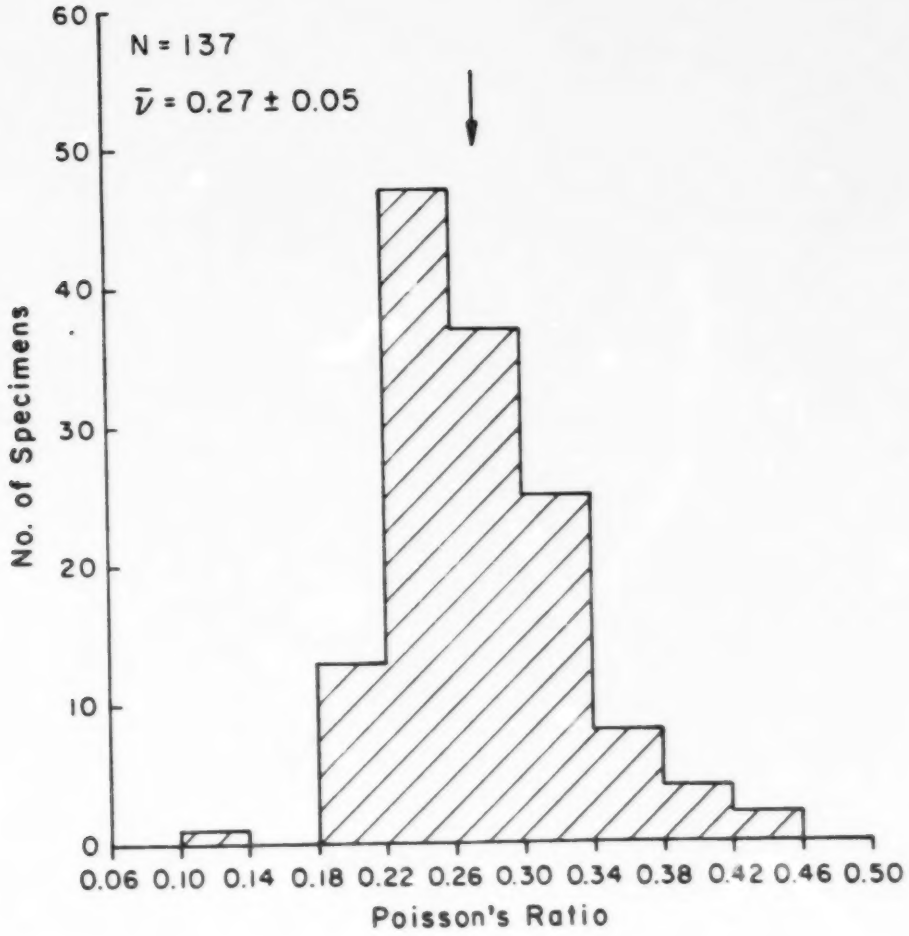

Fig. 29 - Histogram of Poisson's ratio for Lac du Bonnet granitic samples (URL and WNRE combined data)

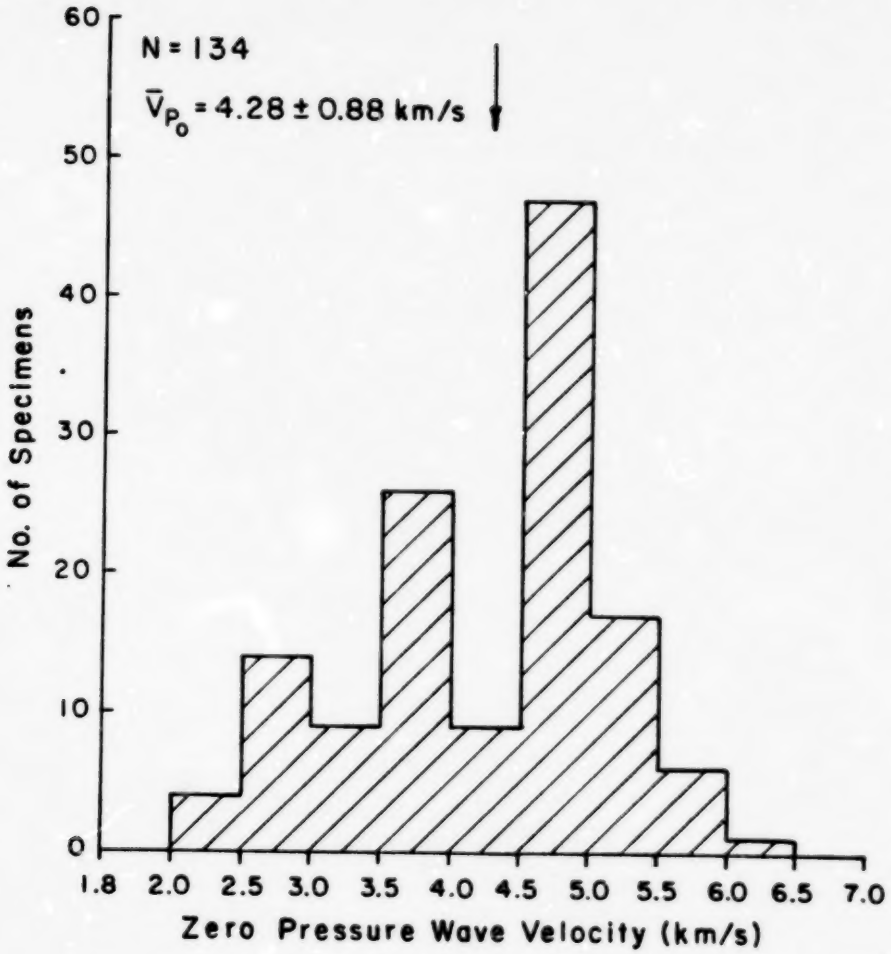

Fig. 30 - Histogram of Brazilian tensile strength for Lac du Bonnet granitic samples (URL and WNRE combined data)

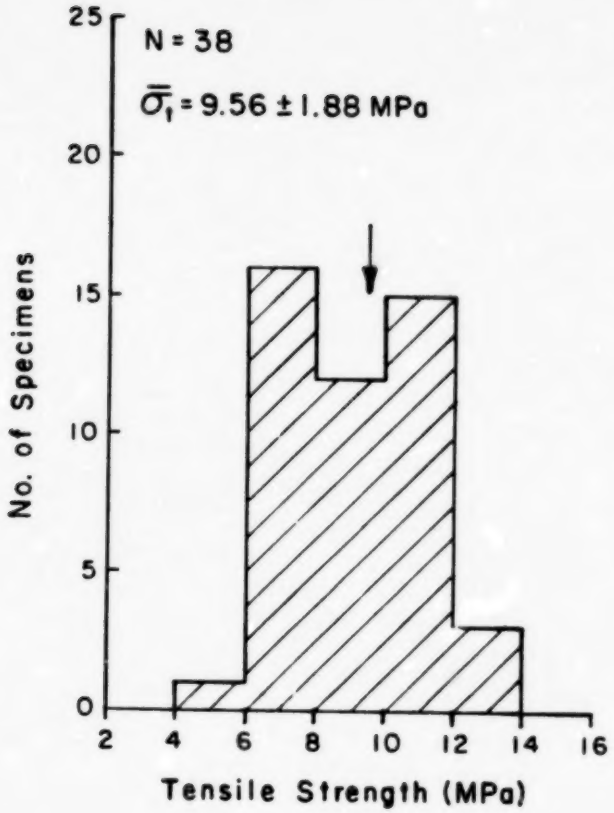

Fig. 31 - Histogram of zero pressure compressive wave velocity for Lac du Bonnet granite samples (URL and WNRE combined data)

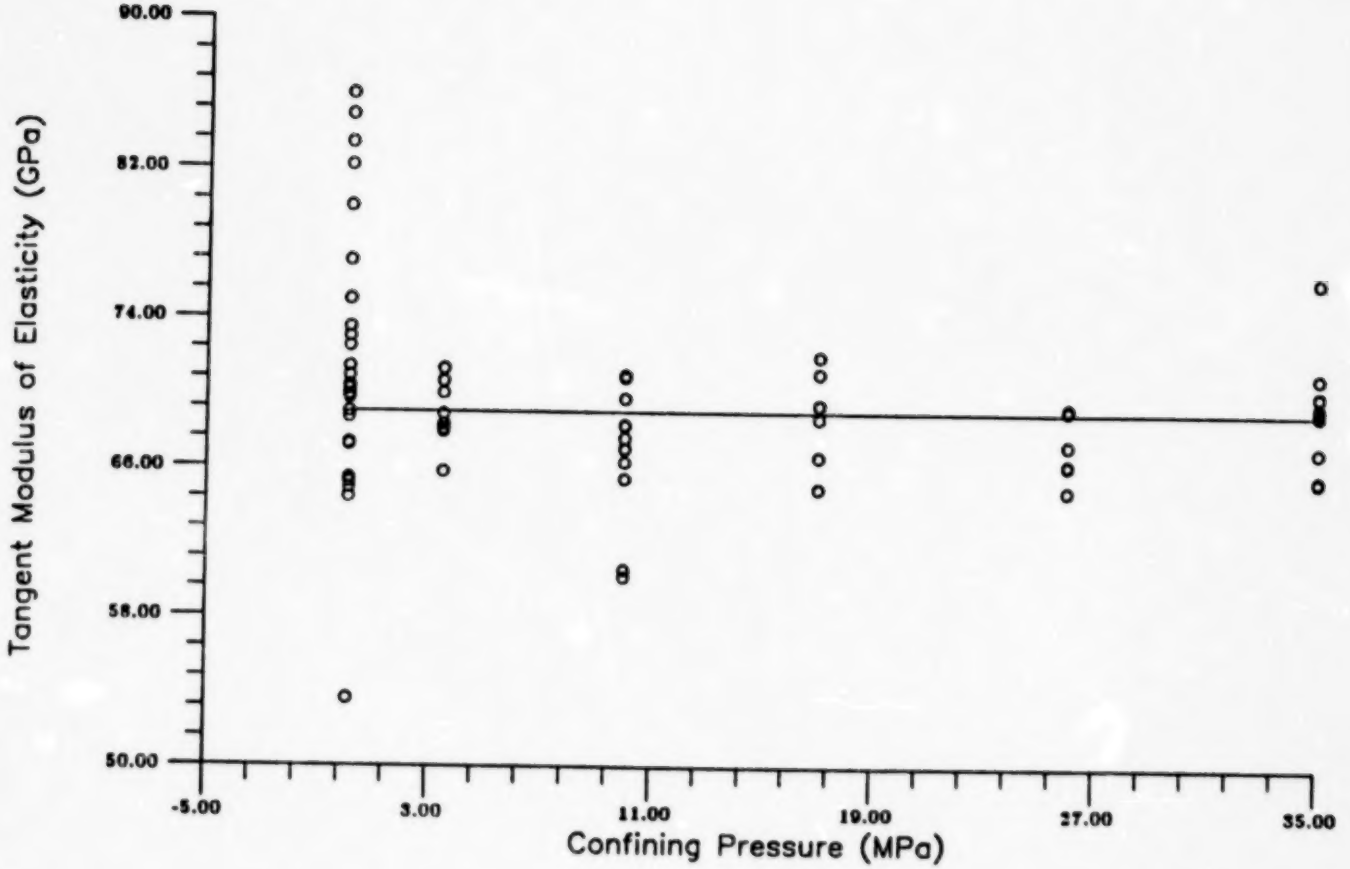

Fig. 32 - Variation of tangent modulus of elasticity versus confining pressure for URL upper zone samples

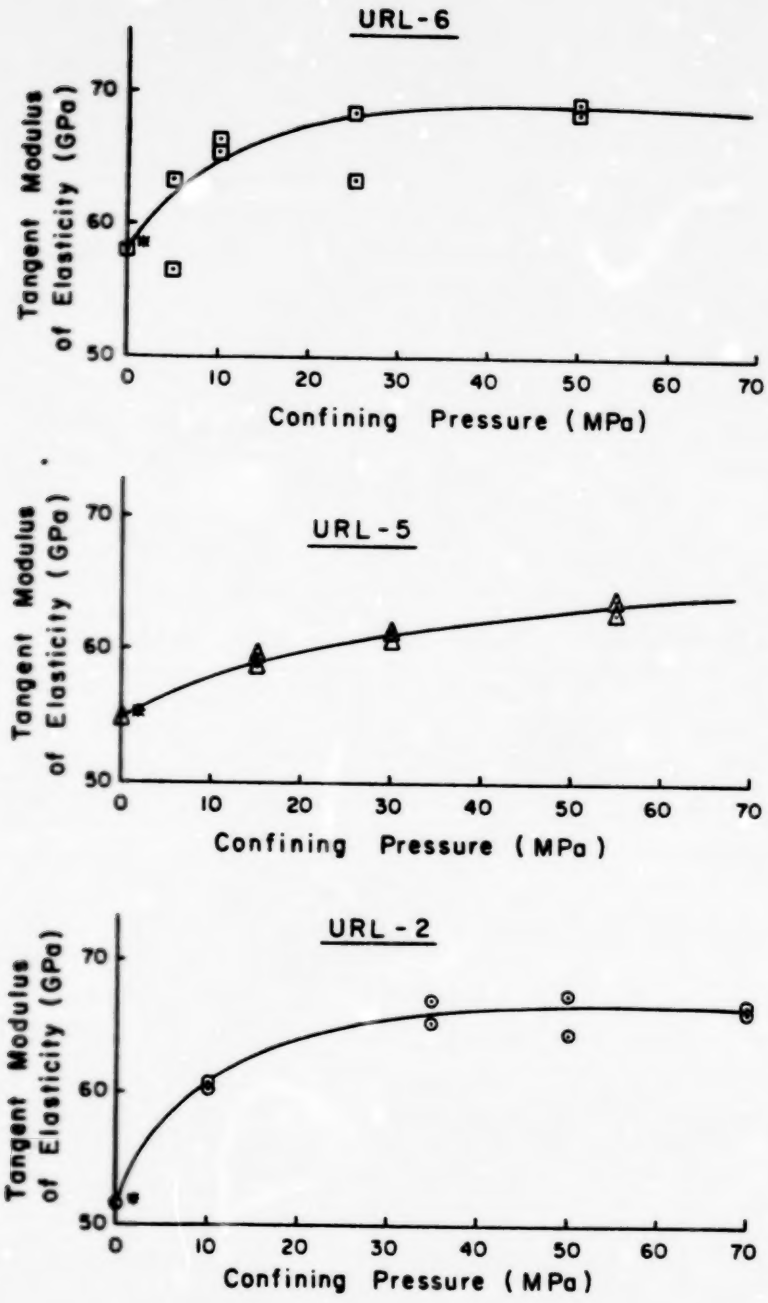

Fig. 33 - Variation of tangent modulus of elasticity versus confining pressure for boreholes URL-2, 5, and 6 deep samples

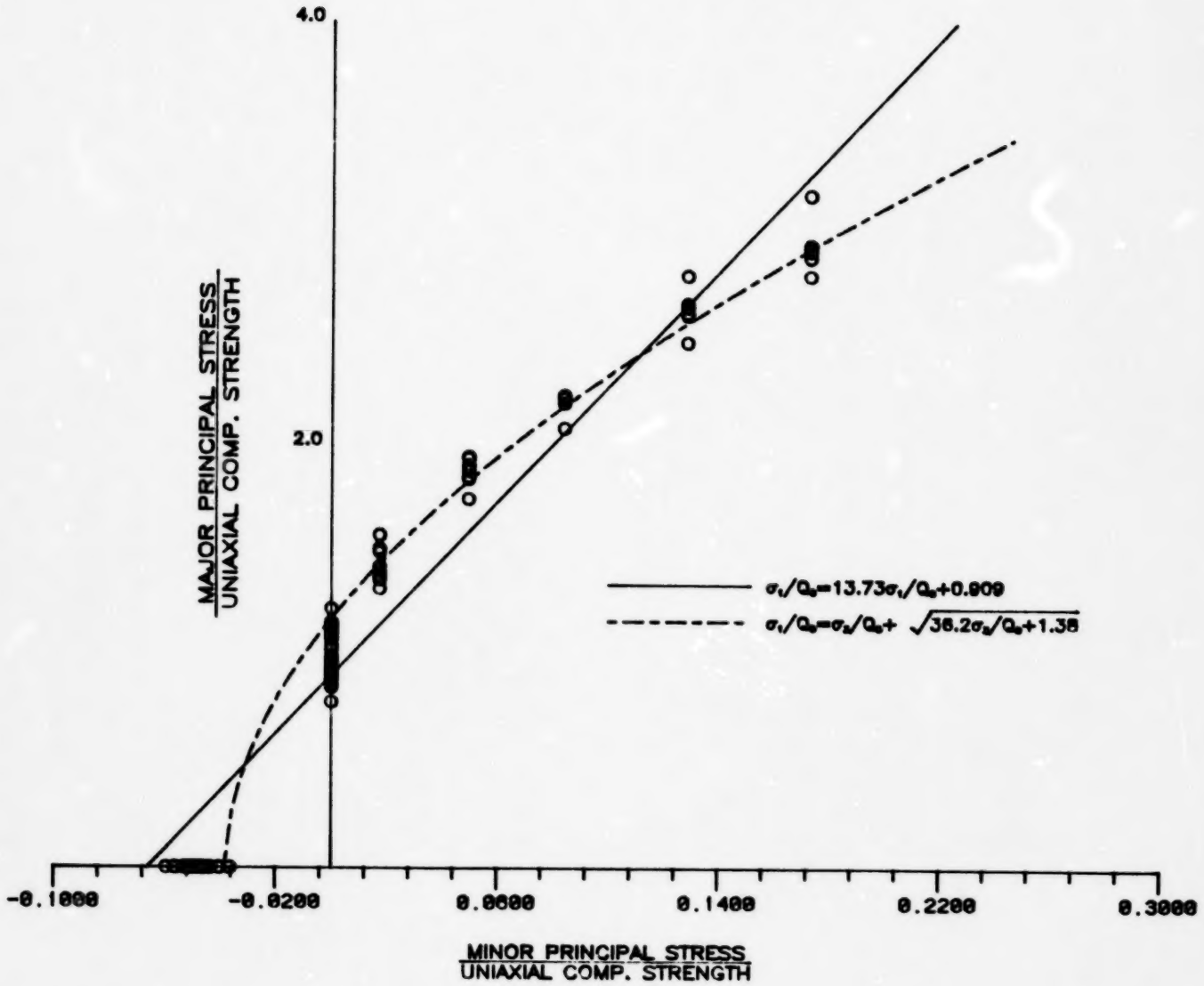

Fig. 34 - Normalized strength envelope for Lac du Bonnet granitic samples from the URL-site

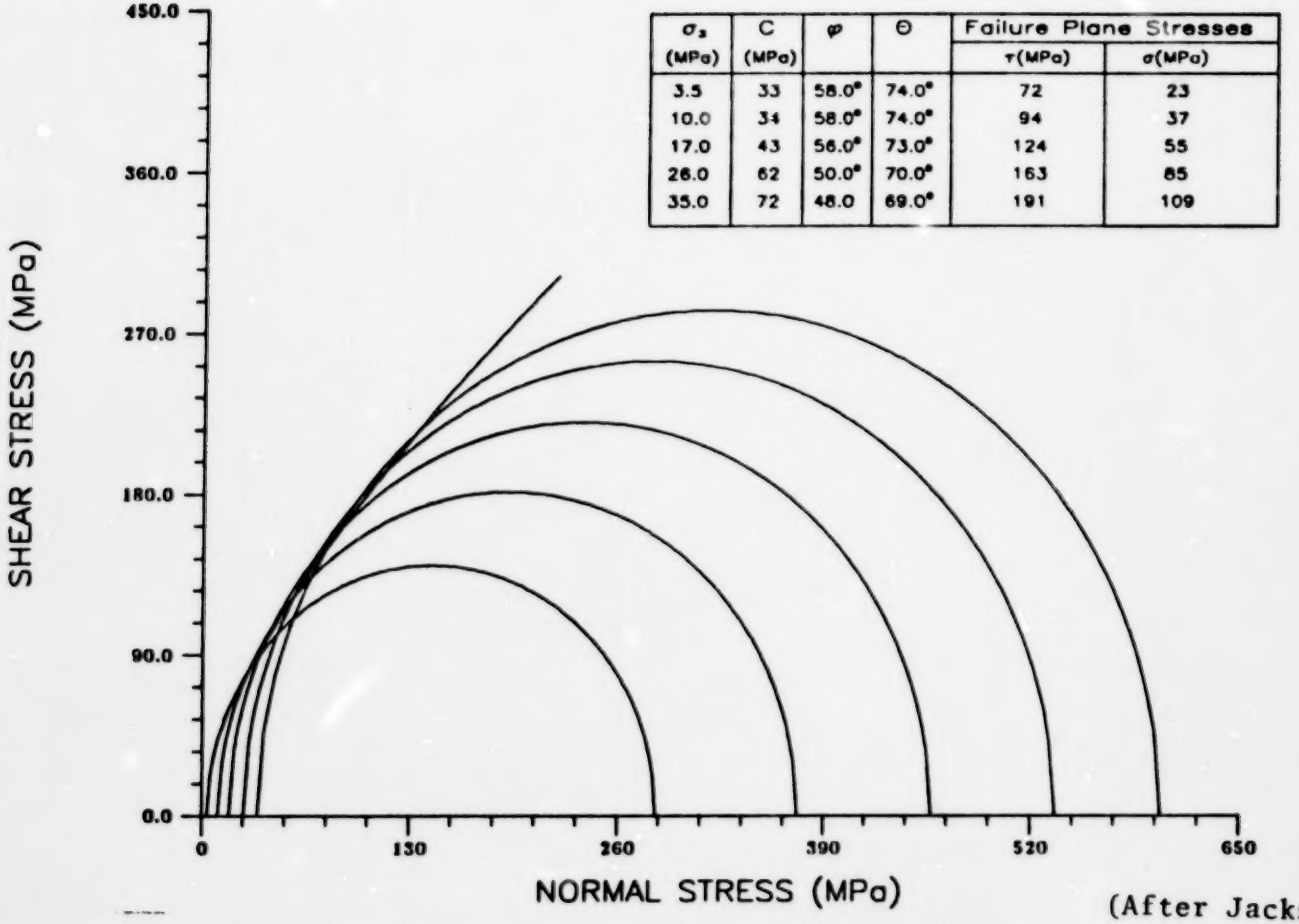

σ_3 (MPa)	C (MPa)	φ	Θ	Failure Plane Stresses	
				τ(MPa)	σ(MPa)
3.5	33	58.0°	74.0°	72	23
10.0	34	58.0°	74.0°	94	37
17.0	43	56.0°	73.0°	124	55
26.0	62	50.0°	70.0°	163	85
35.0	72	48.0	69.0°	191	109

(After Jackson and Annor, 1985b)

Fig. 35 - Mohr's circle and strength envelope for Lac du Bonnet granitic samples at 21°C

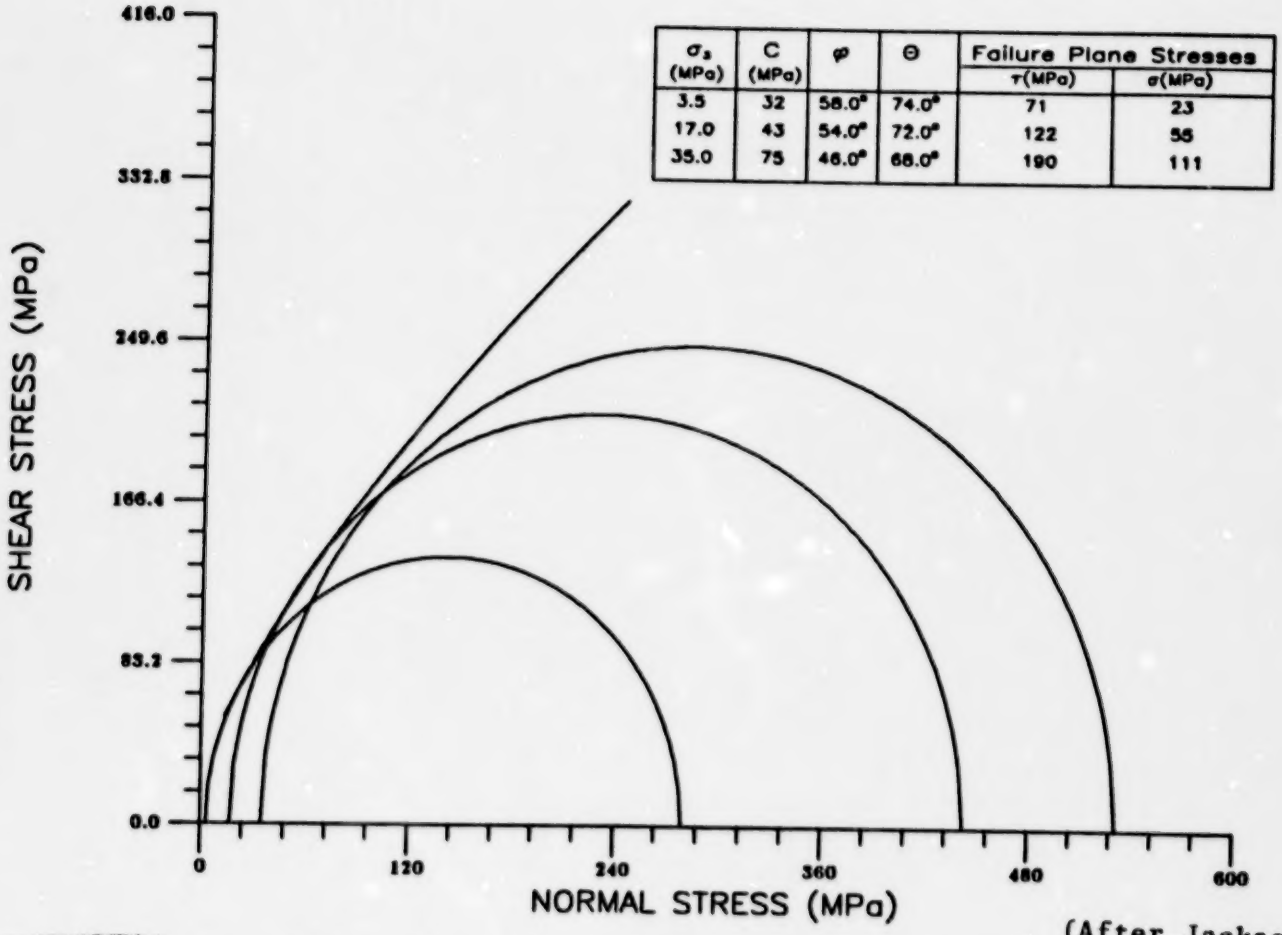

σ_3 (MPa)	C (MPa)	φ	Θ	Failure Plane Stresses	
				τ(MPa)	σ(MPa)
3.5	32	58.0°	74.0°	71	23
17.0	43	54.0°	72.0°	122	56
35.0	75	46.0°	68.0°	190	111

(After Jackson and Annor, 1985b)

Fig. 36 - Mohr's circle and strength envelope for Lac du Bonnet granitic samples at 100°C

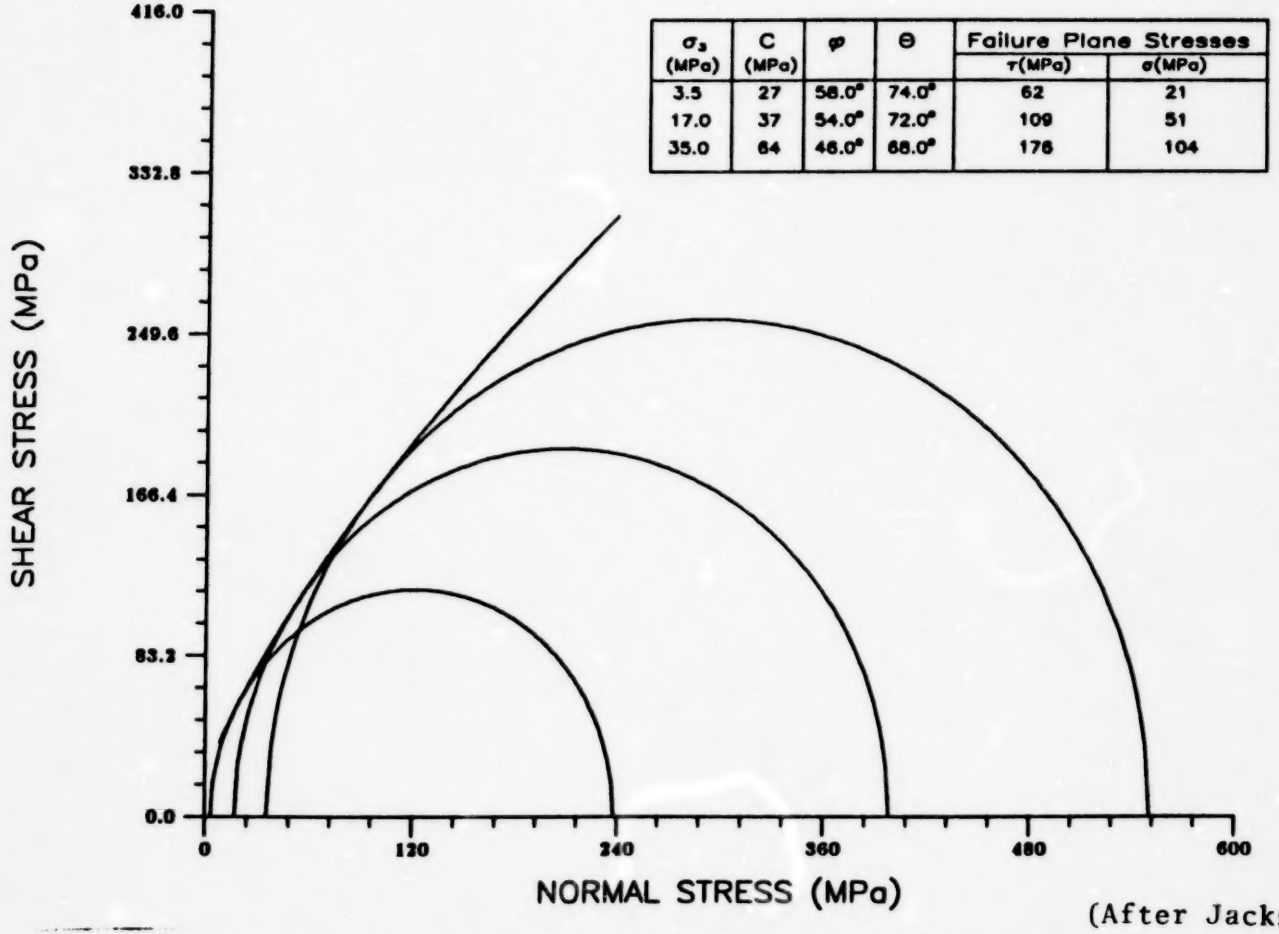

σ_3 (MPa)	C (MPa)	φ	Θ	Failure Plane Stresses	
				τ(MPa)	σ(MPa)
3.5	27	58.0°	74.0°	62	21
17.0	37	54.0°	72.0°	109	51
35.0	64	46.0°	68.0°	176	104

(After Jackson and Annor, 1985b)

Fig. 37 - Mohr's circle and strength envelope for Lac du Bonnet granitic samples at 200°C

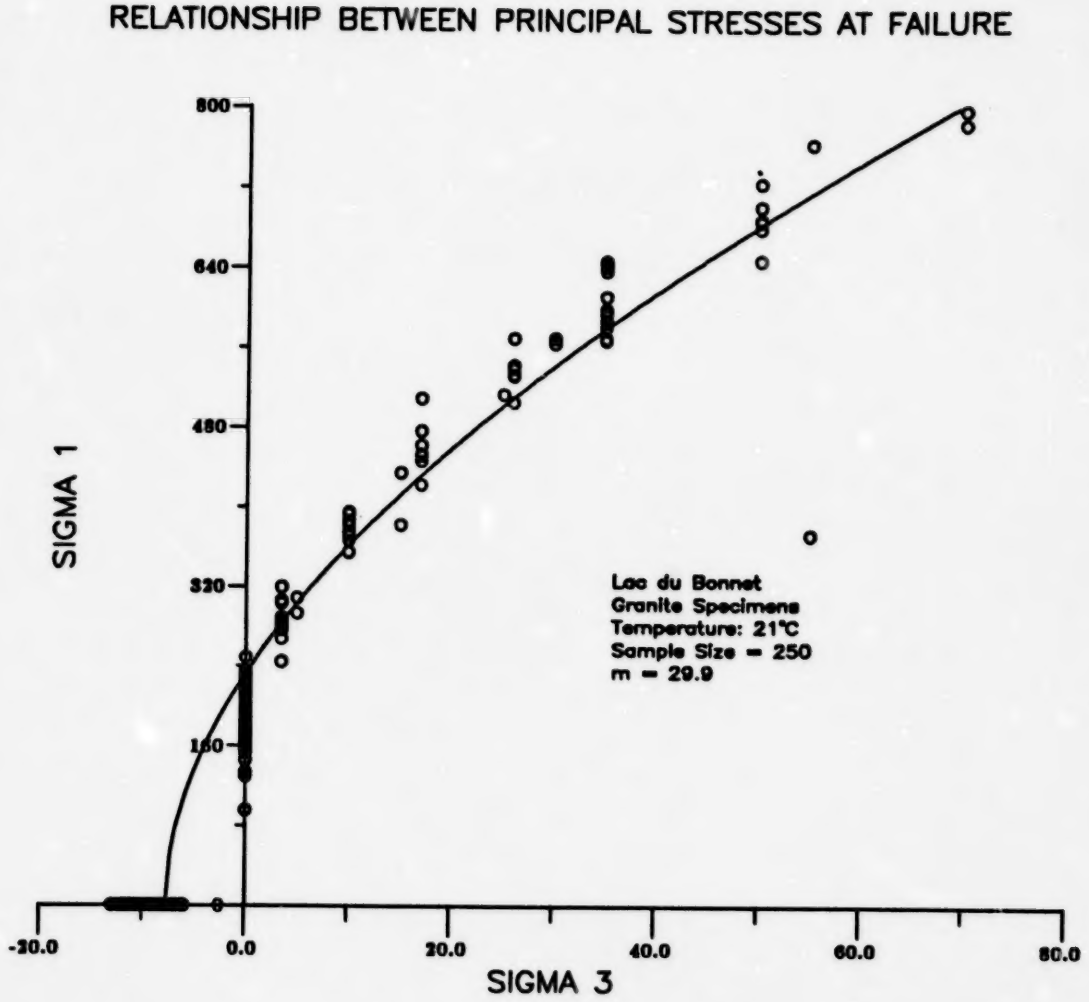

(After Jackson and Annor, 1985b)

Fig. 38 - Relationship between principal stresses at failure for Lac du Bonnet granitic samples at 21°C

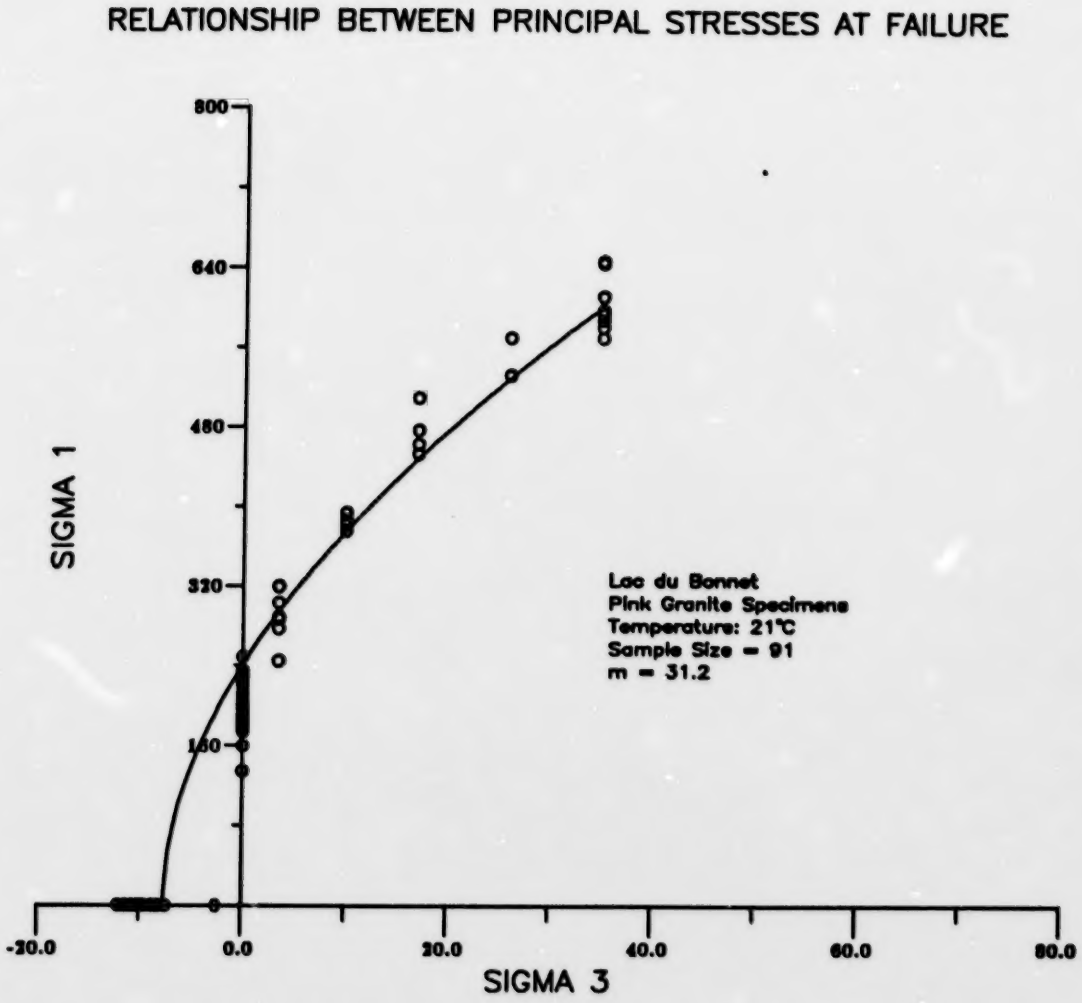

(After Jackson and Annor, 1985b)

Fig. 39 - Relationship between principal stessses at failure for Lac du Bonnet pink granite samples at 21°C

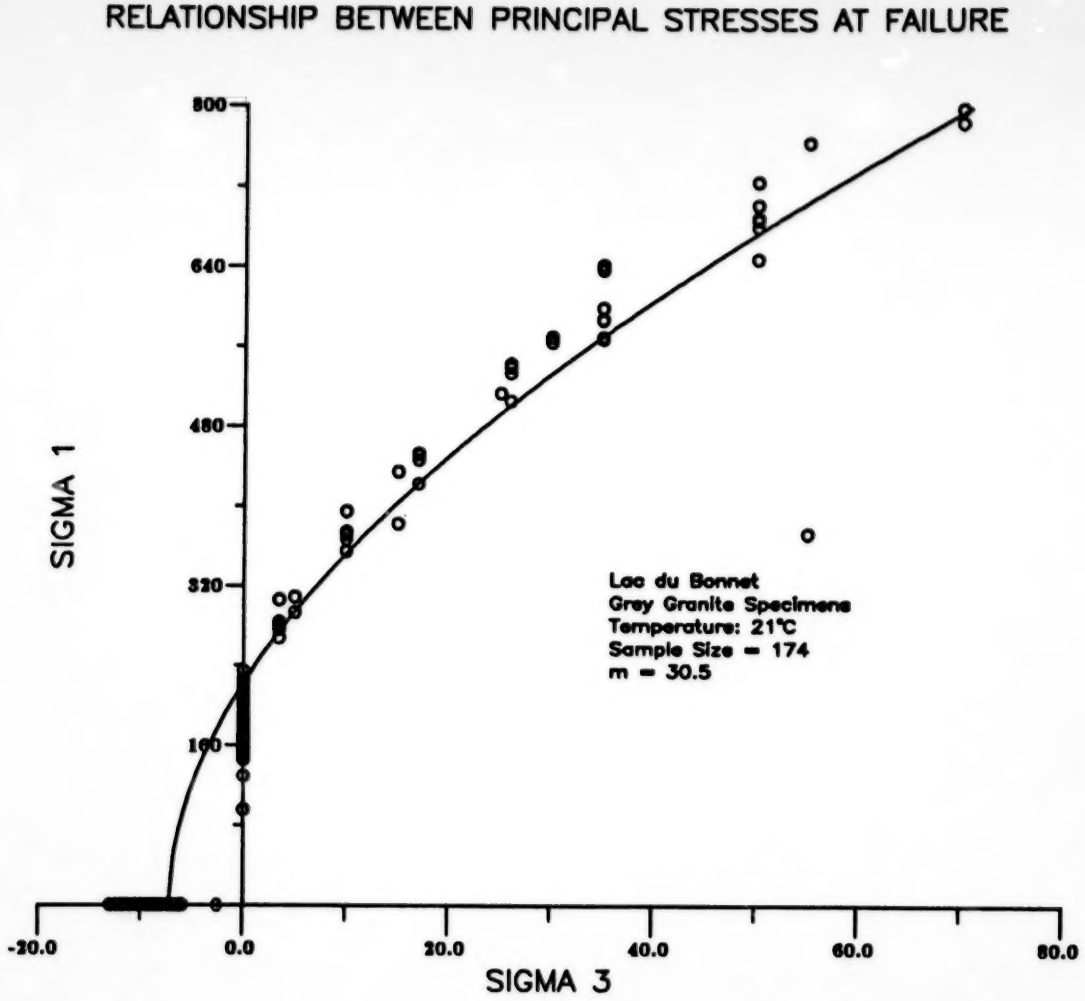

(After Jackson and Annor, 1985b)

Fig. 40. Relationship between principal stresses at failure for Lac du Bonnet grey granite samples at 21°C

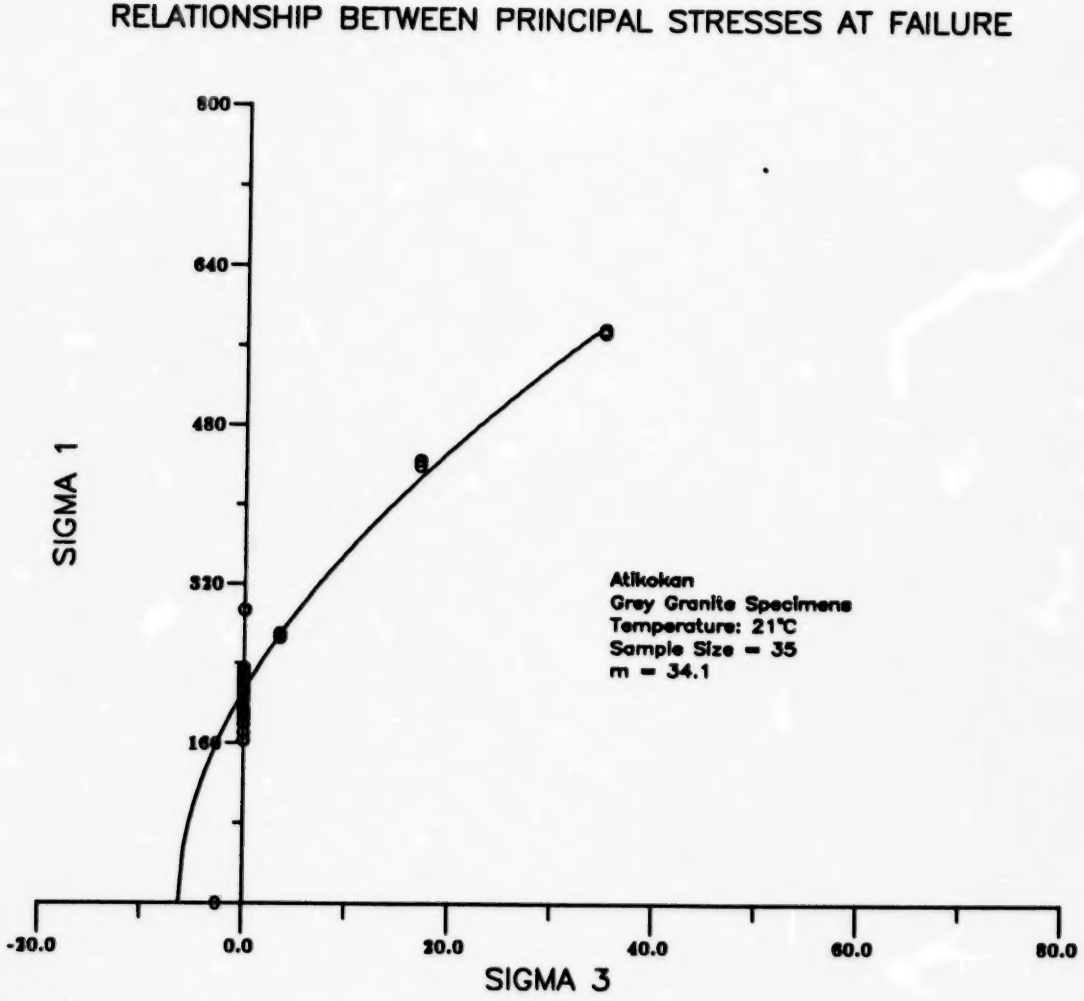

(After Jackson and Annor, 1985b)

Fig. 41 - Relationship between principal stresses at failure for Atikokan granite samples at 21°C

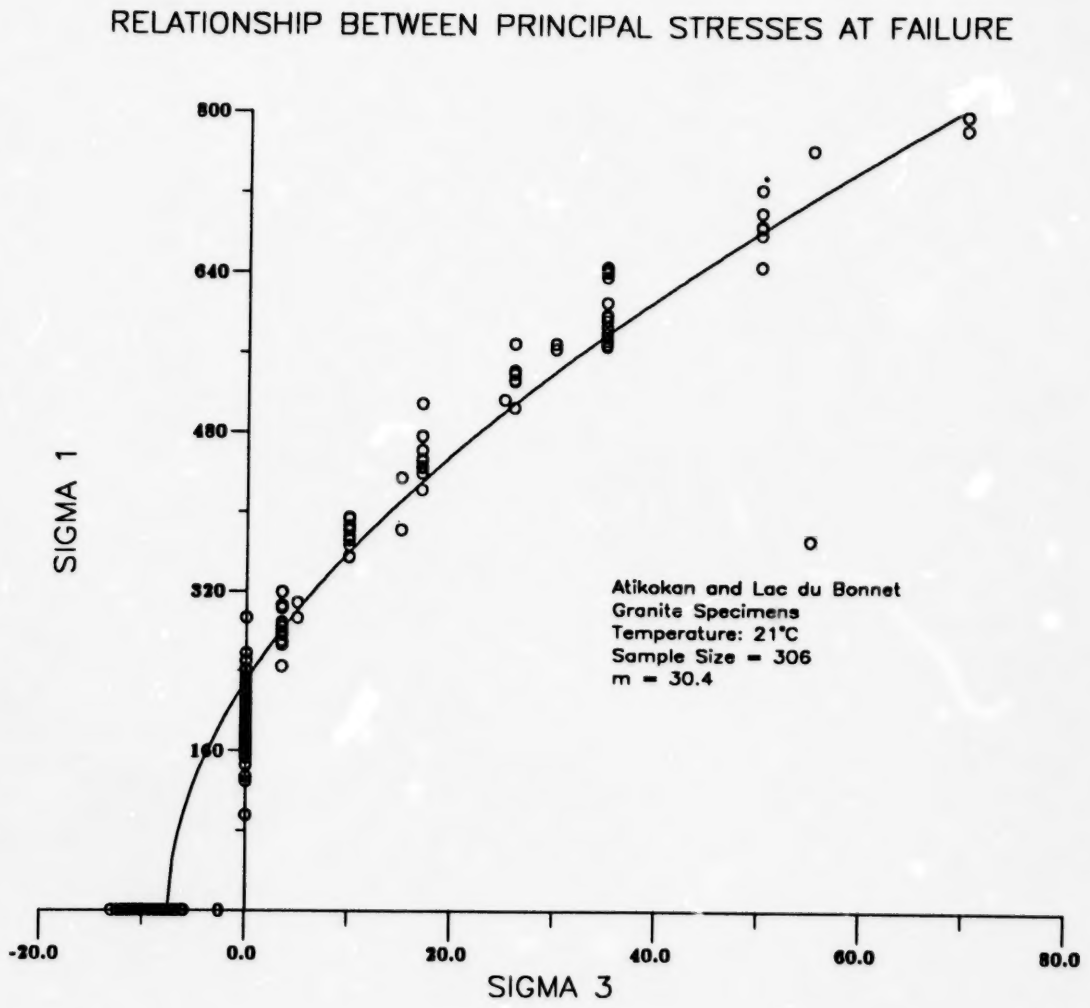

(After Jackson and Annor, 1985b)

Fig. 42 - Relationship between principal stresses at failure for Atikokan and Lac du Bonnet granite samples at 21°C

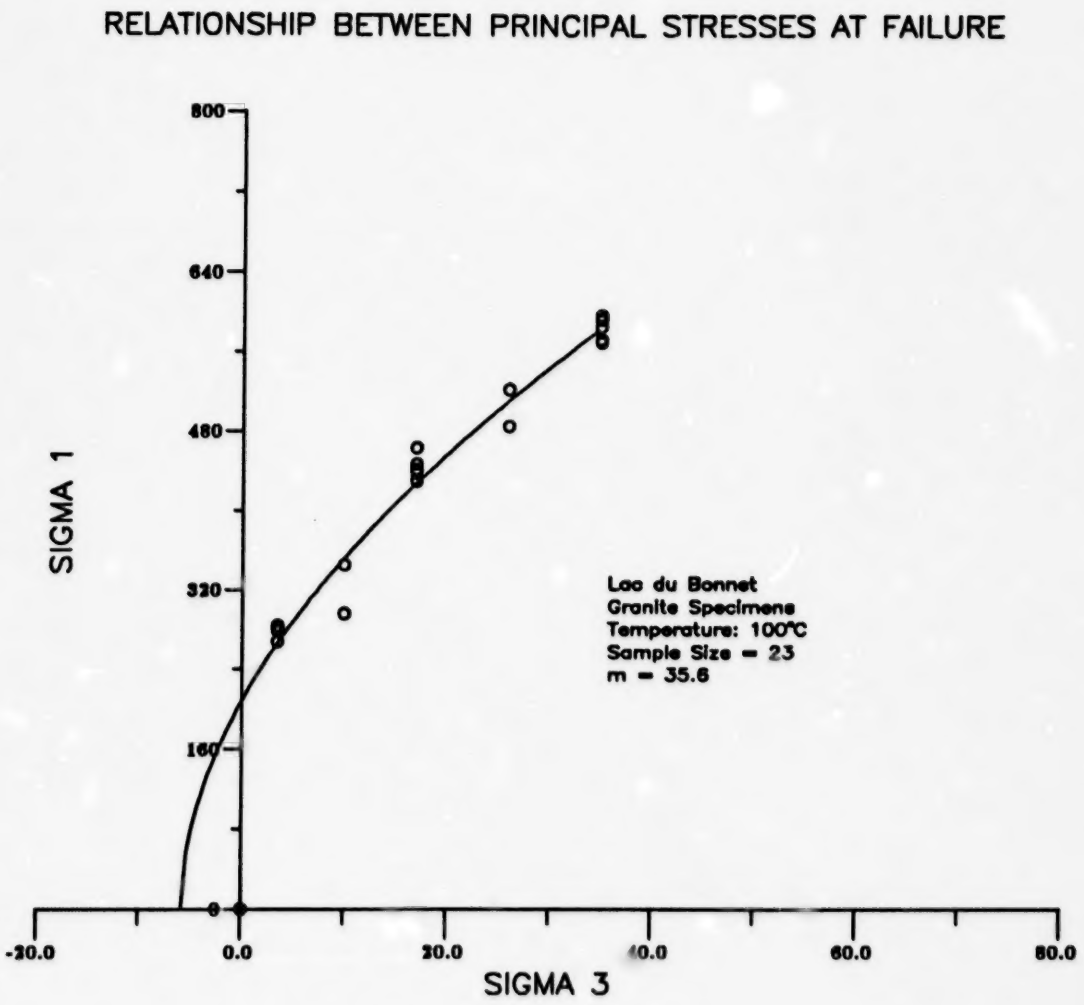

(After Jackson and Annor, 1985b)

Fig. 43 - Relationship between principal stresses at failure for Lac du Bonnet granitic samples at 100°C

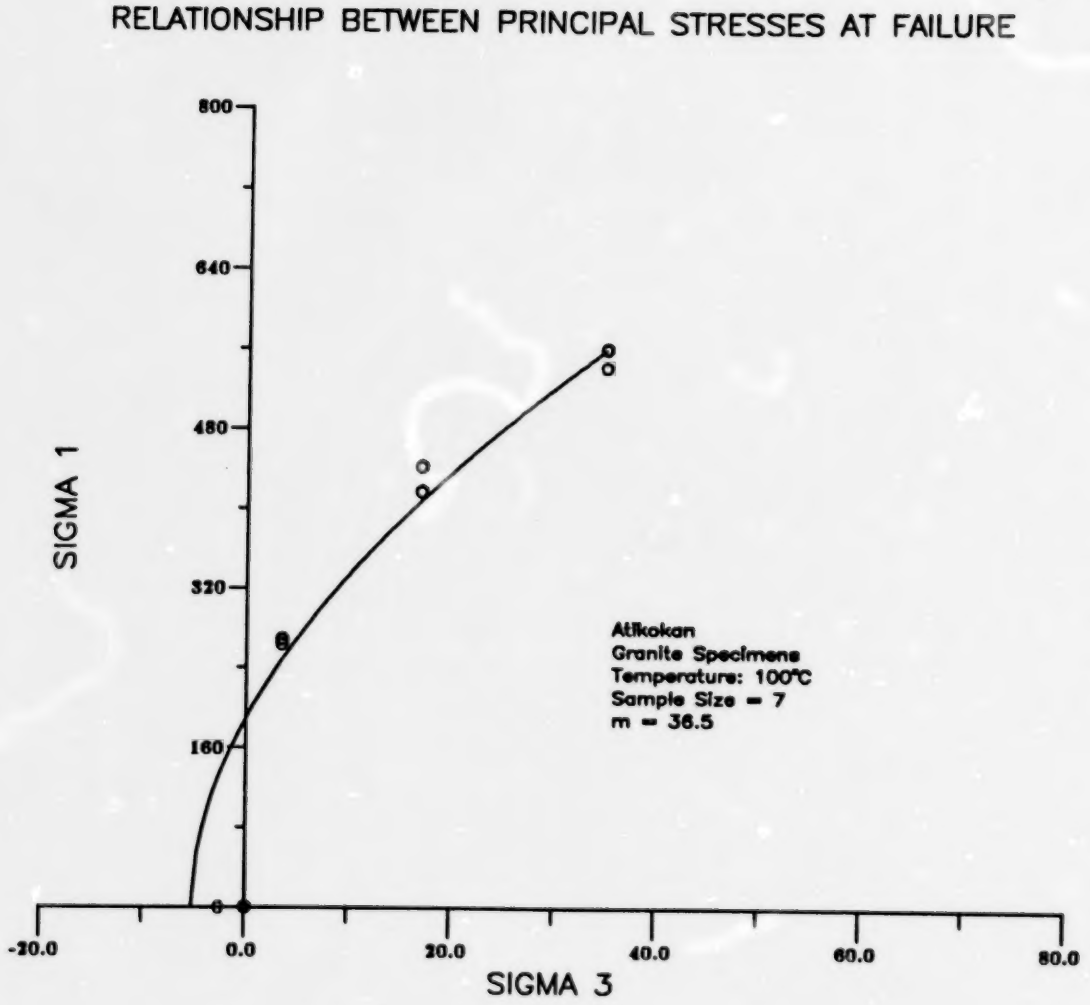

(After Jackson and Annor, 1985b)

Fig. 44 - Relationship between principal stresses at failure for Atikokan granitic samples at 100°C

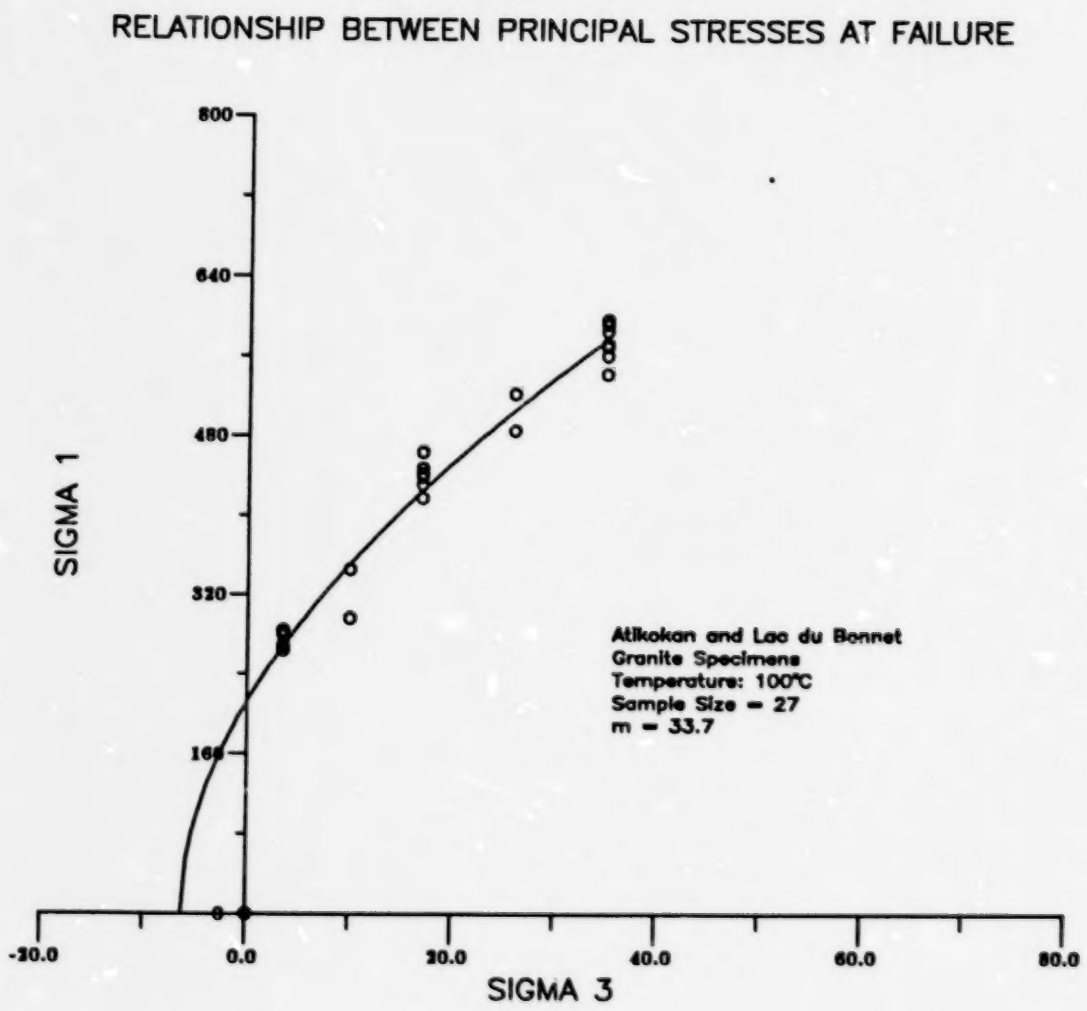

(After Jackson and Annor, 1985b)

Fig. 45 - Relationship between principal stresses at failure for Atikokan and Lac du Bonnet granitic samples at 100°C

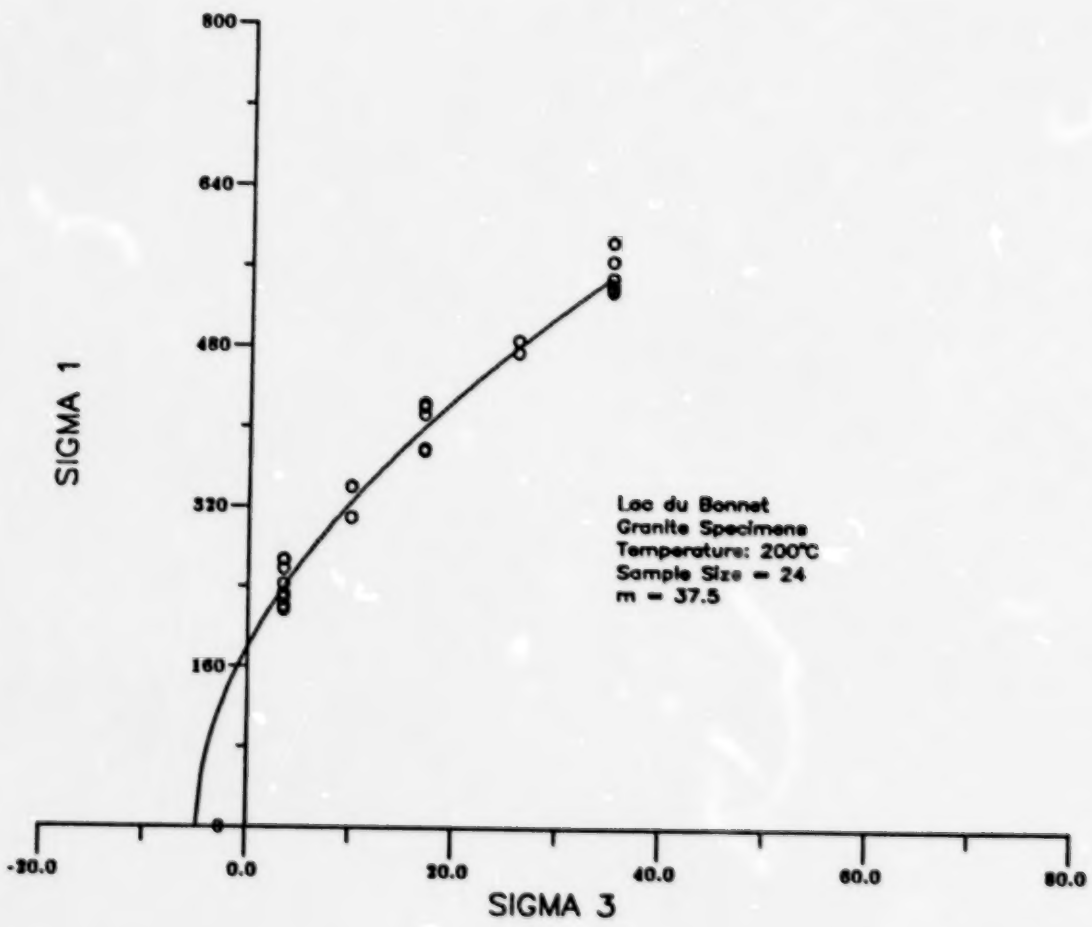

(After Jackson and Annor, 1985b)

Fig. 46 - Relationship between principal stresses at failure for Lac du Bonnet granitic samples at 200°C

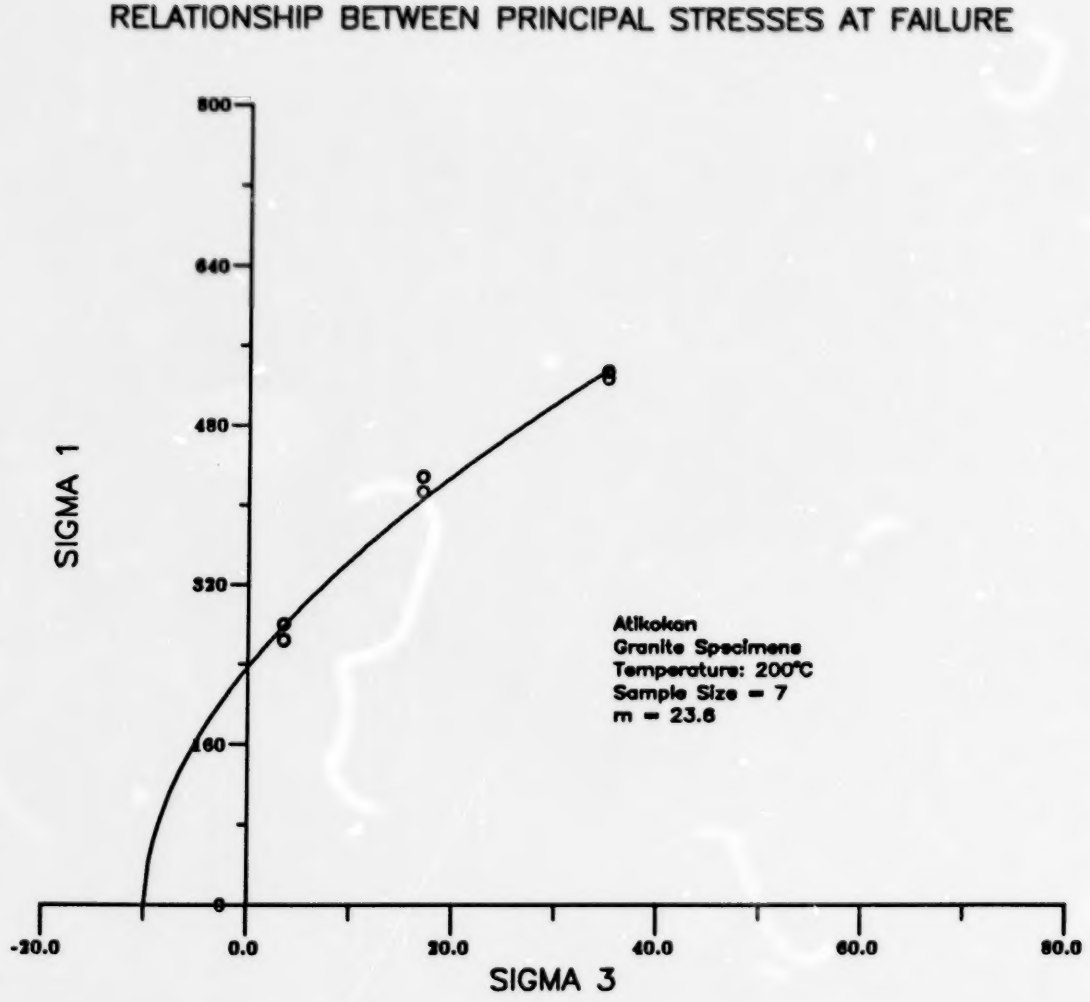

(After Jackson and Annor, 1985b)

Fig. 47 - Relationship between principal stresses at failure for Atikokan granitic samples at 200°C

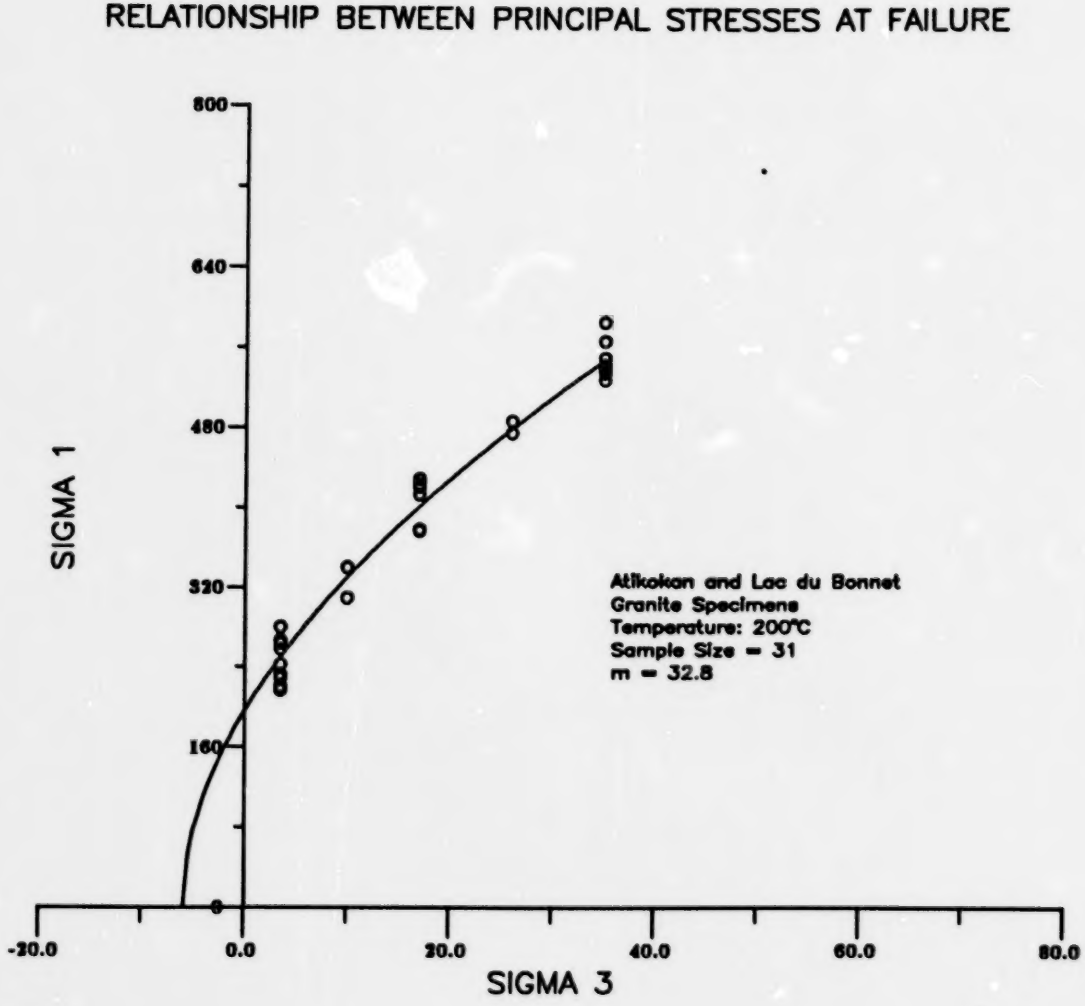

(After Jackson and Annor, 1985b)

Fig. 48 - Relationship between principal stresses at failure for Atikokan and Lac du Bonnet granitic samples at 200°C

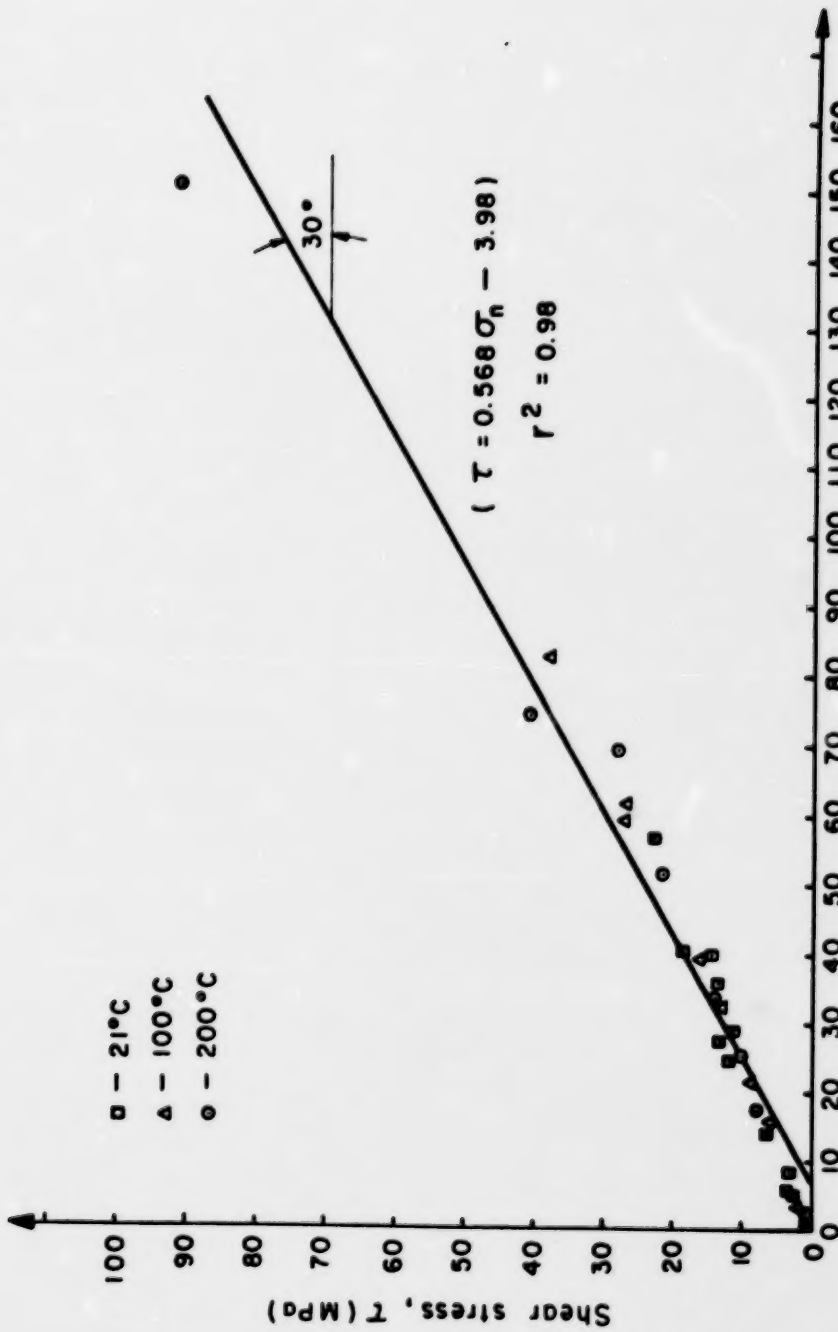

(After Annor et al, 1981)

Fig. 49 - Frictional strength of saw-cuts in Lac du Bonnet granitic samples as a function of temperature